SAND2003-3493
Unlimited Release
Printed October 2003

Experimental Optimization of the FireFly™ 600 Photovoltaic Off-Grid System

David L. King, Thomas D. Hund, William E. Boyson, Mark E. Ralph, Marlene Brown
Photovoltaic Systems R&D Department
Sandia National Laboratories
P.O. Box 5800
Albuquerque, NM 87185-0752

Ron Orozco
Energía Total, Ltd.
451 W. Meadowlark Lane
Corrales, NM 87048

Abstract

A comprehensive evaluation and experimental optimization of the FireFly™ 600 off-grid photovoltaic system manufactured by Energia Total, Ltd. was conducted at Sandia National Laboratories in May and June of 2001. This evaluation was conducted at the request of the manufacturer and addressed performance of individual system components, overall system functionality and performance, safety concerns, and compliance with applicable codes and standards. A primary goal of the effort was to identify areas for improvement in performance, reliability, and safety. New system test procedures were developed during the effort.

ACKNOWLEDGEMENTS

The effort documented in this report was funded by the U.S. Department of Energy as part of the photovoltaic system research and development effort at Sandia National Laboratories in Albuquerque, New Mexico. The initial motivation for the effort resulted from discussions between Ron Orozco of Energia Total, Ltd. and Sandia's Technology Partnerships organization. Marlene Brown formalized the desired scope of work with Energia Total. The array performance test procedure used during this investigation was previously developed and documented by David King, Bill Boyson, and Jay Kratochvil. Tom Hund developed and implemented the new test procedure used to fully characterize the performance and functionality of the entire system. Mark Ralph provided a thorough assessment of the system in regard to compliance with recognized codes and standards associated with photovoltaic systems. Jerry Ginn and Mark Ralph provided test results illustrating the electrical performance of a typical Trace DR2424 inverter. David King conducted the array and system performance modeling, consolidated data analysis procedures, formalized the concept of daily energy efficiency for components and system, and integrated all aspects of the effort documented in this report. John Wiles of the Southwest Technology Development Institute (SWTDI/NMSU) provided valuable consultation on the specifics of photovoltaic system grounding. John Stevens (Sandia), Andy Rosenthal (SWTDI), and Bob Hammond (Arizona Public Service) provided comprehensive reviews of the document. This work was conducted in support of Sandia's photovoltaic system applications project previously directed by Beth Richards.

DISCLAIMER

As part of its research mission, Sandia conducts photovoltaic component, subsystem, and system testing for the purpose of assessing the state of the technology, identifying research needs, and providing information that may assist in the proper use or improvement of a product. **SANDIA NEITHER CERTIFIES NOR ENDORSES ANY PRODUCT.**

CONTENTS

EXECUTIVE SUMMARY **6**
GLOSSARY OF TERMINOLOGY **9**
ARRAY PERFORMANCE CHARACTERIZATION **18**
- **Performance at Standard Reporting Conditions** **18**
- **Energy Available from PV Array** **21**
- **Matching the Array with PCS Components (System Optimization)** **23**
- **Temperature Coefficients** **27**
- **Solar Spectral Influence** **27**
- **Solar Angle-of-Incidence** **28**
- **Array Performance at Other Operating Conditions** **29**
- **Operating Temperature versus Environmental Conditions** **30**

SYSTEM PERFORMANCE TESTING **33**
- **System Energy Losses** **33**
- **Model for System and Component 'Daily' Efficiency** **35**
- **Outline of System Test Procedure** **36**
- **Load Selection for System Testing** **38**

COMPONENT TEST RESULTS **40**
- **Initial System Inspection** **40**
- **Compliance with Codes & Standards** **40**
- **Electrical Grounding Discussion** **41**
- **Battery and PCS Enclosure Design** **41**
- **Battery Capacity Measurements** **47**

SYSTEM TEST RESULTS **54**
- **Operation During Typical Cycling** **56**
- **Recovery from Low-Voltage-Disconnect and Tare Loss** **59**
- **Daily Energy Efficiency for System and Components** **62**
  - Daily Array Efficiency 62
  - Daily Array Utilization Efficiency 63
  - Daily Battery Efficiency 64
  - Daily Inverter Efficiency 64
  - Daily System Efficiency 65
- **System Performance Optimization** **66**

CONCLUSIONS **69**
REFERENCES **70**
APPENDIX A – TRACE DR2424 INVERTER TESTS **71**
APPENDIX B - TRACEABILITY STATEMENT **76**

EXECUTIVE SUMMARY

A comprehensive evaluation and experimental optimization of the FireFly™ 600 off-grid photovoltaic system manufactured by Energia Total, Ltd. was conducted at Sandia National Laboratories in May and June of 2001. This evaluation was conducted at the request of the manufacturer and addressed performance of individual system components, overall system functionality and performance, safety concerns, and compliance with applicable codes and standards. A primary goal of the effort was to identify areas for improvement in performance, reliability, and safety. The following bullets summarize the most important results from the investigation.

Photovoltaic Array

- The measured maximum power (P_{mp}=564 W) from the array of eight BP Solar BP275 modules was about 6% below the power expected from individual module nameplate ratings (600W) at the ASTM Standard Reporting Condition.
- The maximum-power voltage (V_{mp}) for the array was significantly higher than the system operating range dictated by the Nationwide batteries and charge controller, resulting in low array utilization with about 15 to 20% of the available dc energy lost on an annual basis.
- Adjustment of the array tilt angle for winter operation resulted in about 10% more energy available from the array in the months of December and January, relative to a latitude-tilt orientation.
- The daily array efficiency (dc energy out divided by solar energy in) varied seasonally and was determined to be highest in winter at 11.2% and lowest in summer at 9.5%.

Battery Subsystem

- The hydrogen venting provision on the Zomeworks H_2Vent™ battery enclosure was inadequate for the Nationwide lead-acid batteries used in the system. For summer operation in Albuquerque, the hydrogen concentration in the enclosure readily exceeded the 4% lower-explosive-limit during battery charging near full state-of-charge. The venting needs to be enhanced to eliminate the potential safety hazard, or different batteries with less hydrogen generation need to be selected.
- The thermal design for the insulated battery enclosure needs to be modified to keep the batteries cooler in the summer. The current design will result in battery temperatures over 45°C in the summer, undesirably reducing battery lifetime and increasing the 'watering' frequency. Ideally, the batteries in the enclosure should spend the majority of the time in the range from 15°C to 35°C.
- The close-packed physical layout of battery monoblocks inside the battery enclosure resulted in undesirably high cell-to-cell temperature differences. During testing, cell-to-cell temperature differences of over 15°C were measured during battery equalization (boost) charging. Physically separating the monoblocks to provide air gaps between vertical surfaces will increase thermal convection and give more uniform cell-to-cell temperatures. Temperature differences less than 3°C are desirable.
- The capacity of the Nationwide battery bank at a discharge rate of 18A and an average temperature of 30°C to a voltage of 21.0 Vdc was measured to be 434±15 Ah. For one-year-old batteries, this value was consistent with the manufacturer's specification of 440 Ah at 25°C.
- The 'usable' capacity for the battery bank depended on the low-voltage-disconnect (V_{LVD}) setpoint. At V_{LVD} = 21.7 Vdc for a 22-A discharge rate and an average temperature of 30°C, the battery capacity was measured to be 425±15 Ah, or in units of energy 10.2±0.4 kWh. However, for the battery manufacturer recommended value of V_{LVD} = 22.8 Vdc, corresponding to a 12% state-of-charge, the usable capacity was 375 Ah, or 9.0 kWh.

- The low-voltage-disconnect setpoint, V_{LVD} = 21.7 Vdc, established by a dynamic 'over-discharge protection' feature in the Trace DR2424 inverter was too low for the Nationwide batteries. This setpoint was not adjustable and will likely result in a significant loss of capacity and shortened battery lifetime. A V_{LVD} value of 22.8 Vdc, or higher, is recommended for lead-acid batteries.
- The low-voltage-reconnect voltage setpoint, V_{LVR} = 24.9 Vdc, established by the Trace DR2424 inverter was also too low for reliable system operation. After full discharge, the batteries had regained only 18% state-of-charge at the 24.9-Vdc setpoint. A preferred value of V_{LVR} = 26 Vdc would allow the batteries to recover about 50% state-of-charge before the ac load is reconnected.
- The daily energy efficiency of the Nationwide battery (daily energy out of the battery divided by daily energy into the battery) was determined to be about 73%, during a 30-day test period in the summer in Albuquerque using a 'conservative' ac load. Optimization of setpoints and charging strategy could increase this daily energy efficiency to about 85%.
- If the Nationwide batteries are fully charged, the system will provide about 6.0, 4.5, and 3.5 'days of autonomy' for daily ac energy requirements (loads) of 1.5, 2.0, and 2.5 kWh/d, respectively.

Power Conditioning Subsystem (PCS)

- A fundamental incompatibility between the Trace DR2424 inverter and the Trace C40 charge controller was identified. Basically, the upper limit for dc input voltage to the inverter (31 Vdc) was too low to accommodate the setpoint range, the low temperature battery voltage compensation, and the battery equalization provision of the Trace C40 charge controller. For winter operation, the consequence will be periodic inverter shut-downs and dissatisfaction with system reliability.
- As tested in the summer with an average inverter enclosure temperature of 30°C, the daily energy efficiency of the Trace DR2424 inverter (ac energy out divided by dc energy in) including tare loss was determined to be about 87±1%. The peak inverter efficiency at an ac load of 475 W was about 91±1%.
- The tare loss for the DR2424 inverter ("search" mode defeated) plus the Trace Meter was determined to be 17.5±1 Wdc which accounted for a significant fraction of the energy 'loss' in the system. Reducing this tare loss to <5 W would effectively raise the ac energy available from the system in the winter months by about 0.2 kWh/d, or 15%.
- The thermal design for the Zomeworks insulated steel enclosure used to house the inverter, charge controller, and Trace Meter needs improved ventilation in summer in order to reduce equipment temperatures. As designed, temperatures above 45°C will be realized in summer. The peak inverter efficiency for the Trace DR2424 dropped by about 1 percentage point for every 10°C rise in temperature, and the output from the Trace C40 charge controller will be limited for temperatures above 40°C.

System Performance

- The FireFly™ 600 system had an overall daily energy efficiency of about 54% (ac energy out divided by dc energy available from the array), as tested over a 30-day period in Albuquerque. System optimization that minimized inverter tare losses and excess energy used to overcharge batteries could increase the overall system efficiency to about 67%.
- The daily ac energy production capacity of the system varies seasonally, depending on three things: array orientation (latitude-tilt or seasonal adjustment), battery 'overcharge' procedure, and inverter efficiency including tare loss. In winter in Albuquerque with array at latitude-tilt and 0.57 kWh/d daily battery overcharge and 0.33 kWh/d tare loss, the system will deliver about 1.55 kWh/d ac energy daily. By adjusting the tilt-angle of the array seasonally, the system will deliver 1.70 kWh/d in winter.
- The Trace DR2424 inverter had a 'search mode' intended to reduce the dc energy (tare) loss at times when an ac load was not present. If the devices making up the ac load are compatible with the

inverter's 'search mode,' then the winter ac energy capacity of the system will increase to about 2.10 kWh/d in Albuquerque.

System Optimization

- Implementation of all proposed design modifications for the FireFly™ 600 system will eliminate a hydrogen safety hazard, improve the efficiency and lifetime of batteries, increase overall system energy efficiency to about 73%, and increase the winter ac energy capacity by over 50%, to about 2.4 kWh/d in Albuquerque.
- Obtaining optimum ac energy production capacity will require the following: an array that meets its nameplate power rating, seasonal adjustment of array tilt-angle, an array whose V_{mp} range closely matches the battery operating voltages (or a 95%-efficient charge controller with maximum-power-point-tracking capability), an average of less than 0.2 kWh/d dc energy used to overcharge batteries, and an inverter with 90% daily energy efficiency plus less than 0.1 kWh/d tare loss.

Codes and Standards

- A variety of relatively minor modifications were identified as being required for compliance with the National Electrical Code (NEC) pertaining to photovoltaic systems. The most significant change will be wiring revisions for compliance with grounding requirements for equipment, dc circuit, and ac circuit.

GLOSSARY OF TERMINOLOGY

The terminology used by module manufacturers, system integrators, power conditioning component manufacturers, and battery manufacturers is often different and can be confusing. The following glossary is an attempt to consolidate terms and to provide explicit definitions as used in this report.

Absolute air mass, AM_a. A dimensionless term used to describe the optical depth, or path length, that sunlight must traverse through the atmosphere before reaching the ground. When adjusted for the altitude or atmospheric pressure of a site, it is called absolute or pressure-corrected. The reference value of 1.0 is for a site at sea level with the sun directly overhead.

Amp-hour, Ah. An engineering unit used by the battery industry to describe energy flow into and out of a battery. This is not a standard SI unit, but is in common usage. The unit is not a measure of energy in that it does not account for the battery voltage associated with the value, and in particular for PV systems the battery voltage varies significantly with the battery state-of-charge.

Array. The photovoltaic (solar to electric) system component composed of separate photovoltaic modules. The photovoltaic modules are in turn composed of individual solar cells that are wired in series-connected strings within the module.

Array maximum-power voltage, V_{mp}. The voltage corresponding to the maximum-power-point on the array's current-voltage (I-V) curve.

Array open-circuit voltage, V_{oc}. The voltage produced by the photovoltaic array in an open-circuit condition.

Array maximum power, P_{mp}. The maximum power available from the photovoltaic array at a given environmental operating condition; occurs at the maximum-power-point on the I-V curve.

Array power rating at SRC, P_{mpo}. The maximum power available from the photovoltaic array at the Standard Reporting Condition (SRC) specified by ASTM. The SRC commonly used by the PV industry is for a solar irradiance of 1000 W/m^2, a PV cell temperature of 25°C, and a standardized solar spectrum referred to as an air mass 1.5 spectrum (AM=1.5).

Array utilization. The percentage of daily dc energy available from the photovoltaic array that is actually used by the system. This value provides a gauge of how well the system's power-conditioning-system tracks the maximum-power-point of the array's current-voltage (I-V) curve.

Battery rated capacity, Ah or Wh. Manufacturer's rating for the total energy available from a battery taken from a fully charged to a fully discharged condition. For lead-acid batteries this rating is typically stated for a battery temperature of 25°C when discharged to a voltage representing 1.75 volts per cell, or 21.0 Vdc for a 24-V battery bank.

Battery usable capacity, Ah or Wh. Specifically for photovoltaic systems, the energy available from the battery at 25 °C when the battery is discharged from a fully charged condition to the low-voltage-disconnect, V_{LVD}, setpoint. The setpoint selection is a tradeoff between maximizing battery lifetime and minimizing initial system cost. For deep-cycle lead-acid batteries, the usable capacity to a voltage of about 1.9 volts-per-cell, or 22.8 Vdc for 24-Vdc battery bank, is typically about 85% of the rated capacity.

Battery discharge rate. The rate at which current is extracted from a battery. Usually expressed in amps, or in terms of hours required to fully deplete the battery. A 20-hr discharge rate is commonly used when measuring battery capacity.

Battery specific gravity, SG. The chemical specific gravity of the sulfuric acid solution (electrolyte) in cells of the battery. SG is measured using a hydrometer and is typically adjusted to a battery temperature of 25°C. Typical value is about 1.3 for a fully charged lead-acid battery.

Battery charge controller. The system component that controls the charging process for the battery bank by setting voltage limits and regulating the current flow into the battery from the photovoltaic array.

Battery state-of-charge, SOC. The percentage of energy remaining in a battery relative to energy contained when fully charged.

Battery daily deficit charging. An operating condition where, on a daily basis, less energy is added to the battery than removed, resulting in a reduction of the battery state-of-charge. Continuous deficit charging will result in a low-voltage-disconnect condition, and repetitive occurrences can result in reduced battery capacity and lifetime.

Battery daily overcharge, Ah or kWh. The daily energy (kWh), or current flow (Ah), added to the battery after a specified voltage condition has been reached. As defined in this document, the specified voltage condition was the point in the charging process where average battery voltage reached the float charging setpoint, V_{FLOAT}. Since the amount of overcharge necessary to maintain battery health varies with battery type, this definition provides a specific test condition relative to which an energy balance can be conducted.

Battery equalization charging. A periodic charging process that overcharges or boost charges the battery for an extended period of time in order to fully mix the battery electrolyte and maximize battery lifetime. For deep-cycle lead-acid batteries, the equalization process may last several hours at a maximum voltage of 2.50 to 2.55 volts-per-cell (30 to 31 Vdc for 24-V battery).

Battery bulk charging voltage, V_{BULK}. The maximum voltage that the charging system (charge controller) allows the battery to achieve during the charging process prior to achieving a full state-of-charge.

Battery float charging voltage, V_{FLOAT}. The voltage at which the charging system (charge controller) holds (regulates or floats) the battery after a full state-of-charge has been achieved, also called the regulation voltage.

Battery high-voltage-disconnect, V_{HVD}. The battery voltage at which the charging system disconnects the charging source (PV array) to prevent damage to the battery.

Battery low-voltage-disconnect, V_{LVD}. The battery voltage at which the system load is disconnected to prevent battery damage, and to allow the battery to recover from a low state-of-charge.

Battery low-voltage-reconnect, V_{LVR}. The battery voltage at which the system load is reapplied following the occurrence of a low-voltage-disconnect condition and the subsequent addition of energy to the battery.

Battery monoblock. Term used to describe the physical enclosure used to house multiple battery cells. For deep-cycle lead-acid batteries, there are often three cells per monoblock.

Battery voltage-per-cell, vpc. Batteries are composed of individual cells that are electrically connected in series. A 24-V battery has twelve cells in series, each cell with nominally 2 volts-per-cell. For lead-acid batteries, the individual cell voltage can vary from 1.75 volts-per-cell to about 2.6 volts-per-cell depending of the state-of-charge.

Daily solar insolation, kWh/m^2. The cumulative daily solar irradiance in the plane of the photovoltaic array. This quantity is either measured directly or calculated from typical meteorological year (TMY) data for a specific geographic location. Sometimes expressed in "sun-hours" where the daily insolation is divided by the standard solar irradiance of 1000 W/m^2. That is, 5 kWh/m^2/d is referred to as 5 sun-hours.

Daily sun-hours, h/d. This is an alternative term used to quantify the daily solar insolation. In this case, the daily solar insolation in kWh/m^2/d is divided by the standard solar irradiance of 1000 W/m^2 to give units of hours per day.

Daily array-to-load energy ratio, A:L. A ratio used to gauge the daily energy available from the photovoltaic array relative to the daily energy required by the load attached to the system. The ratio is both site dependent and system design dependent. There is currently no standardized method for calculating this ratio, so the values documented elsewhere for PV systems vary widely. In this report, A:L was determined by measuring PV array performance and using the resulting array performance parameters along with typical meteorological year (TMY) solar resource data to calculate the daily average energy available from the PV array. For a resistive load, the daily average A:L ratio can be calculated for each month of the year. For a system with an ac load, the calculated A:L ratio will be lower than for a system with an equivalent dc load because of the energy losses associated with the inverter. For system design purposes, the A:L for the month with the lowest solar resource, December or January, is typically used. For systems with a dc load, this design A:L ratio is typically in the range from 1.3 to 1.6. For systems with an ac load, the A:L ratio is typically in the range from 1.4 to 2.0.

The following 'daily efficiency' terms are illustrated by example in the text of this report. They provide an alternative and more realistic means of quantifying component and system performance that is based on energy flow rather than instantaneous power at a prescribed operating condition.

Daily array efficiency, η_{PV}. The ratio of the daily energy available from the photovoltaic array at its maximum-power-point divided by the daily total solar insolation on the array, varies seasonally.

Daily MPPT efficiency, η_{MPPT}. The ratio of the daily energy actually provided by the photovoltaic array divided by the total daily energy available from the array if operated at its maximum-power-point.

Daily battery efficiency, η_{BAT}. The ratio of the daily energy extracted from the battery divided by the total daily energy provided to the battery from the photovoltaic array.

Daily inverter efficiency, η_{INV}. The ratio of the daily ac energy provided by the inverter divided by the total energy provided to the inverter from the battery and/or photovoltaic array.

Daily system efficiency, η_{SYS}. The ratio of the daily ac energy provided by the inverter divided by the total daily energy available from the array if operated at its maximum-power-point.

Days-of-autonomy. The maximum length of time that the photovoltaic system can provide power to the load in the absence of power provided from the photovoltaic array. Directly related to the 'usable' battery

capacity and the average daily ac energy required by the load. Four days is commonly considered adequate for a residential off-grid photovoltaic system.

Design load, kWh/d. Photovoltaic system design and optimization requires an accurate definition of the expected daily ac energy required from the system (load). The worst situation for a photovoltaic off-grid system is typically the winter months where the solar resource is minimum; therefore, the 'design load' is typically chosen as the daily ac energy expected on a typical winter day.

Design month. The month chosen during system design to ensure that the photovoltaic system adequately meets the system load over the entire year. Typically the design month is one of the winter months, December or January, when the solar resource is lowest.

Electrical inverter. The system component that converts the direct current (dc) electrical energy from the photovoltaic array or battery to alternating current (ac) electrical energy required by the system load.

Equipment-grounding conductor. A conductor attached to metal surfaces of equipment that does not normally carry current, except during a fault condition. It is connected to earth ground, helps prevent electrical shocks, and also helps over-current devices to operate properly. The equipment grounding conductor is usually either a bare copper wire, a wire with green insulation, or the metal raceway containing the circuit conductors.

Grounded. Term indicating that parts of an electrical system are connected to an earth ground.

Grounded-circuit conductor. An electrical conductor that normally carries current in the system circuit, which is connected to earth ground. Examples are the neutral conductor in ac wiring and the negative conductor in a grounded photovoltaic array. Note that this conductor is distinct from the equipment-grounding conductor, which carries no current during normal operation.

Grounding electrode. The 'ground rod' or metallic device used to make physical contact with the earth; it is typically a 5/8-in diameter, 8-ft long copper rod.

Grounding-electrode conductor. The electrical conductor (wire) between the common single grounding point in a photovoltaic system and the grounding electrode.

Grounding-electrode system. A wiring scheme with two or more grounding electrodes connected together. An example would be a home with an existing ac grounding electrode when a new dc grounding electrode is added for a photovoltaic system.

Grounding 'bond.' In common usage, 'bond' refers to the connection between the grounded conductor, the equipment-grounding conductor, and the grounding electrode conductor. Often a single common grounding point in the system.

Plane-of-array irradiance, E_{poa}, W/m^2. The total (global) solar irradiance in the plane of the photovoltaic array, measured using a pyranometer.

Solar angle-of-incidence, AOI, degrees. The angle between the direct beam from the sun and a line perpendicular (normal) to the surface of the photovoltaic array.

Standard Reporting Condition (SRC). The reference condition used by the photovoltaic industry for rating the power from photovoltaic modules, which has been standardized by organizations such as ASTM, IEEE, IEC, UL, and others. This condition has a solar irradiance of 1000 W/m^2, photovoltaic cell temperature of 25°C, and a solar spectral distribution specified for an air mass equal to 1.5 (AM1.5). The condition is also commonly referred to as the standard test condition (STC).

System load, kWh/d. The daily energy required by the energy consuming devices (load) attached to the photovoltaic system. Depending on the system, the load may require either ac or dc energy.

System load control. The system component that controls when the system load (power consuming device) is electrically disconnected from the system, usually to prevent damage to the battery bank. This component usually establishes the setpoints for V_{LVD}, V_{LVR}, and V_{HVD}.

SYSTEM DESCRIPTION

The FireFly™ 600 solar-electric (photovoltaic) system manufactured by Energia Total, Ltd. in Albuquerque, New Mexico, is a 120 Vac electrical power source designed for powering small residential loads in remote or off-grid applications [1]. Photos of the photovoltaic (PV) array, battery enclosure, and power conditioning hardware in separate enclosure are shown in Figure 1. The PV array had eight BP Solar, BP275, 75-W_p crystalline silicon modules with a combined power rating of 600-W_p at the ASTM Standard Reporting Condition (1000 W/m^2, 25°C, AM1.5). Each module-string had two modules connected in series, and there were four parallel module-strings. The individual module area was 0.630 m^2 resulting in a total array area of 5.04 m^2. The modules were mounted on a horizontal pivot tube that enabled orientation of the array at different tilt-angles for performance optimization during different months of the year.

Figure 1. Photos of FireFly™ 600 photovoltaic off-grid system, insulated battery box with lid removed, insulated box containing Trace DR2424 inverter and Trace C40 charge controller, and Trace Meter used for monitoring battery state-of-charge.

Array wiring was rated for 90°C operating temperature, and was terminated in a "dc combiner box" with circuit breakers. The ac wiring from the inverter terminated in an "ac distribution panel." This panel was equipped with circuit breakers and a provision for power input from an auxiliary charging source (generator).

Separate steel enclosures manufactured by Zomeworks Corporation were used to house the batteries and the power conditioning hardware [2]. The battery enclosure had an external width of 28 in, length of 40 in, and height of 24 in, with an internal volume of about 15.5 ft^3 (0.44 m^3). Both enclosures were lined with 2-in-thick Styrofoam providing R-10 insulation. The battery enclosure was equipped with an H_2Vent™ system designed to passively remove hydrogen gas produced during the battery charging process. The intent of the hydrogen venting system was to keep the hydrogen gas concentration in the enclosure from exceeding the lower-explosive-limit (LEL) established by safety organizations as 4% hydrogen gas by volume.

The battery bank in the 24-V system had a total of eight 6-V Nationwide deep-cycle lead-acid (golf cart) batteries, with two parallel strings of four batteries each. The rated capacity of each individual battery was 220 Ah resulting in a 440-Ah capacity at 24-V for the battery bank, or 10.5 kWh of energy storage.

Battery 'charge control' and system 'load control' were provided by two system components: the charge controller (Trace C40) and the inverter (Trace DR2424). Both the bulk charging voltage (V_{BULK}) and the float charging voltage (V_{FLOAT}) were controlled by the Trace C40 charge controller. The DR2424 inverter controlled the three voltage setpoints at which the ac load was either disconnected or reconnected: the low-voltage-disconnect voltage (V_{LVD}), the high-voltage-disconnect voltage (V_{HVD}), and the low-voltage-reconnect voltage (V_{LVR}). Table 1 summarizes the system components, ratings, and setpoints.

The Trace DR2424 (s/n V019834) was a "modified sine wave" or "pulse width modified square wave" inverter equipped with an additional capability for battery charging using an auxiliary power source (ac generator) [3]. The input voltage range for the DR2424 was specified as 21.6 to 31.0 Vdc. Input voltages outside this range will result in the inverter shutting down, and then resuming operation once the voltage is back inside the range. The inverter had an adjustable "search mode" used to minimize parasitic power loss in the inverter when there was no ac load on the system. The operating (ambient) temperature range for the DR2424 inverter was specified as 0 to 50°C with inverter efficiency decreasing as the temperature increases. (See Appendix A for Sandia's performance test results on a typical Trace DR2424 inverter.)

For load control, the Trace DR2424 had a dynamic, but basically not adjustable, "over discharge protection or ODP" feature that automatically adjusted the V_{LVD} value as a function of the battery discharge rate. At high discharge rates, the ODP feature could set the V_{LVD} as low as 18 Vdc and for low discharge rates as high as 24 Vdc. However, the lowest value for the automatic V_{LVD} is also constrained by the lower input voltage limit for the inverter, that is 21.6 Vdc. For example, at a battery discharge rate of 22 A, the V_{LVD} would be adjusted by the ODP feature to 21.2 Vdc, but prior to that inverter operation would shut down at the lower input limit of 21.6 Vdc. Trace personnel also indicated that the over discharge protection circuitry would trip immediately if a large instantaneous discharge rate was detected, but would take about 1 minute to trip after V_{LVD} was detected during normal discharge rates. The other load control setpoint, low-voltage-reconnect, V_{LVR}, was not adjustable in the DR2424 but was measured to be about 24.9 Vdc.

In the event that an auxiliary ac generator is used to charge the system batteries, the Trace DR2424 assumes the "charge control" features by controlling the V_{BULK} and V_{FLOAT} voltage setpoints. These setpoints are selected by generic battery type. For the deep-cycle lead-acid batteries in the FireFly system, the values were 30.0 and 26.6 Vdc, respectively.

In the FireFly™ 600 system, the Trace C40 charge controller was used in a "charge control mode" to control only the V_{BULK} and V_{FLOAT} voltages as the PV array charged the batteries [4]. The Trace C40 had a continuous current rating of 40 A with adjustable ranges for V_{BULK} (26 to 30 Vdc) and V_{FLOAT} (25 to 29 Vdc). The Trace C40 provided a 3-stage battery charging process; bulk, 1-hr absorption, and float. In the bulk stage, the battery voltage was allowed to rise to the V_{BULK} setpoint while allowing the maximum current flow available from the photovoltaic array. In the absorption stage, battery voltage was held at V_{BULK} setpoint for a period of 1 hour and current flow into battery gradually decreased as full state-of-charge was reached. In the float stage, the C40 controller limited the voltage to the V_{FLOAT} setpoint and current continued to flow into the battery at a reduced level until there was no longer current available from the photovoltaic array.

A battery temperature compensation feature was provided with the C40 charge controller that adjusted the V_{BULK} and V_{FLOAT} setpoints based on battery temperature relative to a reference temperature (25°C). For a 24-V battery, the temperature compensation rate was -0.06 V/°C, up to a maximum compensation of 1.5 Vdc. Thus, a V_{BULK} setpoint of 30 Vdc would be lowered to 29.1 Vdc for a battery temperature of 40°C, and raised to 31.5 Vdc for a low battery temperature of 0°C. Note that at this low battery temperature which is likely to occur in cold climates, the V_{BULK} value exceeds the input voltage range for the DR2424 inverter, and would likely result in the inverter shutting down. System testing at Sandia was done with the C40 setpoints at the high end of both ranges (V_{BULK}=30 Vdc, V_{FLOAT}=29 Vdc), as originally configured by Energia Total.

The C40 controller had a provision for either manual or automatic "battery equalization." In this process, the battery was held at a voltage 2 Vdc above the V_{BULK} setpoint for a period of 2 hours. As supplied, the C40 was set for a manual equalization process. However, it should be noted that the equalization process is likely to result in a battery voltage (30+2=32 Vdc) which exceeds the upper input voltage (31.0 Vdc) for the DR2424 inverter. As a result, battery equalization could only be performed when the inverter was shut down, or if the V_{BULK} setpoint was reduced to less than 29 Vdc.

The C40 also had "over temperature protection" circuitry, which reduced its output if the ambient temperature exceeded 40°C. For operation in the summer, the air temperature inside the enclosure containing the inverter and charge controller may exceed 40°C, and as a result system performance will be degraded. Additional venting of this enclosure may be needed in the summer.

The FireFly™ 600 was also equipped with a "Trace Meter" for monitoring the status of the battery [5]. The Trace Meter had an LED display and provided six monitoring features: state-of-charge (percent of capacity), battery voltage, battery current, amp-hours removed, days since full SOC, cumulative amp-hours, recharge indicator, low voltage indicator, full charge indicator. This device was not evaluated in detail during our system evaluation.

Table 1. FireFly 600 Photovoltaic System Component Description, Ratings, Setpoints

Component	Manufacturer	Model	Rating	V_{LVD}	V_{HVD}	V_{LVR}	V_{BULK}	V_{FLOAT}
Module	BP Solar	BP275	75Wp at SRC					
Array	BP Solar	8 – BP275	600Wp at SRC					
Battery	Nationwide	Deep Cycle	6V, 220Ah @ C/20					
Battery Bank	Nationwide	Deep Cycle	24V, 440Ah @ C/20, 10.5kWh					
Inverter	Trace Engr.	DR2424	120Vac, 2400 VA, 94 % max	21.6	31	24.9		
Charge Control	Trace Engr.	C40	24V, 40A				30	29
Battery Status	Trace Engr.	TM500	V, A, Ah, SOC					

Notes: V_{LVD} is dynamic using "Over-Discharge Protection Control," value varies with discharge rate.
V_{LVR} is not specified for the DR2424 but was measured to be 24.9 Vdc.
Battery temperature compensation provision adjusts these values by -0.06 V/°C. Battery equalization charging feature (manual or automatic) raises V_{BULK} value by 2 Vdc for 2 hours.

ARRAY PERFORMANCE CHARACTERIZATION

The FireFly 600 photovoltaic array was tested outdoors during the period from 5/3/01 through 5/16/01. Our evaluation provided:

1. Electrical performance at the ASTM Standard Reporting Condition,
2. Calculated annual and monthly energy production potential for the PV array,
3. Temperature coefficients for I_{sc}, I_{mp}, V_{oc}, V_{mp}, and P_{mp},
4. Solar spectral (absolute air mass, AM_a) influence on I_{sc} for clear sky conditions,
5. Solar angle-of-incidence influence on I_{sc} for clear sky conditions,
6. Performance coefficients and model appropriate for other operating conditions,
7. Relationship for operating temperature vs. irradiance, ambient temperature, and wind speed,
8. Array and junction box temperature characterization using infrared (IR) imaging.

Figure 2. Photo of FireFly 600 photovoltaic array with eight BP Solar, BP275, 75-W crystalline silicon photovoltaic modules.

Performance at Standard Reporting Conditions

The array on the FireFly 600 system tested was composed of eight BP Solar BP275 crystalline silicon modules, as shown in Figure 2. Each module-string had two modules connected in series, and there were four parallel module-strings. The serial numbers for the eight modules in the array were the following: 9201015I, 9201295I, 9201589I, 9201503I, 9200996I, 9201410I, 9327154U, and 9201429I. Each of the 36 crystalline silicon cells in the module was approximately 150-cm^2 in area.

All electrical performance testing was done with the array pointed south and oriented at a latitude tilt-angle (35±2 degrees). Electrical connection to the array was made directly to the array wiring inside the array disconnect box ("dc combiner box"). The array was washed prior to performance testing. The array was tested in a manner consistent with ASTM procedures [6]. The instrument used for plane-of-array solar irradiance measurements was a secondary standard Kipp & Zonen CM21 (s/n 990628) thermopile pyranometer calibrated as a function of solar angle-of-incidence (Less than ±2% calibration uncertainty at normal incidence and less than ±3.5% uncertainty for all solar angles-of-incidence less than 60 degrees). Current-voltage (I-V) curves were measured at approximately 30-second intervals over

several hours during clear sky conditions on multiple days. The array was held at the maximum-power condition between scans. About 2600 I-V scans were recorded on three different days under clear sky conditions. The array's I_{sc} at the ASTM Standard Reporting Condition (SRC) was determined at the time of day corresponding to AM_a=1.5 and was normalized to an irradiance level of 1000 W/m^2. In Albuquerque at an AM_a=1.5 clear sky condition, the solar spectrum is very similar to the ASTM standard spectrum which minimizes the need for a spectral correction (<0.5% correction required). In order to characterize array performance on overcast days, an additional 2700 I-V scans were recorded on three days with intermittent overcast conditions. Typical I-V and power-voltage (P-V) measurements at different irradiance levels during clear conditions are shown in Figure 3a and 3b.

Table 2 gives the performance parameters for the array at the ASTM Standard Reporting Condition along with our estimated uncertainty for each parameter (95% confidence limits in terms of percent of value). The efficiency indicated was based on the sum of the individual module areas. The measured performance was about 6% below the 600-W_p rating derived from individual module nameplate values. This discrepancy could be due to module mismatch, wiring losses, resistive terminations in junction boxes, incorrect module nameplate ratings, or measurement error. The measured performance at a higher cell temperature of 50°C is also given in the table.

Table 2. Performance at ASTM Standard Reporting Conditions (1000 W/m^2, AM_a=1.5, 25°C)

Ser. No.	Area (m^2)	PSEL#	I_{sc} (A)	V_{oc} (V)	I_{mp} (A)	V_{mp} (V)	FF	P_{mp} (W)	Eff (%)
BP275 Array (2 series x 4 parallel)	5.04	1865	18.30	43.15	16.61	33.95	.714	563.8	11.2
		95% CL=	2.5%	1.0%	2.6%	1.1%	1.0%	2.9%	3.0%
For T = 50C →			18.46	38.83	16.48	29.45	.677	485.2	9.6

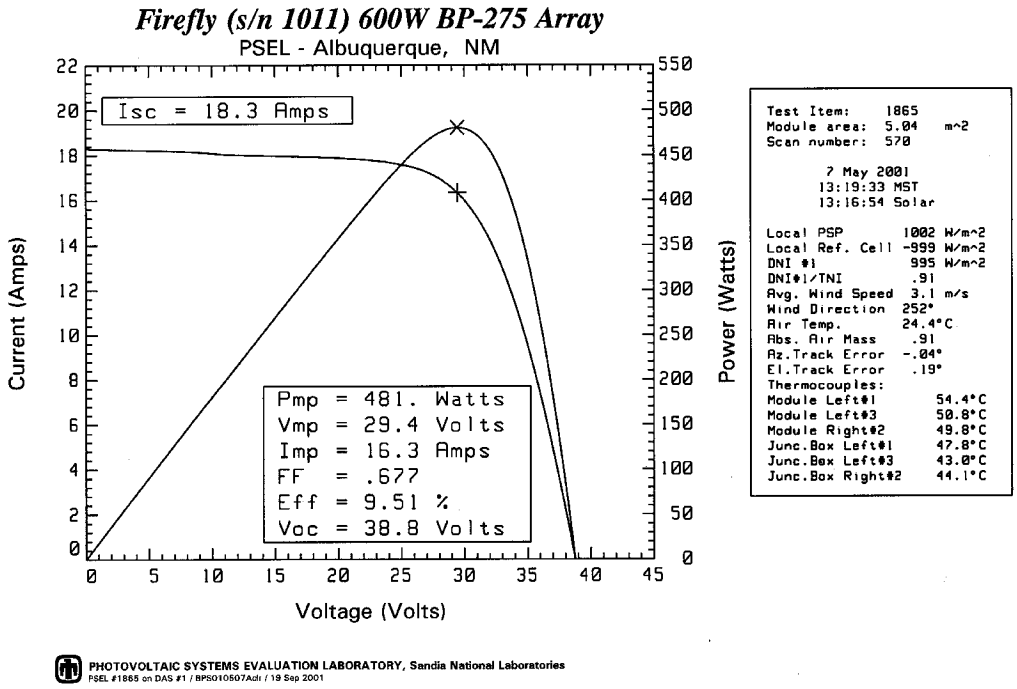

Figure 3a. A typical current-voltage (I-V) curve measurement at 1002 W/m^2 solar irradiance and 52°C module temperature for eight BP Solar BP275 c-Si modules, array pointed south and oriented at a latitude tilt-angle (35 deg).

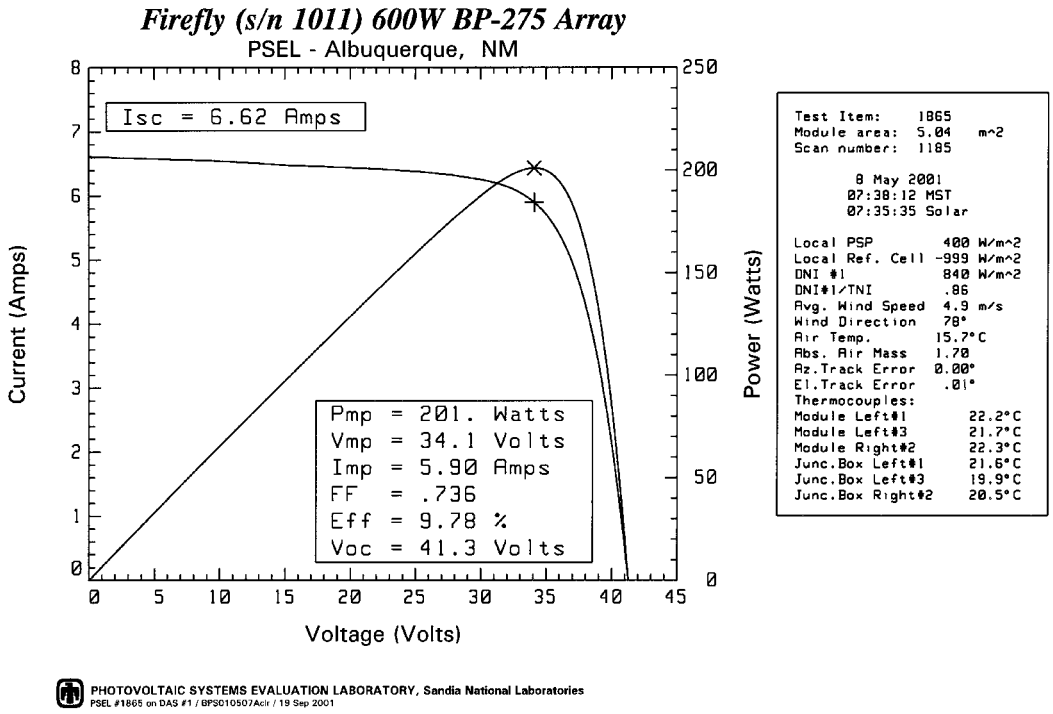

Figure 3b: Typical current-voltage (I-V) curve measurement at 400 W/m^2 solar irradiance and 22°C module temperature for eight BP Solar BP275 c-Si modules, array pointed south and oriented at a latitude tilt-angle (35 deg).

Energy Available from PV Array

The electrical, thermal, and optical performance characteristics measured for the array were used in Sandia's array performance model (PVMOD) to calculate an accurate estimate for the maximum energy available from the photovoltaic array. Assuming that the array was oriented at one of four different tilt-angles and facing south, the performance model was coupled with hourly-average solar resource and meteorological data for Albuquerque to calculate daily average energy production by month. The hourly solar resource and weather data used were "typical meteorological year (TMY)" data from the National Solar Radiation Database (NSRDB) [7]. Figure 4 shows the calculated solar resource for the array tilt-angles considered; 35, 50, 60, and 20 degrees. Figures 5 and 6 show the results of this analysis. The daily average energy values shown in the figures represent the total direct current (dc) energy available from the array in units of either kWh/d or Ah/d. The values given in both figures assume that the array operates at its maximum-power voltage (V_{mp}) throughout the day. Therefore, the daily energy available shown in Figure 6, in units of Ah/d, is not the energy available at a nominal 24-V battery voltage but rather assumes that the system is capable of continuously operating at the array's V_{mp}. How well the energy available from the array is actually utilized by the photovoltaic system depends strongly on the remaining components in the system (charge controller, batteries, inverter, load, etc.). Therefore, these energy values provide an upper limit for the dc energy available from the photovoltaic system.

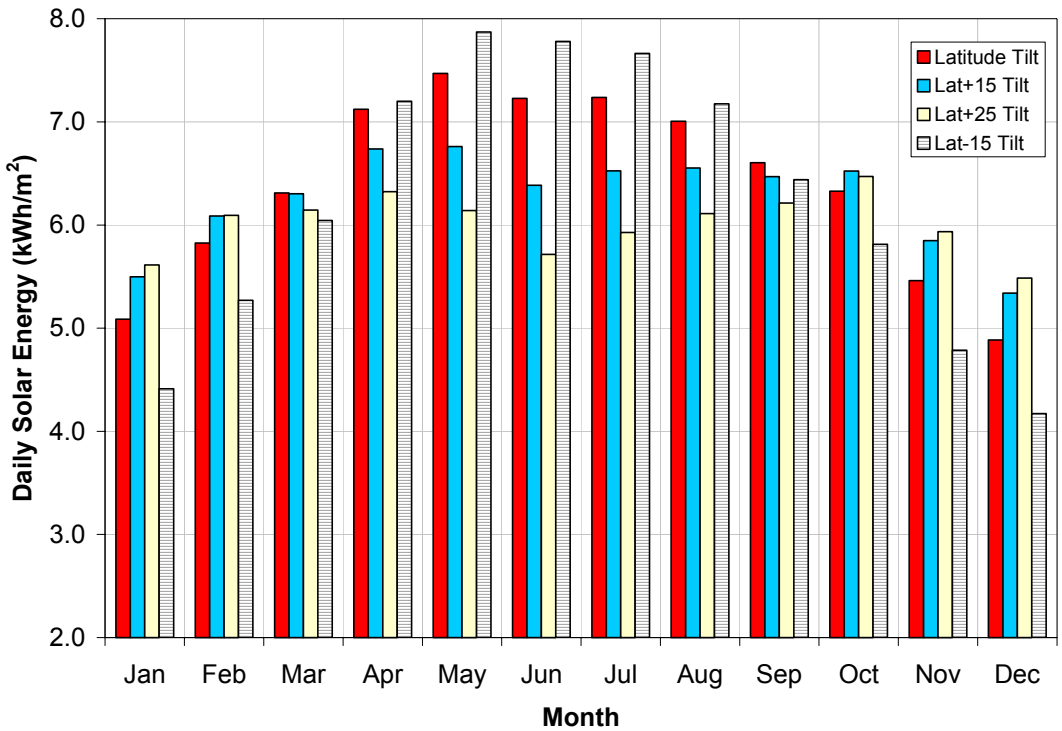

Figure 4. Calculated daily-average solar resource (kWh/m^2) available to the FireFly™ 600 array when located in Albuquerque, pointed south, and oriented at different array tilt-angles. (TMY2 solar resource from NSRDB)

It can be seen from Figures 5 and 6 that the energy available from the array is seasonal, with December and January being the worst months. For this reason, off-grid systems oriented at a latitude tilt-angle are typically designed and sized to power a specified load for the worst case conditions in these months. The

FireFly™ 600 array was also designed with a provision for adjusting the tilt-angle of the array. By increasing the tilt angle, this provision can be used to increase the energy available from the array in the winter months. Similarly, energy available can also be increased in the summer months by decreasing the tilt angle from the typical latitude tilt angle. Figures 5 and 6 show the effect on energy production of seasonal adjustments of the array tilt angle. For instance, a two-orientation strategy could be used during the year instead of a single orientation at a latitude tilt-angle. In mid-September, the array tilt could be increased by 15 to 25 degrees from latitude tilt, and then in mid-March the tilt could be 15 degrees less than latitude tilt. This scheme would increase energy available from the array by 8 to 11% in the worst case months of December and January. Similarly, the energy available in the summer months, May through August, would also increase by about 5% relative to a latitude-tilt orientation.

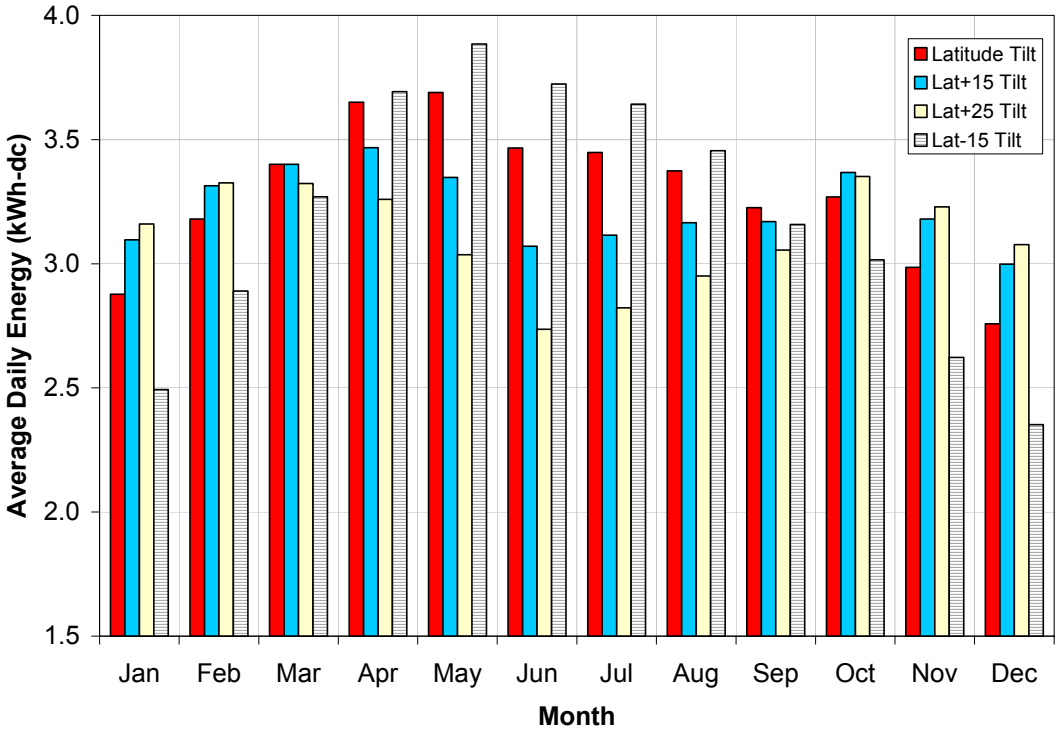

Figure 5. Calculated dc energy available (kWh/d) from the FireFly™ 600 array of BP Solar BP275 modules when located in Albuquerque, pointed south, and oriented at different array tilt-angles.

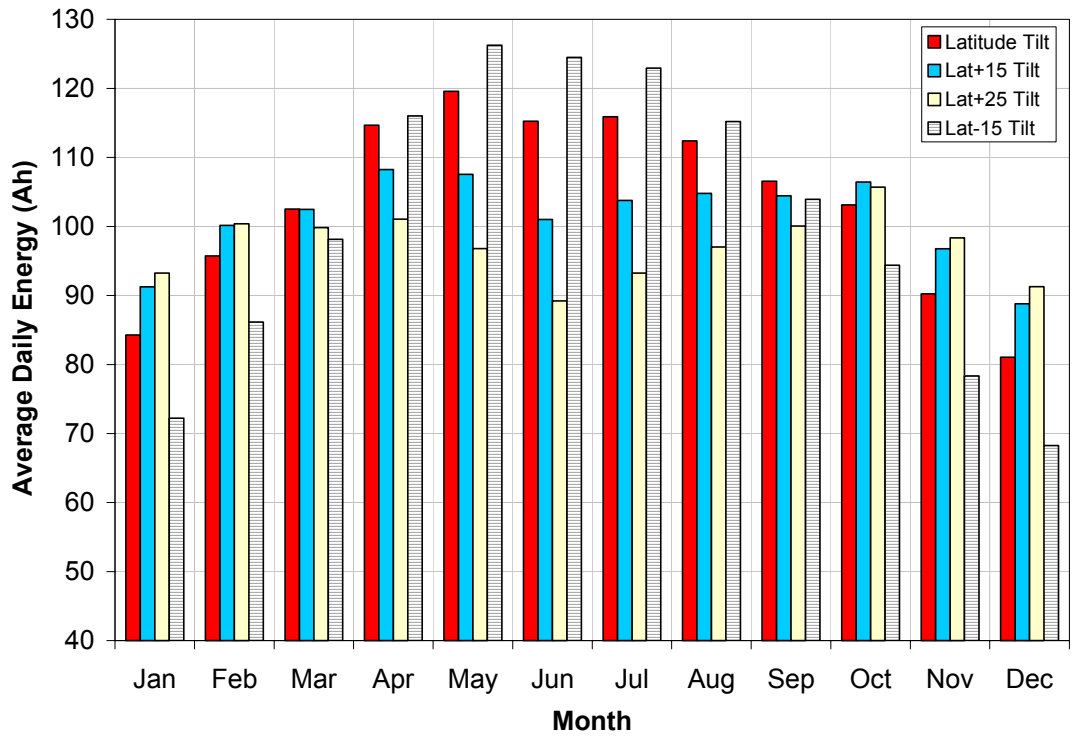

Figure 6. Calculated daily dc amp-hours available from the FireFly™ 600 array of BP Solar BP275 modules when located in Albuquerque, pointed south, and oriented at different array tilt-angles.

Matching the Array with PCS Components (System Optimization)

The PVMOD performance model was also used to investigate how well the performance characteristics of the array matched the operational characteristics of the power conditioning system (charge controller, battery, inverter). The model provided estimates for the energy available from the array on an hourly basis for the entire year. These hourly energy values were used to generate scatter plots of array performance, and they were sorted and accumulated relative to individual array performance parameters, such as maximum-power voltage (V_{mp}) and open-circuit voltage (V_{oc}) providing additional system design insight.

Figure 7a shows a scatter plot of the calculated hourly V_{mp} values plotted as a function of the associated array maximum-power, P_{mp}. Thus, Figure 7a provides a visual assessment of how well the performance characteristics of the array match the actual operating conditions (voltages) dictated by the battery and power conditioning system. In this case, the array V_{mp} is well above the operating voltage of the system for the majority of the year, and as a result a significant percentage (~15%) of the energy available from the array cannot be used by the system. Thus, the overall system efficiency could be improved if the array voltage was about 5 to 7 Vdc lower than the current design.

Figure 7a also gives a rough sense of the seasonal influence of temperature on V_{mp}, the upper edge of the scatter of points generally occurs in the winter months when array temperatures are lower, and the lower edge of the scatter occurs in the summer. More temperate climates, such as in San Diego, would result in a tighter band of V_{mp} values over the year.

The cumulative distribution curve shown in Figure 7a indicates the fraction of the annual energy available as a function of array P_{mp}. For example, this figure indicates that about 85% of the annual energy available from the array occurs at a power level less than 0.5 kW. This is important to know in optimizing the system performance because the efficiency of the Trace DR2424 inverter drops significantly for power levels less than 0.5 kW. The peak inverter efficiency occurs for power levels between 0.5 and 1.0 kW. Thus, a higher power array would be a better match to the inverter efficiency characteristics, resulting in a higher system efficiency. (See Appendix A.)

Figure 7b illustrates the same cumulative array energy information as a function of the array V_{mp} and V_{oc}. It can be seen from this chart that if it were possible to lower the array V_{mp} by about 7 Vdc then the majority of the energy distribution curve would be contained within the battery voltage window.

The magnitude of energy losses associated with mismatched components can also be site dependent. In order to illustrate this site dependence, annual performance analyses were conducted for a hotter climate (Phoenix, AZ) and a colder climate (Alamosa, Colorado). Figures 8a and 8b show scatter plots of the calculated hourly V_{mp} values for the two different sites. It can be seen in these figures that the system "voltage window" is a better match in Phoenix than Albuquerque, but worse in Alamosa. However, for all three sites, the energy available from the array is not being used as effectively as it could be.

There are couple possible alternatives for improving (optimizing) the performance of the FireFly™ 600 system. One alternative would be to use a different array design with an annual distribution of V_{mp} that better fits the voltage window defined by the Nationwide batteries. An array design with both lower voltage and a higher power rating would reduce energy loss in charging the batteries and also increase the inverter efficiency. Incorporation of a charge controller with an array maximum-power-point-tracking (MPPT) capability would further improve the system efficiency, and minimize the need for an array redesign.

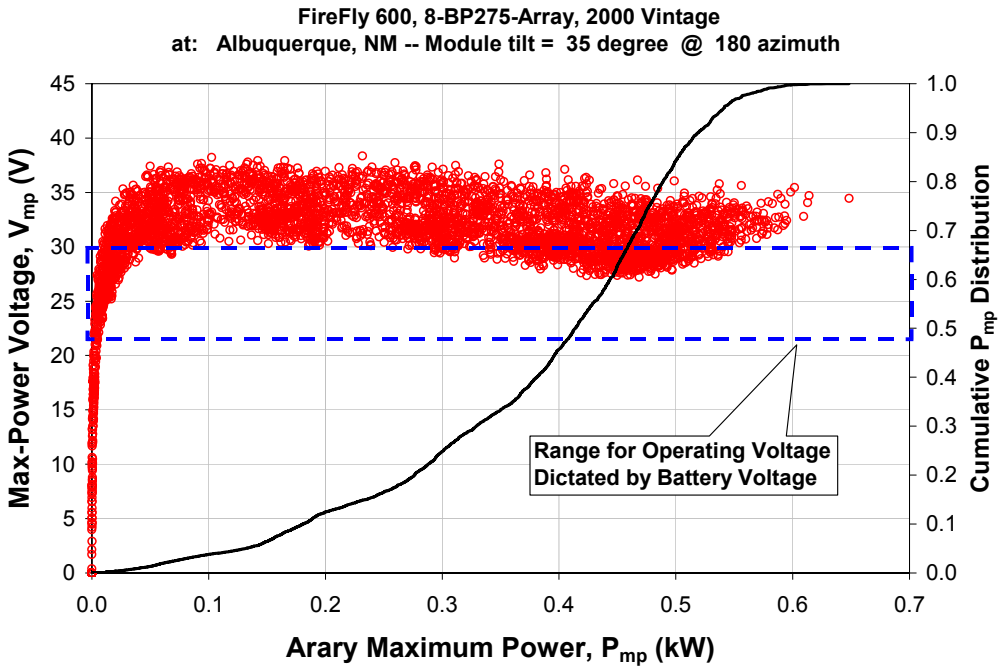

Figure 7a. Scatter plot of hourly values for array V_{mp} as a function of array P_{mp} for year long operation in Albuquerque, with array oriented at a latitude tilt-angle. Array operating voltage will be constrained by battery voltage within the range shown (21.6 to 30 Vdc). The cumulative distribution curve indicates the fraction of the annual energy available as a function of array P_{mp}.

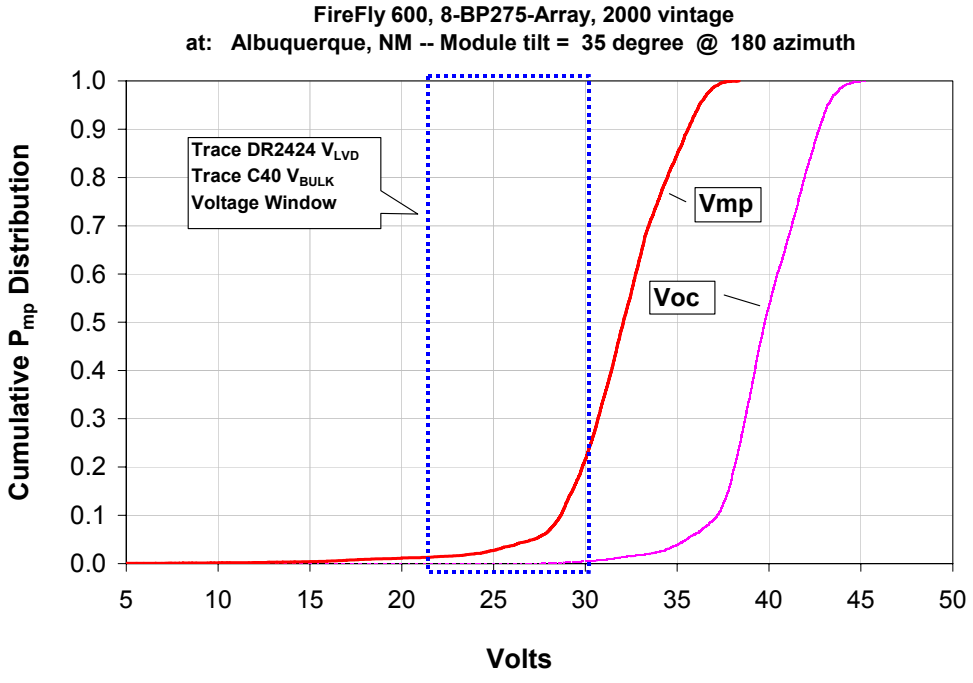

Figure 7b. Cumulative distribution of annual energy available from FireFly 600 array related to the array's maximum-power voltage (V_{mp}) and open-circuit voltage (V_{oc}). The system "voltage window" defining the range for actual operating voltages is also shown. (Albuquerque, NM)

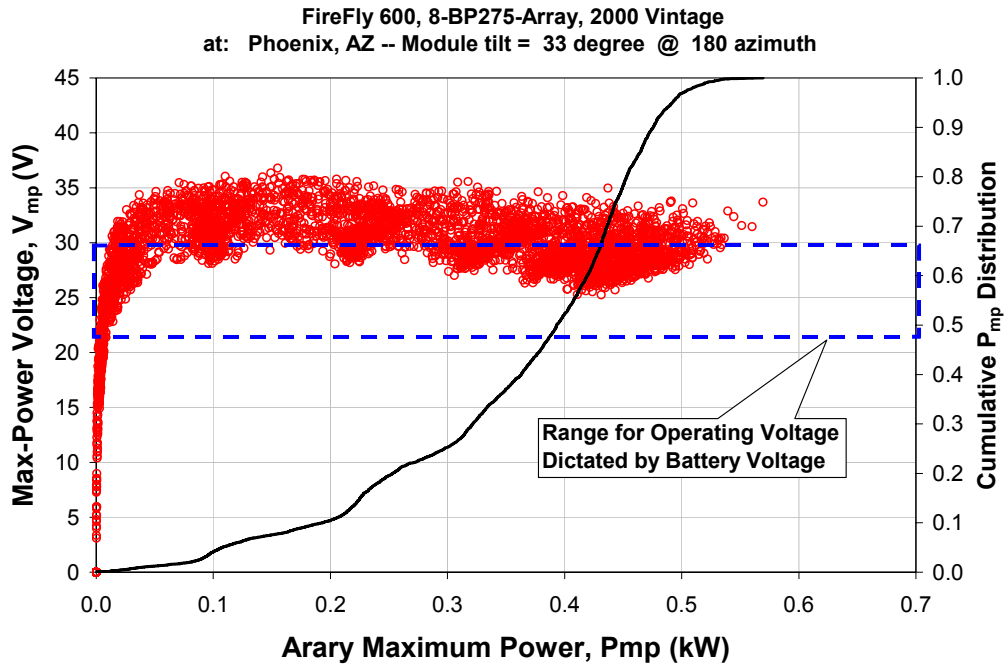

Figure 8a. Scatter plot of hourly values for array V_{mp} as a function of array P_{mp} for year long operation, with array oriented at a latitude tilt-angle. The system "voltage window" defining the range for actual operating voltages is also shown. (Phoenix, AZ)

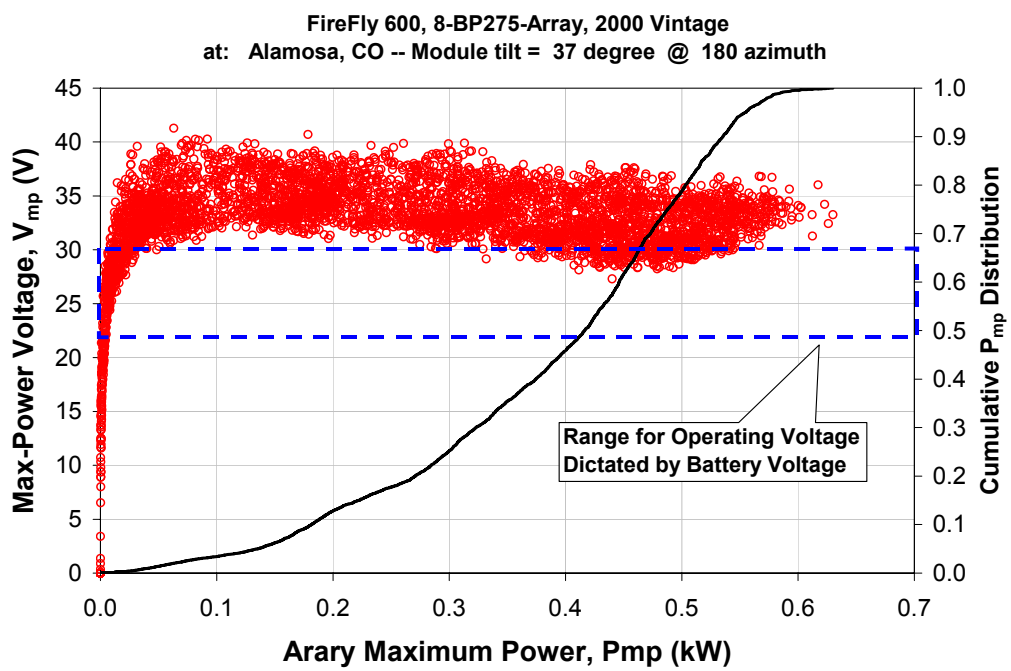

Figure 8b. Scatter plot of hourly values for array V_{mp} as a function of array P_{mp} for year long operation, with array oriented at a latitude tilt-angle. The system "voltage window" defining the range for actual operating voltages is also shown. (Alamosa, CO)

Temperature Coefficients

Temperature coefficients used for the array were based on the average values measured under actual operating conditions for two different BP275 modules, using a procedure described elsewhere [8]. To measure the coefficients, the module was shaded until it cooled to near ambient temperature. Then the cover was quickly removed and I-V scans were recorded at 20-second intervals for about 30 minutes as the array heated up to operating temperature. The three thermocouples used to measure back surface temperature were small gauge (0.010-in diameter) thermocouples attached to the back surface of three different modules with Tefzel™ patches. The thermocouples provided an "average" back-surface temperature. Measurements were performed under clear sky conditions with calm wind speed (< 3 m/s) in order to achieve spatially uniform array temperatures. Linear regression analysis was used to obtain the temperature coefficients for I_{sc}, I_{mp}, V_{oc}, and V_{mp} at an irradiance level of 1000 W/m^2. The temperature coefficient for P_{mp} was calculated using the temperature coefficients for I_{mp} and V_{mp}. Table 3 gives the temperature coefficients for the array, along with an estimate of the 95% confidence limits.

Table 3. Temperature Coefficients for the FireFly™ 600 Array (BP275 Modules)

Ser. No.	PSEL#	dI_{sc}/dT (A/°C)	dI_{mp}/dT (A/°C)	dV_{oc}/dT (V/°C)	dV_{mp}/dT (V/°C)	dP_{mp}/dT (W/°C)	dP_{mp}/dT (%/°C)
BP275 Array (2 series x 4 parallel)	1865	.006	-.005	-.173	-.180	-3.17	-.56
	±95%CL=	.0008	.0008	.015	.015	.50	.08

Solar Spectral Influence

Previous testing of BP Solar BP275 modules quantified the influence of a changing solar spectrum on the performance (short-circuit current). An empirical function, $f_1(AM_a)$, was derived that related the solar spectral influence on I_{sc} to absolute air mass (AM_a), for the range $1<AM_a<8$. This function was used in array performance modeling and outdoor module testing as a means for compensating for time-of-day dependent changes in the solar spectrum. Note that, on an annual basis, the majority (>95%) of the solar energy resource occurs for air mass conditions less than 3.5.

The I_{sc} relationship to air mass was determined using I-V measurements recorded over a range of sun elevation angles [9]. The module was mounted on a solar tracker, so angle-of-incidence optical effects were not present in the measurements, only the influence of solar spectrum. A Kipp & Zonen CM21 pyranometer mounted in the plane of the module was used to normalize the measured I_{sc} values to a constant irradiance. The pyranometer had a thermopile (black body) sensor, thus providing an irradiance measurement that was independent of solar spectrum. The $f_1(AM_a)$ relationship was obtained by translating measured I_{sc} values to a common temperature, normalizing them to an irradiance of 1000 W/m^2 based on the thermopile pyranometer measurement, and then dividing by the I_{sc} value at the AM_a=1.5 condition. Figure 9 illustrates the typical relationship obtained for the BP Solar BP275 module.

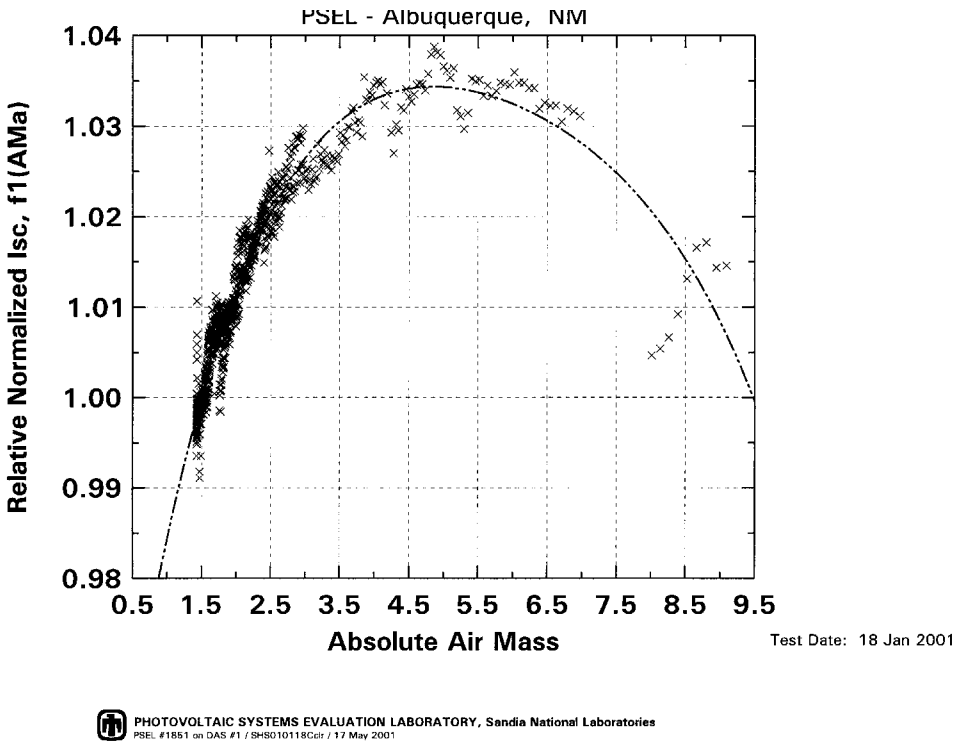

Figure 9. Empirically determined relationship for BP Solar BP275 module showing solar spectral influence on module short-circuit current (I_{sc}), related to absolute air mass.

Solar Angle-of-Incidence

A module's response to the direct (beam) component of solar irradiance is influenced both by the cosine of the solar angle-of-incidence, AOI, and by the optical properties of its front surface. The 'cosine effect' reduces the module output as AOI increases simply because the projected area of the module as seen from the sun is reduced by the factor cos(AOI). For example, at AOI=60 degrees the beam irradiance is ½ that at normal incidence (AOI=0). In addition, the optical reflectance loss from a glass surface increases significantly for AOI > 50 degrees. The influence of this optical property was previously measured for a variety of modules with a glass front surface, and resulted in a generic empirical function, f_2(AOI), that accounts for the influence of optical losses on module I_{sc} [9]. The results measured for the FireFly™ 600 array on multiple days are shown in Figure 10, along with the generic function for glass modules. This generic empirical relationship was used both in analyzing our outdoor performance data for the array and in the performance model used to calculate expected annual energy production.

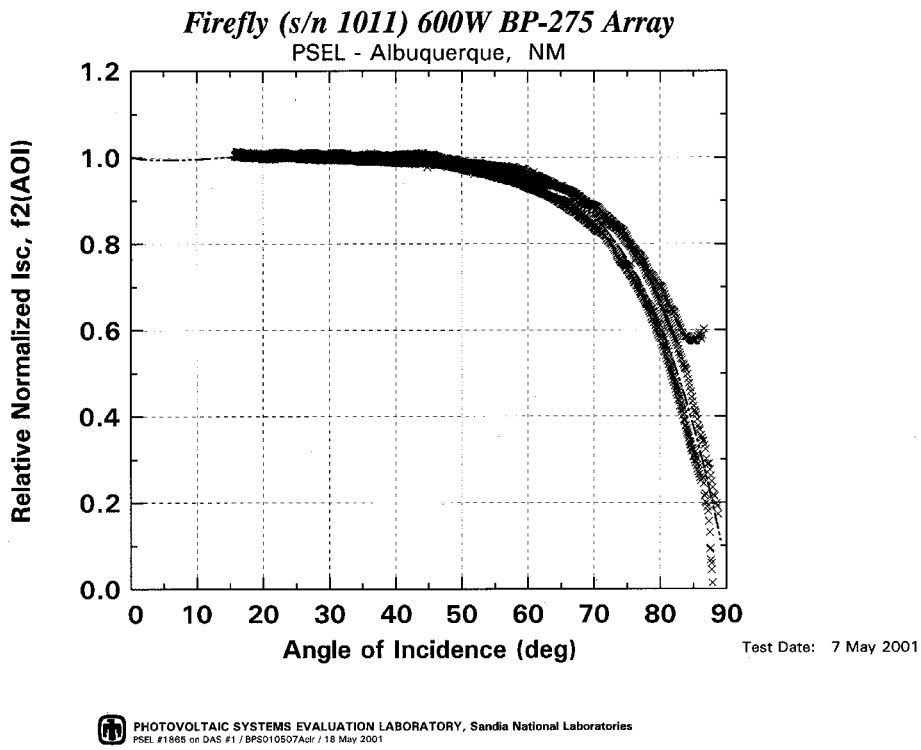

Figure 10. Empirically determined relationship showing solar angle-of-incidence influence on short-circuit current (I_{sc}) for the FireFly™ 600 array. A generic curve fit for modules with glass front surfaces is also shown.

Array Performance at Other Operating Conditions

After quantifying the relative influences of irradiance, temperature coefficients, solar spectrum, and solar angle-of-incidence, it is possible, using an appropriate performance model, to establish module performance parameters for a wide range of operating conditions, including cloudy or overcast situations with very low irradiance levels. The performance model used by Sandia for both modules and arrays has been documented elsewhere [10, 11, 12]. The Sandia performance model is now also incorporated in PV system design software such as PV-DesignPro by Maui Solar Software Corporation [13].

Of particular importance to PV system designers are the open-circuit and maximum-power voltages as a function of irradiance and temperature. Our test procedures capitalize on performance information available during overcast conditions to fully determine this voltage behavior. Figure 11 illustrates the measured V_{oc} and V_{mp} for the array, as a function of the effective irradiance in suns. Voltage characteristics were determined for irradiance levels from less than 100 W/m^2 to over 1200 W/m^2. The results from over 5300 I-V measurements made during both clear and cloudy conditions are illustrated, including a large number of scans (~ 1000) recorded under cloudy or overcast conditions. All measured values shown in the figure were translated to a common temperature of 50°C. The associated performance model was used to calculate the corresponding curves for V_{oc} and V_{mp} at the reference 25°C operating temperature, shown as dashed lines in the figure. It can be seen that the array V_{mp} behaves somewhat differently from Voc in that it is effectively less dependent on irradiance.

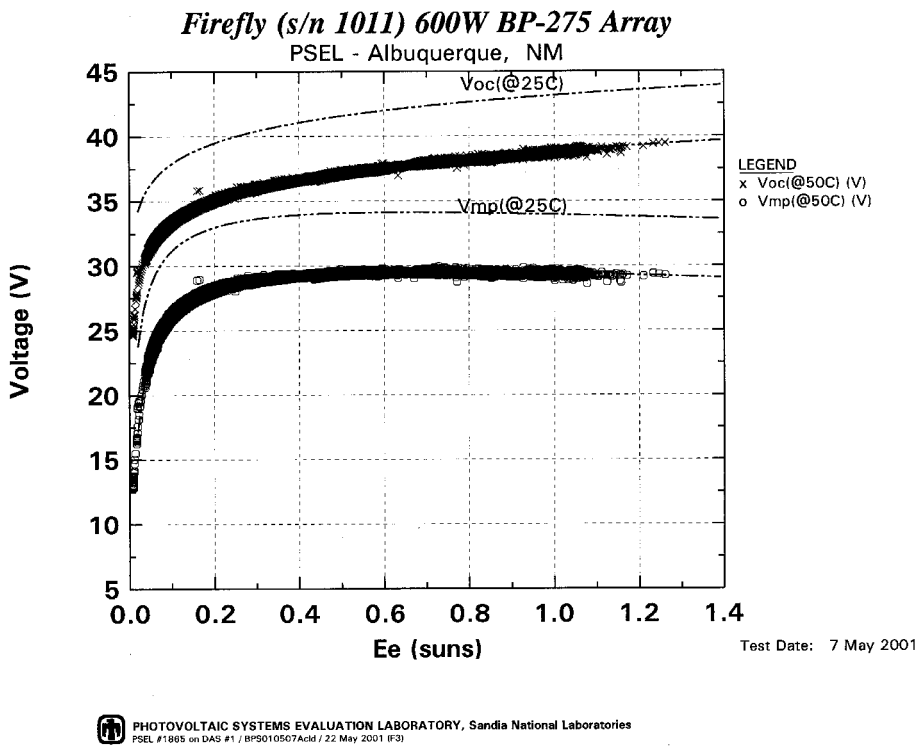

Figure 11. Combined data from both clear and cloudy conditions providing relationship for V_{oc} and V_{mp} versus solar irradiance and temperature for array of BP Solar BP275 modules.

Operating Temperature versus Environmental Conditions

A thermal model relating module operating temperature to environmental conditions (irradiance, ambient temperature, wind speed) is required when calculating expected annual energy production based on hourly data in the National Solar Radiation Database (NSRDB). Figure 12 illustrates measured data recorded at Sandia for the FireFly™ 600 array over a wide range or irradiance, ambient temperature, wind speed, and wind direction. The data illustrated were recorded during predominantly clear sky conditions over a period of several days. Thus, the array was in "quasi" thermal equilibrium for the data illustrated. A linear fit to the measured data provided the coefficients (a = slope, b = intercept) used in Sandia's simple yet effective thermal model, Equations 1 and 2. Variable irradiance due to intermittent clouds, thermal heat capacitance of the modules (response time), and variable wind direction result in random scatter either side of this linear model. Fortunately, these complex influences need not be addressed specifically in the thermal model because they tend to "average out" on a daily, monthly, or annual basis. For the FireFly™ 600 array, the coefficients a = -0.085 and b = -3.56 were appropriate. For stable sunshine conditions, this model should provide estimates of back surface module temperature within about ±5°C, which is adequate for most system design purposes. Intermittent clouds produce random scatter either side of the modeled temperature. This random behavior effectively averages out on a daily, monthly, or annual basis.

$$T_m = E \cdot e^{a \cdot WS + b} + T_a \tag{1}$$

$$T_c = T_m + c \cdot \frac{E}{E_o} \tag{2}$$

Where:
T_m = Back-surface module temperature, °C
T_c = Cell temperature, °C
T_a = Ambient temperature, °C
E = Solar irradiance on module, W/m^2
E_o = Reference irradiance = 1000 W/m^2
WS = Wind speed, m/s
a, b = Empirically determined constants, module and mounting method specific
c = Temperature difference (°C) between module back-surface and internal cell for reference irradiance. This difference is typically 2 to 3 °C for flat-plate PV modules at 1000 W/m^2.

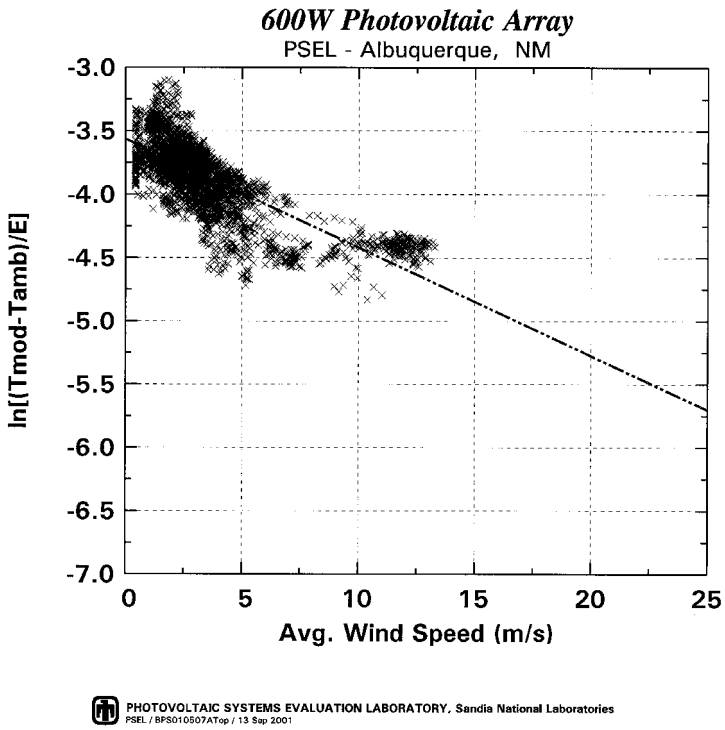

Figure 12. Empirically determined relationship between module back-surface temperature (T_{mod}) and irradiance (E), ambient temperature (T_{amb}), and wind speed. Slope (a = -.085) and intercept (b = -3.56) are used in thermal model.

Additional thermal analyses were also performed on the FireFly™ 600 array. Thermal infrared (IR) imaging was used to illustrate the temperature distribution across the array during operation on a sunny day, with wind speed less than 3 m/s. Figure 13 shows two typical IR images. Cell temperatures were relatively uniform ±3°C, except for the area immediately above the junction boxes. Cells located over the BP Solar junction boxes were about 5°C hotter than the average cell temperature.

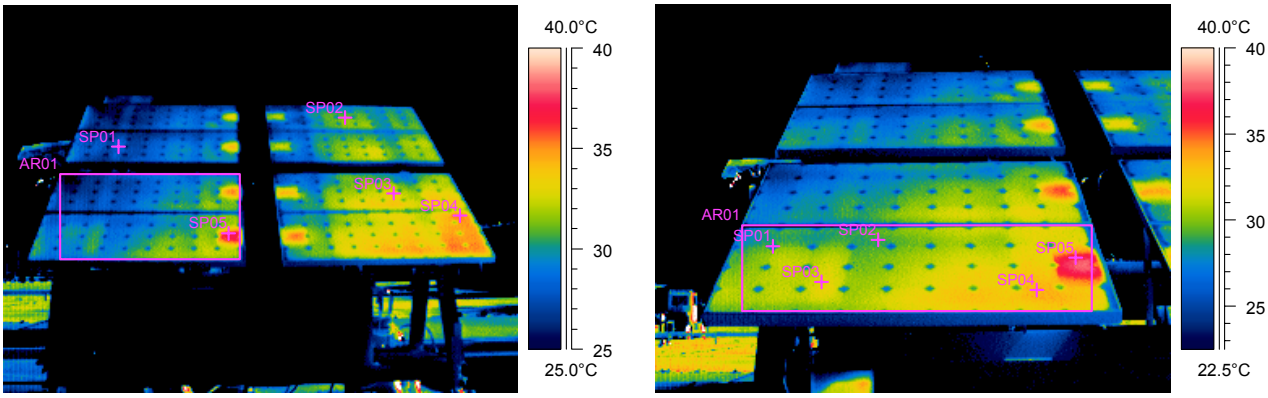

Figure 13. Temperature distribution in FireFly™ 600 array during typical operating conditions on sunny day with wind speed less than 3 m/s.

Compliance with the National Electrical Code (NEC) requires the use of wiring insulation material with a temperature rating consistent with the maximum expected operating temperature [14]. Using the same procedure previously illustrated for back surface module temperature, the temperature of wiring insulation inside the BP Solar junction boxes was measured over a wide range of operating conditions. Small gauge thermocouples were attached directly to wiring insulation about 1 cm from the terminal lugs, in three different junction boxes, as illustrated in Figure 14. The measured insulation temperatures were analyzed using the same model used for module temperature in order to relate insulation temperature to solar irradiance, ambient temperature, and wind speed. A linear fit to these data provided coefficients for the previous model in Equation 1; a = -0.118 and b = -3.68. Using this model, the wiring insulation temperature was calculated for worst case operating conditions. For instance, an insulation temperature of 75°C can be reached in the extreme condition with E = 1200 W/m^2, T_{amb} = 45°C (113 °F), and WS = 0 m/s. Thus, for sunny sites with high ambient temperatures, the NEC will require module wiring with a temperature rating above 75°C.

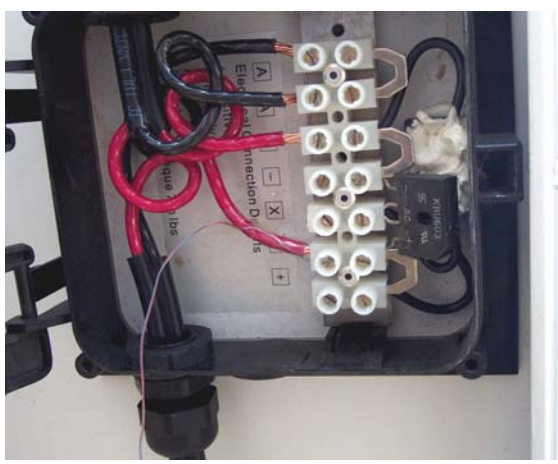

Figure 14. Photo of BP275 module junction box showing wiring, bypass diode, and thermocouple attached to lower wire near terminal lug.

SYSTEM PERFORMANCE TESTING

The goal of our system performance testing was to exercise the system as completely as possible within a relatively short period of time (30 days), without exceeding system design parameters. The test procedure was designed to evaluate the functionality and safety of all system features and to test the performance of the system during 'normal' as well as a 'worst case' operating condition. The 'worst case' operating condition examined the situation where batteries were discharged fully to the low-voltage-disconnect (V_{LVD}) setpoint, and then the system was required to recover to a full state-of-charge (SOC) while still powering the design load. It is important for off-grid PV systems to recharge the battery bank as quickly as possible from a V_{LVD} condition in order to minimize battery damage (capacity loss), as well as to continuously and reliably power the system load. A unique feature of the outdoor test procedure was that it accounted for the unavoidable variation in daily solar radiation. Programmable hardware was used to scale the duration of the nightly ac load in proportion to the preceding day's solar resource.

The system test procedure consisted of eight major parts: (1) installation and inspection of system, (2) calculation of appropriate ac load to use during test sequence, (3) an initial battery test to verify manufacturer's capacity specification and identify appropriate charge control setpoints, (4) multiple days of "cycling" during normal operation, (5) intentional battery discharge to the system low-voltage-disconnect (V_{LVD}) establishing a worst case operating condition and providing a measurement of "usable" battery capacity, (6) multiple day "recovery test" from V_{LVD} including several days of cycling after battery regulation voltage was reached, (7) a second discharge to V_{LVD} to retest "usable" battery capacity, and (8) a second recovery test from V_{LVD} without an ac load applied. Figure 16 shows a photo during the system testing procedure.

Figure 16. FireFly™ 600 photovoltaic off-grid system during performance testing at Sandia.

System Energy Losses

The subtlety and technical complexity of off-grid photovoltaic systems can be put in perspective by appreciating both the magnitude and the value of ac energy produced. On average, small off-grid systems

like the FireFly™ 600 can only produce enough ac energy to power a 100-W light bulb 24 hours per day. So, for typical American homeowners, this total daily energy production is the equivalent of inadvertently leaving the porch light on for 24 hours. Nonetheless, if this quantity of energy is budgeted wisely, it can provide a dramatic impact on the lifestyle of families in remote areas currently without electricity. Using small energy-efficient ac loads along with wisely budgeted energy usage, these systems are capable of powering some combination of lights, microwave, television, computer, and refrigerator. The technical challenge for system designers and engineers is in maximizing ac energy production, minimizing unnecessary losses in the system, designing for high reliability and simplicity, and minimizing life-cycle energy cost. Successful operation of off-grid systems also requires that the user fully understand the magnitude of energy available and the necessity of budgeting energy usage.

In order to understand the rationale used during our test procedure, a brief discussion of the energy balance associated with the entire system is helpful. Figure 17 illustrates the basic components of an off-grid photovoltaic system and the energy flow through them. Each component has energy flowing into it, energy flowing out of it along the desired path, as well as undesirable energy losses. The term "array utilization" is often used to describe the ratio of the dc energy actually provided by the system divided by the total energy available from the PV array. Systems should be designed to maximize the array utilization. Alternatively, the inverse of this ratio, the total dc energy available from the array divided by the energy required by the load, called the "array to load ratio" (A:L), is often used when designing off-grid photovoltaic systems.

Assuming that the energy requirement for the load is relatively constant over the year, then the system is typically designed to ensure that sufficient energy is available to power the load in the worst-case situation, the months with the lowest solar resource (see Figure 4). A rule-of-thumb commonly used for designing systems with dc load is that the A:L ratio should be in the range from 1.3 to 1.6 during winter months in order to ensure that a dc load can be satisfied. The higher the A:L ratio, the higher the probability that there will be adequate energy available to power the load. The energy buffer provided by a high ratio is intended to compensate for non-ideal performance and/or energy losses associated with system components. In terms of array utilization, it is not uncommon in off-grid PV systems to have less than 65% of the energy available from the array actually delivered to the dc load, which is equivalent to saying that an A:L ratio of about 1.5 is needed to meet the energy requirement of the load.

The A:L ratio can also be calculated using an ac load as the divisor, which is more appropriate for the FireFly™ 600 system tested. When ac loads are considered, the typical range for the A:L ratio is 1.6 to 2.0 in order to account for the additional energy losses in the inverter.

The system test procedure developed at Sandia and applied to the FireFly™ 600 system provided a means for quantifying the performance of the complete system as well as individual system components. The performance and energy losses associated with system components were determined during actual operating conditions. Using daily energy measurements, a "daily efficiency" was determined for the array, charge controller, battery, inverter, and the overall system. These test results provided the information required for optimizing and improving the system design.

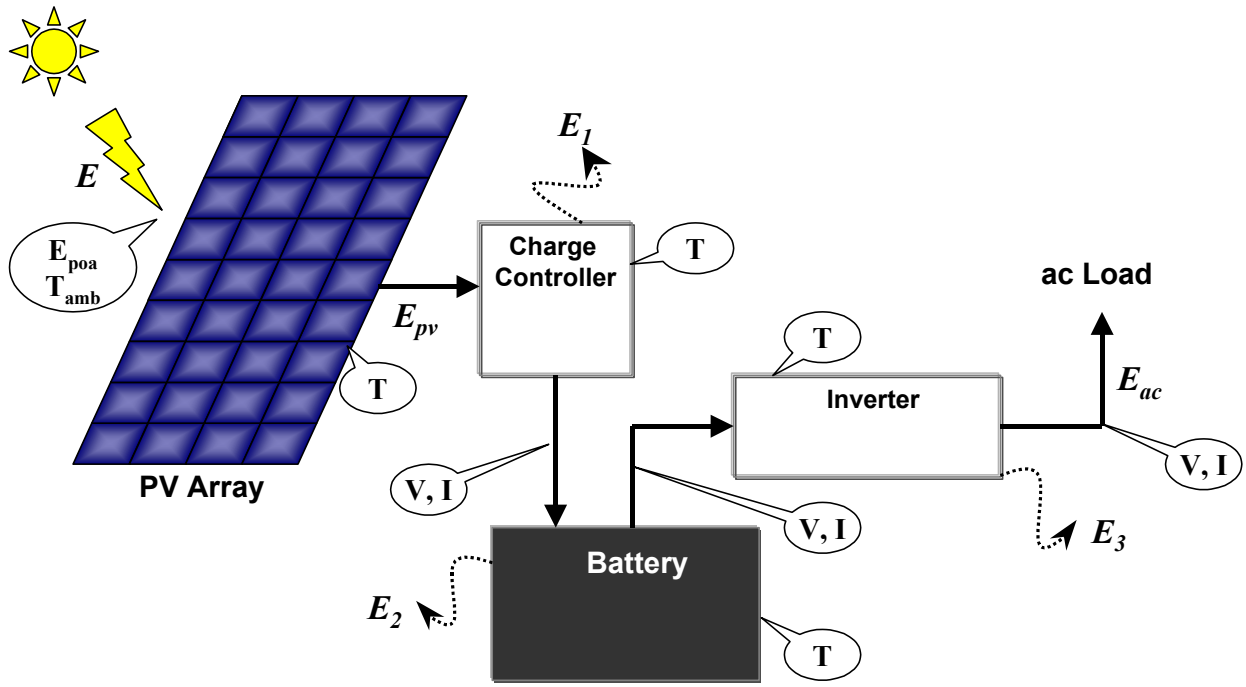

Figure 17. Schematic of an off-grid photovoltaic system indicating the flow of energy from the photovoltaic array to an ac load, including energy losses. Callout ovals indicate the measurements made during the system test procedure (irradiance, temperature, voltage, current).

Model for System and Component 'Daily' Efficiency

Analyzing energy flow on a daily basis is an ideal method for simplifying off-grid system test results, and for putting them in terms that are readily understandable for both the system designer and the system owner. The solar insolation on the array, energy available from the photovoltaic array, energy flow into and out of system components, as well as the ac energy delivered by the system can all be expressed in units of kWh/d. This approach makes it possible to assign a "daily efficiency" to each major component in the system in terms of the ratio of daily energy out of the component divided by the daily energy into the component. In addition, a daily efficiency can be determined for the overall system as the ratio of the daily ac energy provided divided by the daily dc energy available from the photovoltaic array. To be consistent with the format of commonly available solar resource information and to take into account seasonal influences on system performance, the approach can be expressed in terms of average daily efficiency for each month of the year. This approach is expressed in the Equations (3, 4).

$$E_{aci} = (E_{SUNi} \cdot A \cdot \eta_{PVi}) \cdot \eta_{MPPTi} \cdot \eta_{BATi} \cdot \eta_{INVi} \qquad (i = 1,12) \qquad (3)$$

or

$$E_{aci} = E_{PVi} \cdot \eta_{MPPTi} \cdot \eta_{BATi} \cdot \eta_{INVi} \qquad (i = 1,12)$$

and

$$\eta_{SYSi} = E_{aci} / E_{PVi}. \qquad (i = 1,12) \qquad (4)$$

Where:

E_{aci} = ac energy delivered by the system per day in month "i", (kWh/d,ac).
E_{SUNi} = solar energy available per day per square meter, (kWh/m^{2}d).
A = sum of the areas of all modules in the array, (m^2).

η_{PVi} = daily energy efficiency for the photovoltaic array calculated as the ratio of daily dc energy available from the array when operating at its maximum-power-point divided by the daily solar energy incident on the array.

η_{MPPTi} = daily energy efficiency for the charge controller calculated as the ratio of the daily dc energy out of the charge controller divided by the daily dc energy available from the array when operating at its maximum-power-point. This can be thought of as the maximum-power-point-tracking (MPPT) efficiency, and is influenced by the battery state-of-charge.

η_{BATi} = daily energy efficiency for the battery calculated as the ratio of the daily dc energy out of the battery divided by the daily dc energy delivered to the battery from the charge controller.

η_{INVi} = daily energy efficiency for the inverter calculated as the ratio of the daily ac energy from the inverter divided by the daily dc energy provided to the inverter.

E_{PVi} = daily dc energy available from the photovoltaic array when operating at its maximum-power-point continuously, (kWh/d).

η_{SYSi} = overall daily efficiency of the system calculated as the ratio of the daily ac energy provided divided by the daily dc energy available from the array when operating at its maximum-power-point.

It is important to recognize that the successful application of this performance testing and analysis procedure requires that the system is operated in a continuous and 'sustainable' mode for an extended period of time in order to isolate the efficiency of separate components. 'Sustainable' operation requires that the system is powering an ac load in a manner that can be maintained for many days without exceeding design limits. Otherwise, the daily energy efficiency concept can provide meaningless or unrealistic results. For instance, if for some reason the array provides no energy for an entire day then the daily charge-controller efficiency (η_{MPPTi}) becomes zero. Similarly, if no energy is provided from the charge-controller to the battery during the day, but energy is still extracted from the battery then the battery energy efficiency equation becomes meaningless. The 30-day test procedure documented in this report is ideal for this purpose because it compensates for daily variation in solar insolation by scaling the ac load applied thus providing operating conditions that are reasonably uniform from day to day.

Outline of System Test Procedure

The following steps and brief discussion are an attempt to outline the basic steps used during the characterization and experimental optimization of the FireFly 600 system.

Initial Preparations and Component Tests:

1) Install and position photovoltaic system in unobstructed area with array tilted at desired orientation, typically at a latitude tilt-angle.
2) Inspect system to ensure that components are installed properly, functioning correctly, and in compliance with appropriate codes and standards. Determine and record all power conditioning setpoints associated with the charge controller and inverter.
3) Characterize array performance for all operating conditions using the outdoor test procedure previously discussed in order to provide an accurate model for calculating the daily dc energy available from the array for any site, array orientation, and month of the year.
4) Using the array-to-load-ratio concept or estimates of daily component efficiencies, calculate a conservative estimate of the ac load appropriate for a typical wintertime solar resource.
5) Install data acquisition system and the ac load control system. Measured parameters should include battery voltage, battery current into the inverter, battery temperature, inverter and/or charge controller temperature, inverter ac voltage, inverter ac current to the load, ambient temperature, module temperature, and plane-of-array solar irradiance. Program the ac load control system to scale a

resistive ac load in proportion to the solar resource using the A:L ratio previously selected. The ac load should be a simple resistive load without capacitive or inductive components.

6) Measure the specific gravity of individual cells in the battery bank as received from the manufacturer. Identify any abnormal cells and assess the battery bank design in relation to uniformity of cell temperatures and hydrogen venting during the charging process.
7) Fully charge battery bank using an auxiliary source in order to establish a known initial condition. This charging process, for lead-acid batteries, should include a "boost" or "equalization" charge to fully mix the electrolyte in the cells of all batteries. Typically this boost charge should last from 6 to 12 hours at a maximum voltage of 2.50 to 2.55 volts per cell, or 30.0 to 30.8 Vdc for a 24-V battery bank. Measure battery temperature during the boost charge, and measure hydrogen level inside battery enclosure box to ensure adequate ventilation. If the peak hydrogen concentration is greater than 2%, then take steps to ventilate the enclosure. Measure cell or monoblock voltages, electrolyte specific gravity, and cell temperature in the battery bank immediately following the boost charge. At this point, individual cell temperatures should be uniform within about ±5°C, and the specific gravity for individual cells should be uniform, typically in the range from 1.27 to 1.32 SG.
8) Measure battery bank capacity by discharging at a 20-hr rate to the battery voltage (1.75 volts-per-cell or 21.0 Vdc for 24-V battery bank) commonly used by the battery industry. Measure individual cell or monoblock voltage immediately before the discharge is terminated. This test will provide a measured capacity for comparison with the manufacturer's rated capacity. Analysis of measured data also provides a means for selecting appropriate values for V_{BULK}, V_{FLOAT}, and V_{LVD} setpoints. This test will require independent discharge equipment unless the V_{LVD} setpoint for the system can be adjusted to a setpoint equivalent to 1.75 volts-per-cell.
9) Fully recharge battery bank using an auxiliary source or by using the photovoltaic array with no load connected to the system. Measure specific gravity and temperature of individual cells in the battery bank immediately following the boost charge.

Starting Point for System Tests:

10) Operate the system during nominally clear test conditions for a minimum of 5 daily cycles using the ac load selected for testing. Use the data acquisition system to continuously record all test data during this period. At the end of these cycles, measure specific gravity of individual battery cells and verify from test data that the system has fully charged the battery, including a nominal "overcharge."
11) Measure the "usable" battery capacity after the last full day of cycling by continuously discharging through the ac load at a 20-hr discharge rate until the system V_{LVD} setpoint is reached. The photovoltaic array must be disconnected from the system during this capacity test. This test establishes the initial operational capacity and provides information required to calculate the "days of autonomy" for the system.
12) Reconnect the photovoltaic array after V_{LVD} is reached and initiate a multi-day "recovery test" during which the system must return the battery bank to a high state-of-charge while continuously supplying the ac load selected for the test sequence. Continue operating the system for 5 additional daily cycles after the battery bank first reaches the V_{FLOAT} (regulation) voltage. Terminate the recovery test at the end of the 5th day where battery regulation voltage was reached. Disconnect the array. Measure specific gravity and temperature of individual cells in the battery bank immediately after terminating the test. Analyze the test data to determine the battery voltage, low-voltage-reconnect-voltage (V_{LVR}), at which the system reconnected the ac load during this recovery test.
13) Remeasure the "usable" battery capacity by continuously discharging through the ac load at a 20-hr discharge rate until the system V_{LVD} setpoint is reached. The photovoltaic array must be disconnected from the system during this capacity test. This test provides a second measurement of usable capacity and determines if battery capacity was lost during the recovery test. Measure cell or monoblock voltages immediately before terminating the discharge. The variation in cell or monoblock voltages should be small (within ±0.2 Vdc for individual cells), otherwise battery damage during the test sequence may be indicated.

14) Initiate a second multi-day recovery test without ac load in order to recharge battery bank. This test not only recharges the battery bank but also provides a final evaluation of the functionality of all system components. Analyze the test data to determine the battery voltage, V_{LVR}, at which the system reconnected the ac load during this recovery test.
15) Analyze all test data to establish system and component performance characteristics, to identify problem areas, and to identify opportunities for improvements in system performance and reliability.

Load Selection for System Testing

Selecting an appropriate ac load is a critical step in the successful execution of the test sequence previously outlined. However, it is impossible to know in advance what maximum ac load the system is capable of successfully providing on a daily basis because of system design constraints and daily variations in solar radiation. Consequently, it is necessary to conservatively estimate an appropriate ac load likely to result in successful completion of the test sequence. The A:L ratio concept, or estimates of the daily component efficiencies given in Equation (3), can be used in combination with array performance modeling to select an appropriately sized ac load.

From left to right, Table 4 gives calculated values for daily solar resource, array efficiency, daily dc energy available from the array, as well as an estimate for the daily dc energy and ac energy available from the system. The estimates for daily dc and ac energy from the system correspond to the A:L ratios indicated. The table provides daily energy values for each month of the year, as well as for the entire year. The FireFly™ 600 system was tested at Sandia during the month of June, so this month is highlighted in the table.

Table 4. Estimated ac load for FireFly™ array at latitude-tilt in Albuquerque. Assumptions correspond to dc-ratio A:L = 1.57 and ac-ratio A:L = 1.85. Array area is 5.04 m^2

Month	Average Solar @ Tilt (kWh/m^2)	Calculated Array Efficiency	Calculated PV Available (kWh/d, dc)	Calculated PV Available (Ah/d, dc)	Estimated dc Load (Ah/d, dc)	Estimated ac Load (kWh/d, ac)
Jan	5.09	0.112	2.88	84.3	53.7	1.56
Feb	5.82	0.108	3.18	95.7	60.9	1.73
Mar	6.31	0.107	3.40	102.5	65.3	1.84
Apr	7.12	0.102	3.65	114.7	73.0	1.98
May	7.47	0.098	3.69	119.6	76.2	2.00
Jun	***7.23***	***0.095***	***3.47***	***115.3***	***73.4***	***1.88***
Jul	7.24	0.095	3.45	115.9	73.8	1.87
Aug	7.01	0.096	3.37	112.4	71.6	1.83
Sep	6.60	0.097	3.23	106.6	67.9	1.75
Oct	6.33	0.102	3.27	103.1	65.7	1.77
Nov	5.46	0.108	2.98	90.2	57.4	1.62
Dec	4.89	0.112	2.76	81.1	51.6	1.50
Year	6.38	0.102	3.28	103.5	65.9	1.78

Figure 7 previously illustrated that the V_{mp} for the array was not well matched to operating voltages as constrained by the battery's requirements and PCS hardware. Therefore, since the Trace C40 charge controller does not have maximum-power-point-tracking capability, an estimate of the fraction of the daily energy available from the array actually delivered to the battery can be made. We estimated 0.85.

Similarly, estimates of the daily efficiency of the battery and the inverter can be made; we estimated 0.75 and 0.85, respectively. Thus, for the month of June when system testing was performed, the estimated average daily ac energy provided by the system would be 3.47 x 0.85 x 0.75 x 0.85 = 1.88 kWh/d. This ac energy corresponds to an 'average' June day in Albuquerque with a solar insolation of 7.23 kWh/m^2. A very clear day in June with 7.8 kWh/m^2 would scale to 2.0 kWh/d. Scaling the ac energy in June to a clear winter day with solar insolation of 5.5 kWh/m^2 gives an estimated ac energy of 1.4 kWh/d.

Using this rationale, the load selection used during the FireFly™ system testing assumed 5.5 kWh/m^2 as a reference daily insolation along with a corresponding "conservative" load of 1.4 kWh/d. During our testing, the resistive load was then scaled in proportion to the measured daily solar insolation. Note that during the first couple days of the initial "cycling" phase of the test sequence, the appropriateness of this load selection can be verified and then adjusted if necessary.

COMPONENT TEST RESULTS

The following sections of this report summarize the test results obtained while executing the test procedure previously outlined. Initial inspection and assessment of code compliance are discussed first, followed by an investigation of the battery enclosure design in terms of venting and thermal behavior, then battery 'usable' capacity measurements, and finally a discussion of charge control setpoints.

Initial System Inspection

Initial inspection of the FireFly™ 600 system identified design modifications that could improve performance, reliability, and safety. The most important design improvements related to the battery box (enclosure) where improved venting could eliminate a potential safety hazard, and the addition of physical separation (air spaces) between battery mono-blocks would improve uniformity of battery temperature and increase battery lifetime.

Compliance with Codes & Standards

As part of Sandia's evaluation of the FireFly™ system, the electrical design and wiring were reviewed for NEC compliance, good design practice, and workmanship. Overall, the system was well designed and installed in a neat and workman-like manner. Below is a list of items that were identified as either NEC compliance issues, manufacturing instruction issues [the NEC requires that equipment is installed in accordance with the manufactures installation instructions, NEC 110-3(b)], or the opinion of the authors. Ultimately, the successful compliance with codes is strongly dictated by local practices and the specific inspectors involved. The formal requirements of the National Electric Code (NEC) are available from the National Fire Protection Agency [14], and interpretations of the code as applies to photovoltaic systems are periodically published elsewhere [15].

1) The label on the modules indicated that they were rated for a maximum 10-amp series fuse. The 15-amp circuit breaker does not meet this requirement since the current rating is higher than 10 amps. A 10 amp or smaller series fuse could be added in each of the four module-strings to satisfy this requirement. (Manufacturer instructions)
2) The cable connectors on the module junction boxes appear to be designed for a single round conductor. The round inserts may not seal well around the two-conductor, twin-axial cable.
3) The dc load center, "DC Summing Enclosure", is not dc rated. The breakers are dc rated, but not the load center itself. If load centers are available with dc rating, they should be used. The dc circuit breakers are 'backfed,' power is supplied to the side of the breaker where the load is usually connected. If a 'backfed' breaker is removed from the panel, it could still be energized via the wire, presenting a possible safety hazard. Back-fed circuit breakers are required to be secured to the enclosure. Square D sells clips that can be used to secure the breakers to the enclosure. [NEC 384-16(g)] This problem may also apply to the generator breaker, depending on how it is connected.
4) The 250-A circuit breaker for the battery was mounted with foam insulation next to the breaker. The foam obscured the labeling on the breaker such that the voltage rating of the breaker could not be verified. Also, the foam will reduce heat dissipation from the breaker, and may cause the breaker to trip at lower than rated current. The foam should be cut back from the breaker.
5) The inverter is clearly labeled as having a 'top' side. However, the inverter was mounted on its side, which violated the manufacturer's instructions. The inverter was also mounted

towards the top of the box, which was not optimal from a thermal standpoint. If the inverter were mounted lower in the box, it would get better ventilation. (Manufacturer instructions)

6) Part of the label on the 'ac distribution panel' was obscured by the "Generator" label. The generator label should be moved so it does not obstruct the label on the panel. Also, the electrical connection point for the generator was not identified (labeled). (Recommendation)

7) The ac receptacle is required to be a GFCI type, or protected by a GFCI circuit breaker because it is located in an outdoor, and potentially wet, location. A GFCI receptacle should be used. [NEC 210-8(a) or 550-8(b)]. The sheathing on the UF cable should be removed inside the ac panel and outdoor clamps should be used. Sheathing should not be left on cables inside enclosures. Alternatively, instead of wiring the receptacle with UF cable, a conduit would be preferred 'best practice.' (Recommendation)

8) Black conductors sized #6 AWG and smaller cannot be used as equipment-grounding conductors or grounded-circuit conductors. The insulation must be green for equipment-grounding conductors and white for grounded-circuit conductors. On wire larger than #6, the entire exposed end of the wire must be taped. (NEC 200-6 & 250-119) Also, since both the ac and dc grounded-circuit conductors are in the same raceway, or enclosure, they must be differentiated by color. One wire can be plain white, but then the other has to be white with a stripe (not a green stripe). (NEC 200-6 & 250-119)

9) The ac grounded-circuit conductor was not grounded in the ac distribution panel. This panel is the service entrance for the system, and it is recommended that the dc grounded-circuit conductor be bonded to the single-point system ground here. Usually a screw comes with the enclosure for bonding the neutral bus to the enclosure (ground). This screw needs to be installed. (Recommendation)

Electrical Grounding Discussion

Figure 18 illustrates alternative procedures for electrically grounding metallic surfaces of system components (equipment ground), dc circuit conductor, and ac circuit conductor for off-grid photovoltaic systems in a manner that complies with NEC requirements. A variety of alternatives and exceptions may apply; however, the final assessment of code compliance is subject to the discretion of local electrical inspectors.

Battery and PCS Enclosure Design

A safety concern was raised during the initial system inspection concerning the ability of the Zomeworks battery enclosure to adequately vent the hydrogen generated during the charging process. Hydrogen generated by the Nationwide flooded lead-acid batteries during the charging process must be prevented from reaching concentrations inside the enclosure that exceed the "lower-explosive-limit" of 4% established by safety organizations. In addition, heat will be generated inside both the battery enclosure and the enclosure housing power conditioning components. Both enclosures were thermally insulated. So, an investigation was conducted to determine if excessive temperatures were reached inside the enclosures during summer operation.

In order to investigate the extent of hydrogen generation inside the enclosure, and to ensure a safe operating configuration during our system testing, a General Monitors hydrogen detection instrument was installed inside the battery box with the lid closed during battery charging. Figure 19 shows the hydrogen detector sitting on top of the batteries inside the enclosure. The air intake for the General Monitors instrument was located about 1.5 cm from the top of the battery enclosure (inside surface of the lid). The instrument was calibrated in-place by flowing premixed gas with known concentrations of hydrogen (1% and 2%) into the battery box.

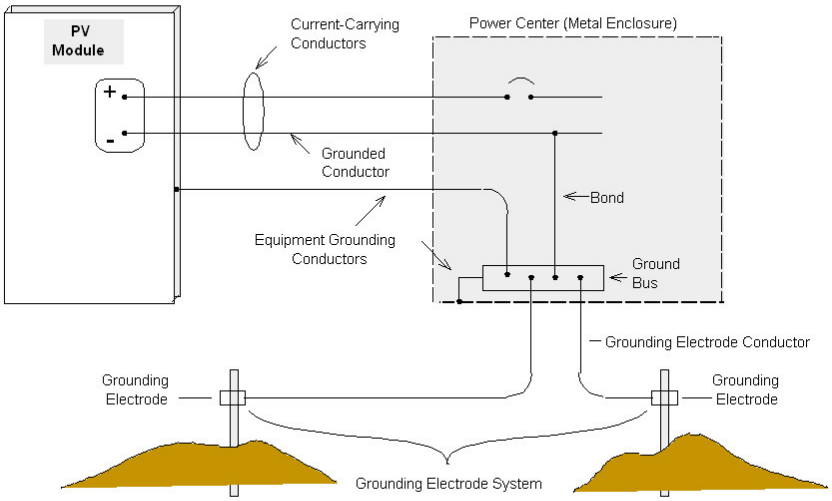

Figure 1. Grounding Electrodes

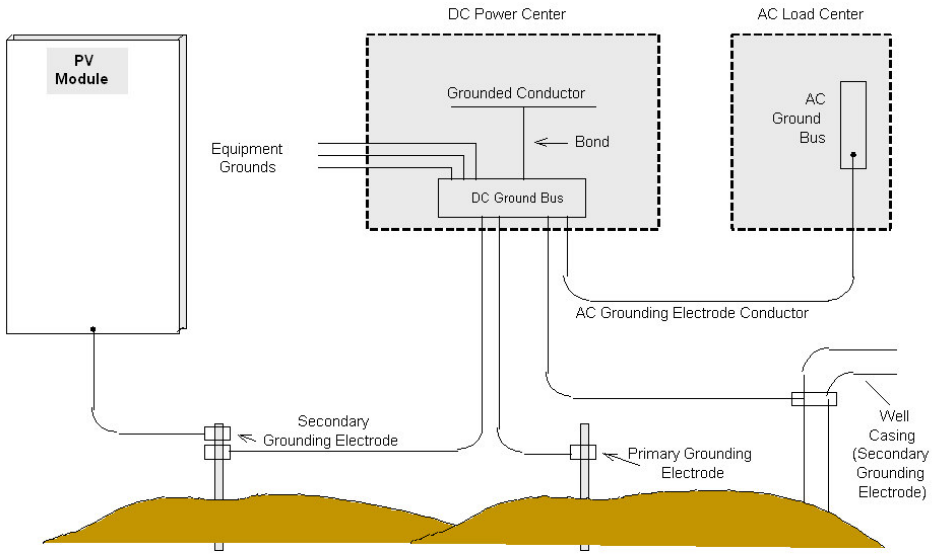

Figure 2. Multiple Grounding Electrodes

Figure 18. Alternative procedures for electrically grounding off-grid photovoltaic systems in a manner consistent with NEC requirements. *[Figures courtesy of John Wiles, Southwest Technology Development Institute, NMSU]*

Figure 20 shows hydrogen concentrations measured at two different charging rates (16A and 8A), with the batteries near a full state-of-charge. At the higher charging rate with the lid closed, the hydrogen sensor saturated (>3.8% hydrogen) after about 8 minutes. Decreasing the charging rate to 8A increased the time required to saturate the sensor to about 13 minutes. In both situations, the hydrogen generation rate of the Nationwide batteries exceeded the capability of the H_2Vent™ system on the Zomeworks enclosures. As seen in the figure, disconnecting the photovoltaic array immediately stopped the hydrogen

generation from the batteries. After the array was disconnected, the hydrogen concentration initially dropped rapidly, and then more slowly decreased over the next 30 to 40 minutes. Opening the lid to the enclosure rapidly dropped the hydrogen concentration to zero. The initial rapid drop in hydrogen concentration after disconnecting the array was attributed to the influence of the H_2Vent™ system. The subsequent slow decrease in hydrogen concentration was probably caused by hydrogen slowly diffusing back out of the Sytrofoam insulation inside the enclosure. The Zomeworks H_2Vent™ system may be entirely adequate for sealed (VRLA type) batteries, or even other flooded lead-acid batteries, but did not provide sufficient hydrogen venting for the Nationwide batteries in the FireFly™ 600 system.

To ensure safety during the 30-day system test procedure, the lid on the battery box was raised about 3.75 cm (1.5 in) allowing direct hydrogen ventilation around the lid perimeter. Figure 21 shows that with the lid raised the resulting hydrogen concentration was negligible. However, the battery temperature during the charging process was still undesirably high (>40°C) for summer operation in Albuquerque. These tests indicated that an improved battery enclosure design for the FireFly™ 600 was needed.

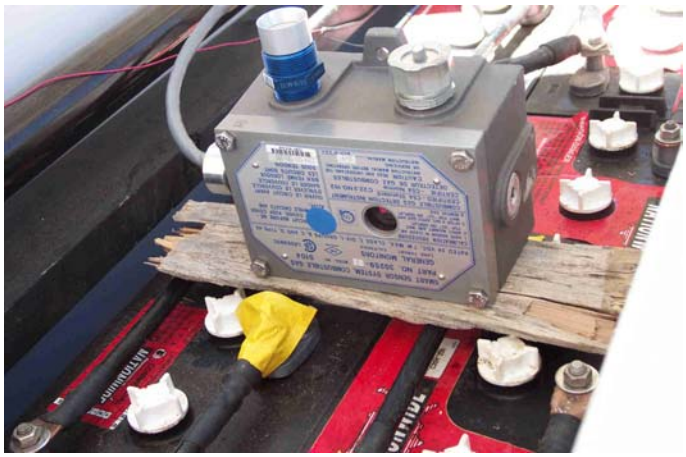

Figure 19. General Monitors hydrogen concentration sensor positioned above batteries in the FireFly™ 600 battery enclosure.

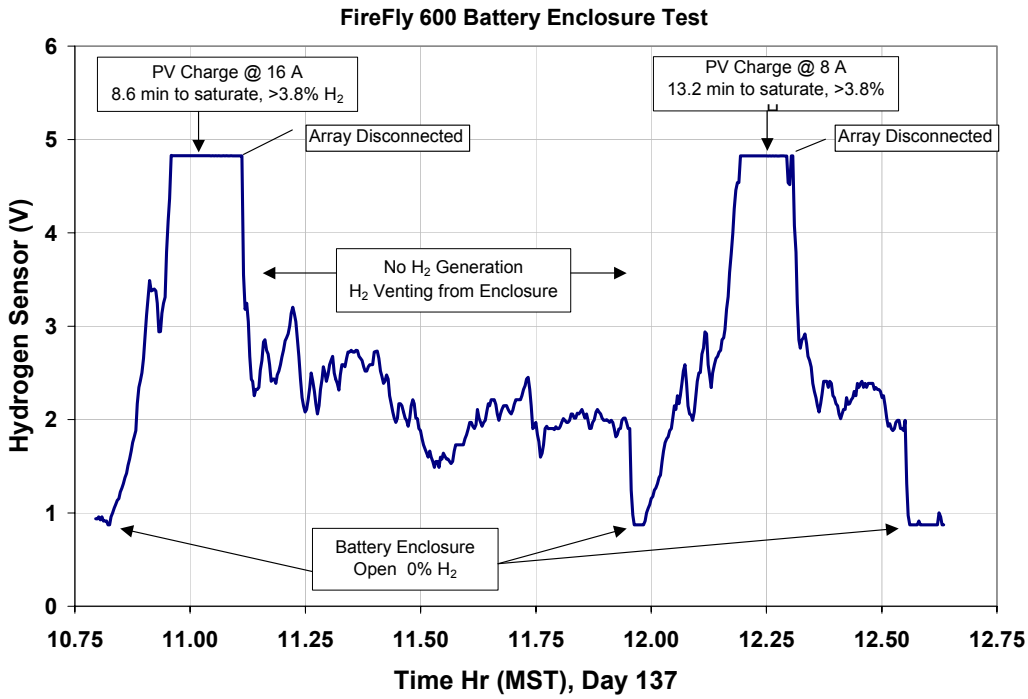

Figure 20. Hydrogen concentration measurement inside the FireFly™ 600 battery enclosure, near full state-of-charge with battery temperature about 35 °C. Note: A hydrogen sensor voltage of 4.8 V corresponded to a hydrogen concentration of 3.8%, and 0.9 V corresponds to 0% hydrogen.

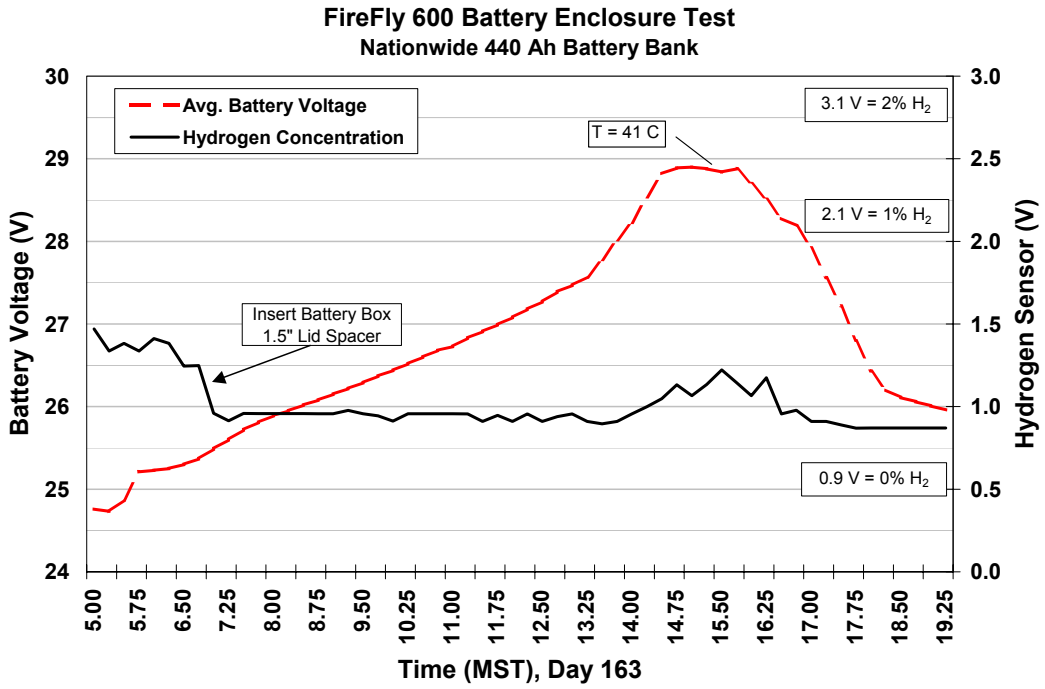

Figure 21. Measurement of hydrogen concentration with lid on battery box raised to allow ventilation around the perimeter. The result was negligible hydrogen concentration even at elevated battery temperature.

The thermal design of both the battery enclosure and the PCS enclosure was also investigated in order to understand the expected diurnal variation in battery temperature and inverter temperature. These data provided an estimate of the expected operating conditions for the batteries and PCS hardware during different seasons of the year. Ideally, the entire battery bank temperature should be uniform (< 3°C difference) from cell to cell within the battery bank, and the battery temperature should be maintained over the year within the range from 15°C to 35°C. Battery manufacturers often indicate that life expectancy for batteries operated at 35°C will be reduced by about 50% relative to continuous operation at 25°C. Battery capacity is also influenced by operating temperature, at 15°C it is reduced by about 12% relative to a 25°C battery temperature. Inverter and charge controller hardware also have lower and upper limits for operating temperature, and their performance and reliability would benefit from air temperatures in the range from 15°C to 35°C. Inverters and charge controllers typically go into a 'self protection' mode when air temperatures exceed about 40ºC, in which case power output from the system will be intentionally reduced.

Figures 22 and 23 illustrate temperatures measured for the battery, in the PCS enclosure (heat sink fin on charge controller), and ambient air temperature during typical operation with the lid closed on both the Zomeworks insulated enclosures. In order to avoid unacceptable hydrogen concentration levels in the battery enclosure with the lid closed, these data were recorded during the 'recovery' periods following battery capacity measurements. During the recovery period with the battery at a relatively low state-of-charge, the hydrogen generation rate was very low. On day 155 (6/4/01), the battery state-of-charge was about 50%, and on day 162 the battery was approaching a full state-of-charge. These data indicated that due to the mass of the batteries the diurnal variation in battery temperature was relatively small, with the difference between maximum and minimum temperature being less than 5°C. During the 10-day recovery period, the battery temperature peaked at a value from 2 to 7°C above the peak ambient air temperature for the day, reaching undesirably high temperatures above 40°C on several days.

Temperature measurements were also recorded during 'cycling' conditions with the battery fully charged, but with the lid on the battery enclosure raised providing a 1.5-in gap for ventilation. Figure 24 illustrates the temperature measurements in this situation. With the lid raised, the minimum to maximum temperature variation for the battery increased to about 7°C, but more importantly the peak battery temperature dropped to less than 35°C for environmental conditions very similar to those shown in Figure 23. For summertime operation in sites such as Albuquerque or Phoenix, battery lifetime can be significantly increased if the daily-average battery temperature can be kept below the peak daytime ambient air temperature.

In the insulated enclosure housing PCS components, the diurnal variation in charge-controller temperature was typically less than 10°C. However, operating temperature of the Trace C40 charge controller reached undesirably high levels during the day. During our tests in Albuquerque at an ambient temperature of 35°C, the charge controller reached a temperature of 40°C, and this is the temperature at which the C40 temperature protection circuitry starts limiting its output. If the FireFly™ 600 system were installed in Phoenix, C40 temperatures over 50°C would result, along with a significant loss in system performance.

The conclusion from these thermal tests on the battery and PCS enclosures was that improved designs were needed to improve both the performance and the reliability of the FireFly™ 600 system.

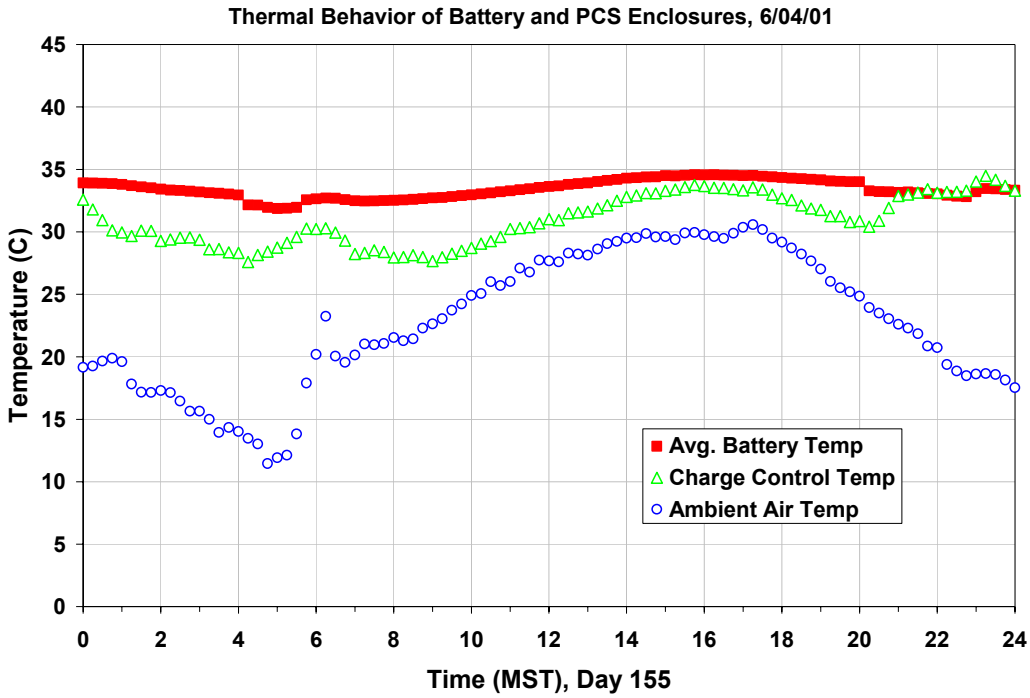

Figure 22. Temperature measurements recorded for battery, charge-controller fin, and ambient temperature during 'recovery' from low-voltage-disconnect condition. Lid closed on battery enclosure with battery at about 50% SOC.

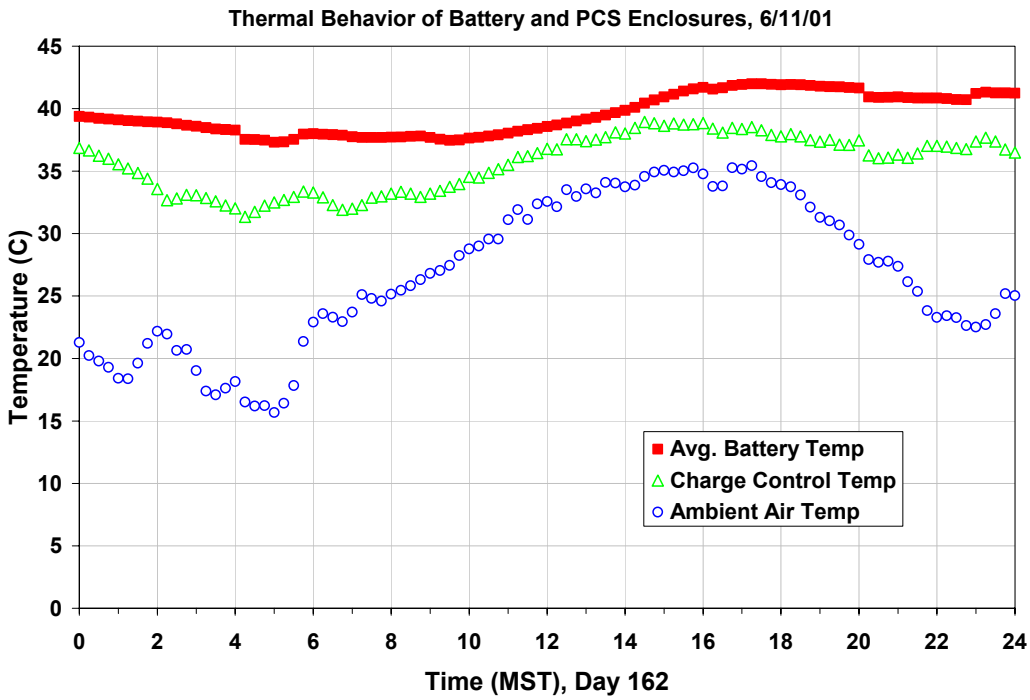

Figure 23. Temperature measurements recorded for battery, charge-controller fin, and ambient temperature during 'recovery' from low-voltage-disconnect condition. Lid closed on battery enclosure with battery approaching a full state-of-charge.

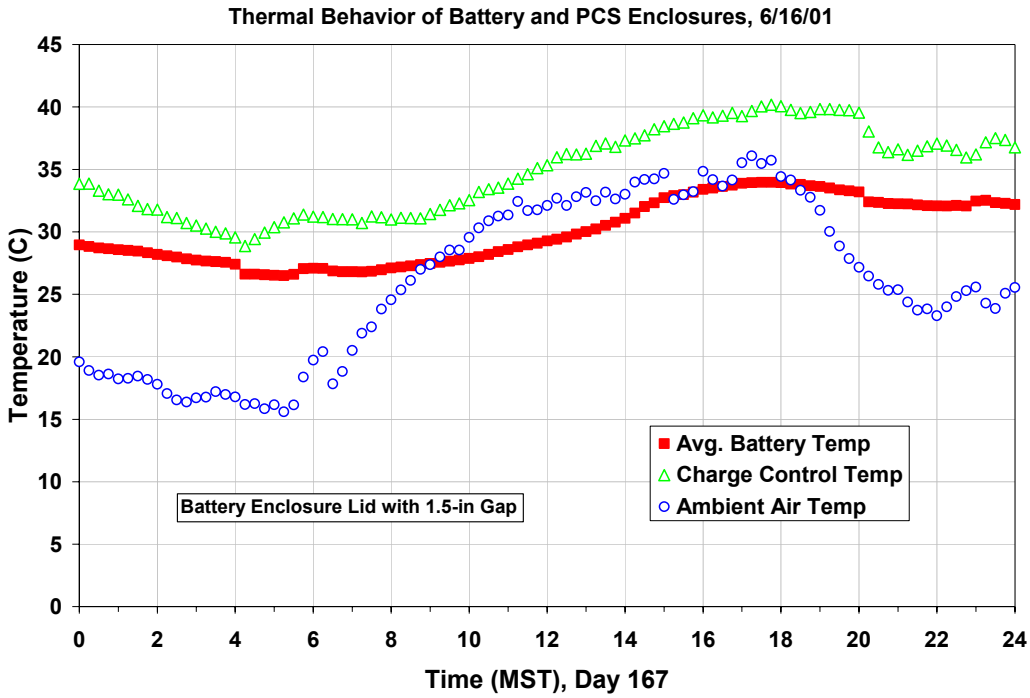

Figure 24. Temperature measurements recorded for battery, charge-controller fin, and ambient temperature during typical 'cycling' condition. Lid on battery enclosure was raised for ventilation with battery at a full state-of-charge.

Battery Capacity Measurements

The FireFly 600 system uses eight Nationwide 6-Vdc deep-cycle lead-acid batteries for energy storage. The battery bank had four series-connected batteries in two parallel battery strings, for an operating voltage of 24 Vdc. As previously discussed in the outline of the system test procedure, battery capacity measurements were performed three different times. An initial battery capacity measurement was performed prior to initiating the 30-day test procedure, and then two additional 'operational or usable' capacity measurements were performed as an integral part of the test procedure. The initial capacity measurement was performed in a manner consistent with the battery industry practice by discharging the battery bank to 21.0 Vdc (1.75 volts-per-cell) over a 24-hr period. The two 'usable' capacity measurements performed during system testing used a similar discharge period but stopped at the low-voltage-disconnect (V_{LVD}) condition controlled by the Trace DR2424 inverter. Electrolyte specific gravity measurements were also recorded for each cell in the battery bank at five different times during the test sequence. Specific gravity was measured using an Anton Paar, model 35N, hydrometer with measurement uncertainty of about ±1%. This hydrometer provided measurements of both electrolyte specific gravity and temperature, and specific gravity measurements were translated to the standard 25°C.

Prior to fully charging the battery bank for the initial capacity test, electrolyte specific gravity (SG) was measured in order to establish the state-of-health of all cells. Initial specific gravity measurements gave an average of 1.267 with a maximum of 1.279 and a minimum of 1.249. This range for SG indicated there were no significant battery problems, but the battery bank was not at a full state-of-charge. As a rule of thumb, SG of about 1.28 indicates a full charge and about 1.12 indicates a fully discharged condition. An overnight boost or 'equalize' charge using an industrial automotive battery charger resulted in specific gravity recovery to an average of 1.297, however, it also identified a significant

temperature imbalance between the two battery strings. Electrolyte specific gravity and temperature measurements during the initial battery bank capacity measurement, as well as during the two subsequent 'usable' capacity measurements, are shown in Figures 25 and 26. All cases shown in Figure 25 illustrate a distinct difference in specific gravity between cells in string #1 and string #2, likely due to continuous operation with non-uniform battery temperature.

Immediately following the initial boost charge, the average temperature of cells in battery string #1 was about 48°C while the average for battery string #2 was about 36°C. This temperature imbalance was significant, resulting in typical SG for string #1 of 1.310 and for string #2 of 1.285. Over the long-term, this temperature difference will result in a growing imbalance between battery strings, and significantly reduce the service lifetime of the battery bank. In an attempt to illustrate the temperature differences measured between the two battery strings, an infrared (IR) camera was used to record the image shown in Figure 27. The IR image was recorded after the array was used to recharge the battery bank following the initial capacity test. Although a direct beam of sunlight saturated the IR image in a strip across the batteries, it can still be seen that string #1 against the right-side insulated wall of the battery enclosure is noticeably hotter than string #2 on the left side. With better access, the IR camera provides a very diagnostic method for evaluating battery temperature distribution and for identifying resistive connections at battery terminals. The left vertical face of string #2 was directly exposed to air-cooling as was one end of both strings at the top of the image. A straightforward design solution to this problem can be achieved by physically separating the individual batteries providing at least a 2-in air space on all sides of the batteries. This air space will allow effective heat transfer by convection on all vertical surfaces and provide more uniform battery temperatures.

The initial battery capacity measurement gave a result of 434±15 Ah when continuously discharged to 21.0 Vdc (1.75 volts-per-cell) at a discharge rate of 18.0 amps and at a battery temperature of 30°C. This capacity measurement when translated to a 25°C battery temperature was 407±14 Ah. A standard procedure for translating battery capacity measurements to different temperatures is documented in IEEE Standard 450 [16]. This capacity measurement was about 7.5% less than the 440 Ah manufacturer's rating; however, the batteries were about 1-yr old and may have degraded somewhat due to the non-uniform temperature previously discussed. Early in the system test sequence, the 'usable' battery capacity was measured during 'capacity test #1,' and the results are shown in Figure 28. In this case, the capacity was measured to be 427±15 Ah at a battery temperature of about 29°C when discharged at a 22-amp rate over a 20-hr period to an average battery voltage of 21.7 Vdc. The 21.7 Vdc value for V_{LVD} was dictated by the Trace DR2424 inverter and was not adjustable. Later in the test sequence, the capacity was measured again in 'usable capacity test #2' at 422±15 Ah. When differences in battery temperature, discharge rate, termination voltage (V_{LVD}) were considered, all three battery capacity measurements gave the same results within measurement uncertainty.

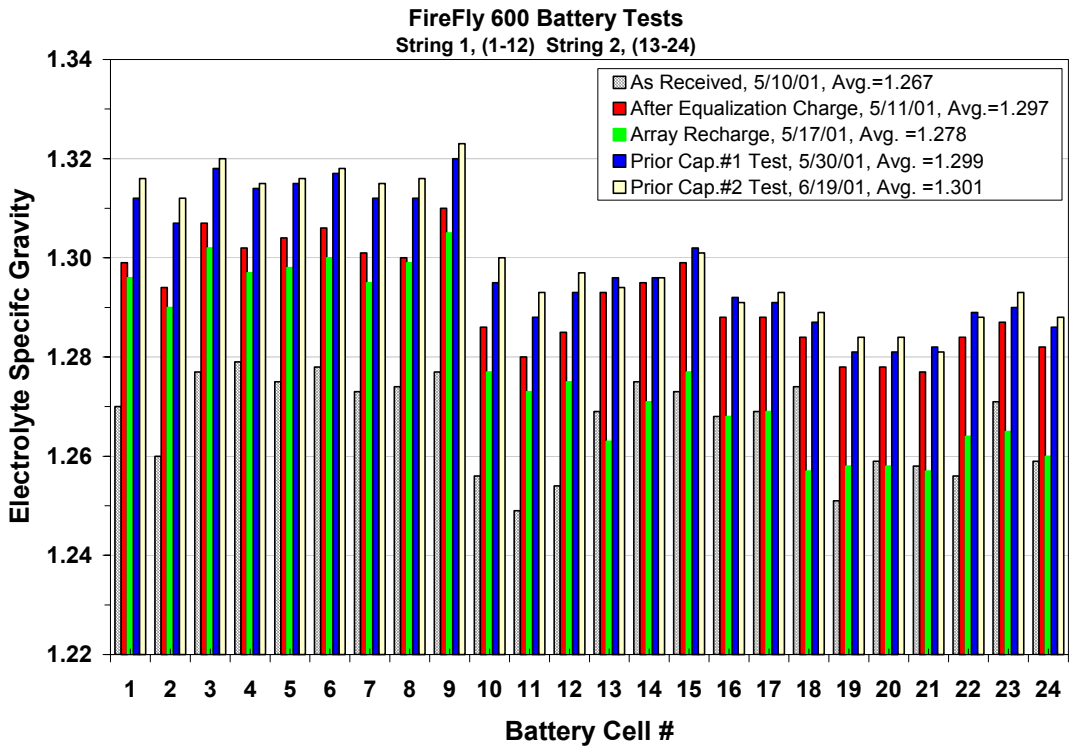

Figure 25. Electrolyte specific gravity measurements for individual cells in the battery bank recorded at different times in the system test sequence.

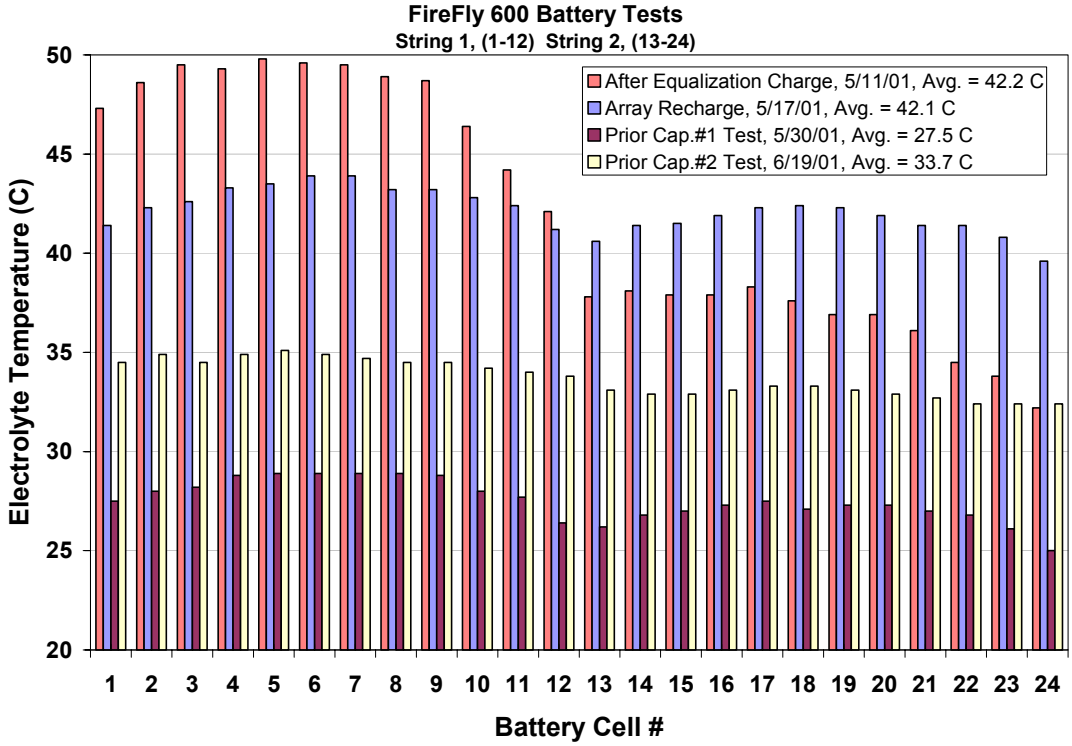

Figure 26. Electrolyte temperature measurements for individual cells in the battery bank recorded at different times in the system test sequence.

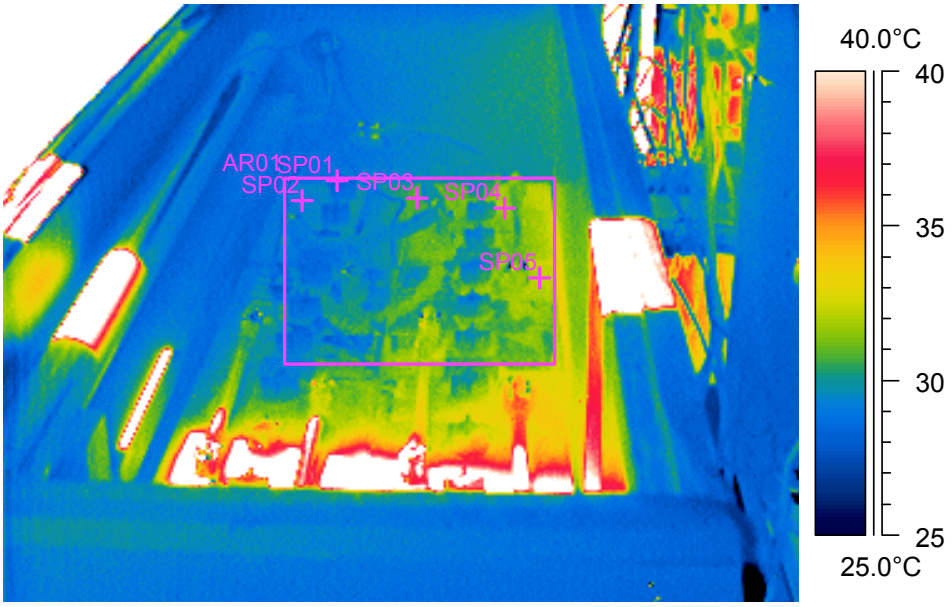

Figure 27. Thermal infrared (IR) image showing temperature distribution between string #1 (right) and string #2 following battery recharge using the PV array. White regions across the image are sunlight shining between the halves of the array.

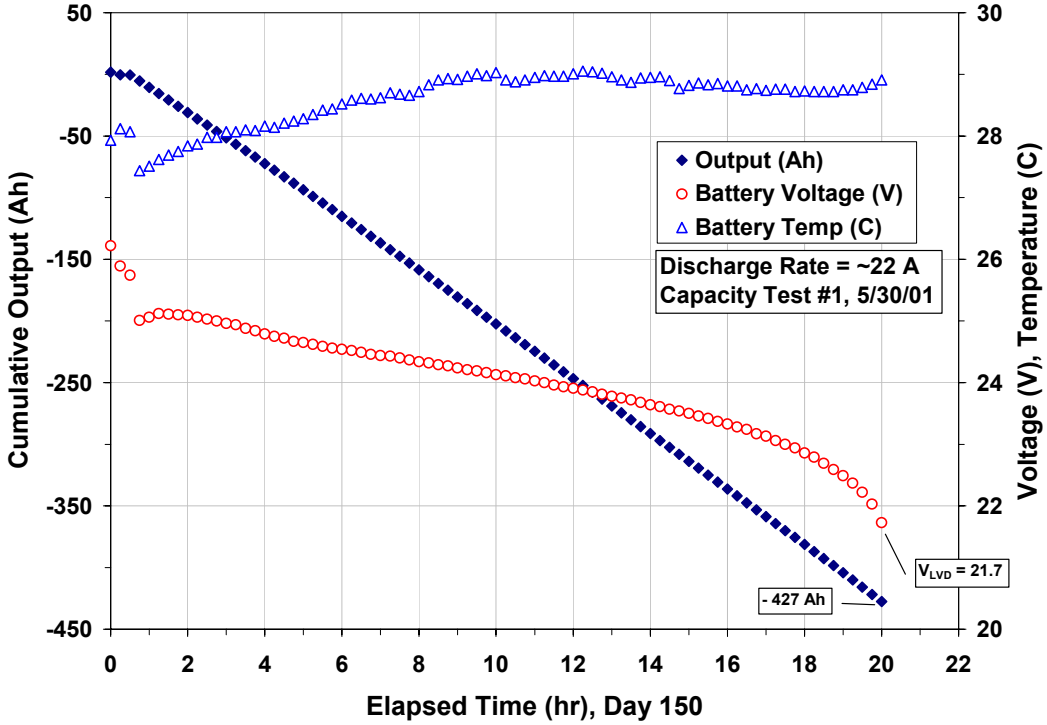

Figure 28. First measurement of 'usable' battery capacity performed during system test procedure. The V_{LVD} setpoint was controlled by the Trace DR2424 inverter.

Figures 29 and 30 present the results from the two 'usable capacity' tests. Data are presented in a way that more clearly illustrates the relationship between battery capacity and battery voltage. Figure 29 expresses battery capacity in the units (Ah) common to the battery industry, and Figure 30 gives battery capacity in units (kWh) more common to the photovoltaic and utility industries. Units of kWh also provided a common unit for reference, starting with solar irradiance and ending with ac energy delivered by the system. The 'usable' capacity indicated in these figures corresponds to a discharge down to 22.8 Vdc, the low-voltage-disconnect voltage recommended by the battery industry. Also shown in the figures is the V_{LVD} value (21.7 Vdc) established by the Trace DR2424 inverter, which results in an undesirably low state-of-charge. If the system frequently reaches this low-voltage-disconnect condition, the battery lifetime will be degraded significantly. A modification should be made to the Trace DR2424 inverter firmware making it possible to increase the setpoint for V_{LVD} to a value at or above 22.8 Vdc.

The relationship between battery capacity and voltage is distinctly different when recharging compared to discharging. Fully recovering from a discharged state requires more energy returned to the battery than was withdrawn, and it requires maintaining the battery at an elevated voltage for a period of time (overcharge) in order to reestablish the battery chemistry. This capacity versus voltage relationship during the recharging process was characterized in order to establish the degree of overcharge required, and to establish a value for the low-voltage-reconnect voltage (V_{LVR}). The V_{LVR} establishes the point during the recharge process where the inverter reconnects the ac load to the system.

Figure 31 shows the capacity versus voltage relationship for the Nationwide battery bank measured while recharging. This test was performed following the initial capacity test for the battery bank. Also shown in Figure 31 is the V_{LVR} value (24.9 Vdc) used by the Trace DR2424 inverter. The V_{LVR} setting in the inverter was not adjustable. If the V_{LVR} setting is too low, then after a low-voltage-disconnect condition has occurred a prolonged period may be required for the battery to recover to a full state of charge because the ac load is reconnected prematurely. A low setting may also result in power to the load may cycle on and then off again during the day as the system oscillates between the V_{LVD} and V_{LVR} conditions. As a rule-of-thumb, sufficient energy should be returned to the battery bank to power the ac load for about two days before the load is reconnected to the system. For the FireFly system, this rule-of-thumb suggests a V_{LVR} of about 26 Vdc, corresponding to about 50% state-of-charge.

A second modification needs to be made to the Trace DR2424 inverter by either increasing the setpoint for V_{LVR} or making it adjustable.

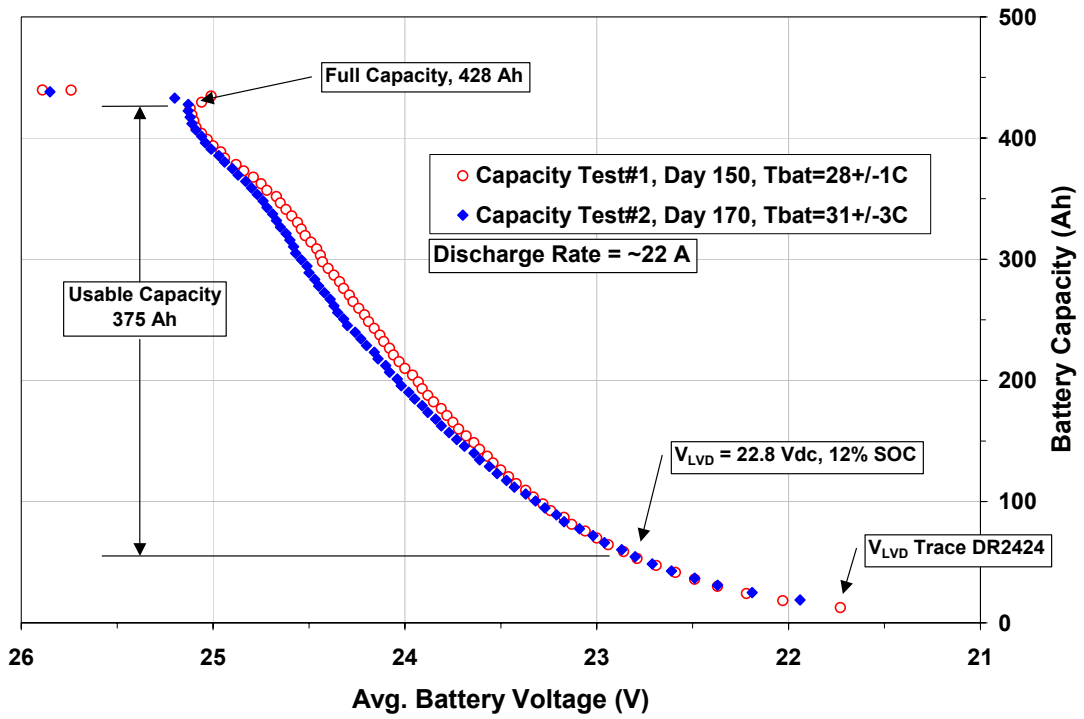

Figure 29. Measured battery capacity in units of Ah versus average battery voltage. The recommended V_{LVD} and the value actually used by Trace DR2424 inverter are indicated.

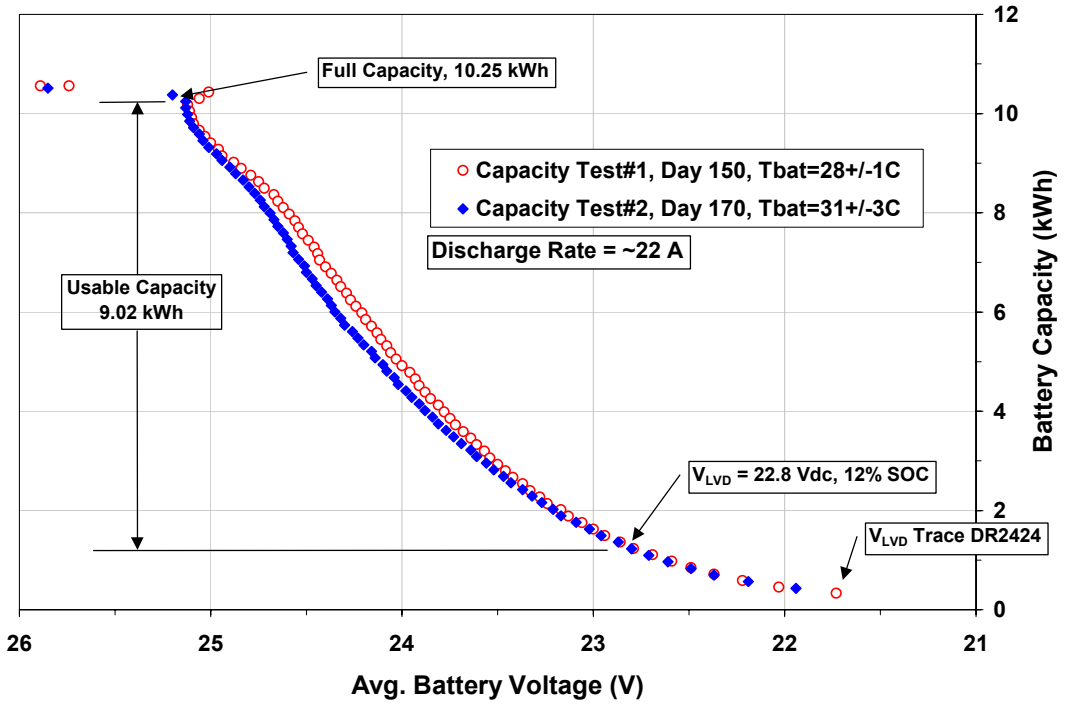

Figure 30. Measured battery capacity in units of kWh versus average battery voltage. The recommended V_{LVD} and the value actually used by Trace DR2424 inverter are indicated.

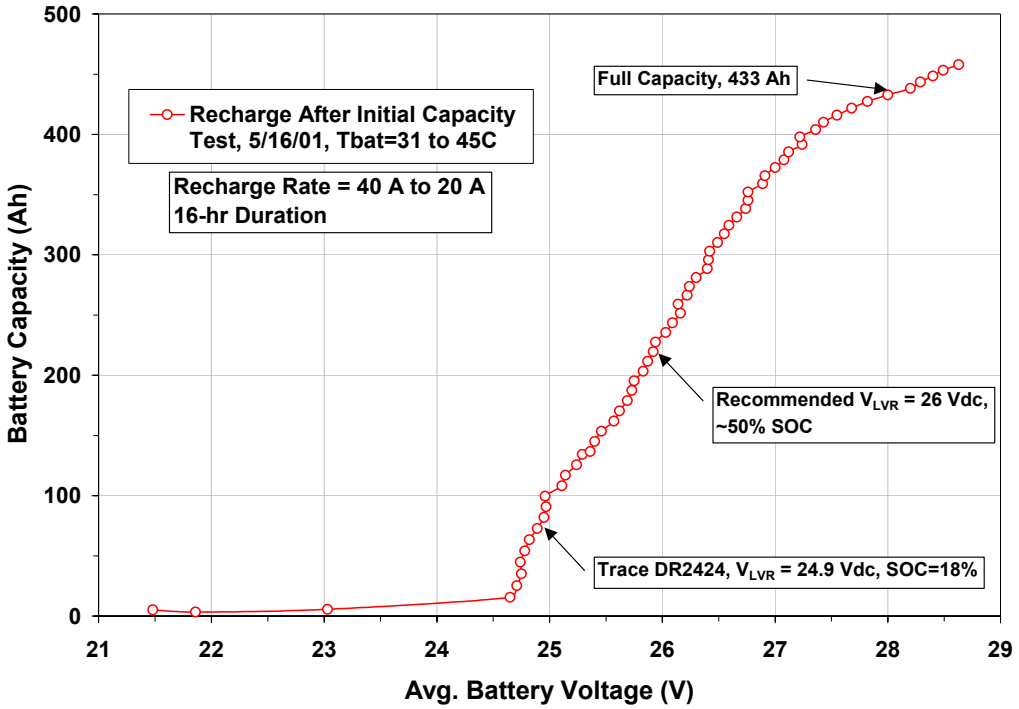

Figure 31. Battery capacity versus battery voltage, measured while recharging from a low-voltage-disconnect condition. A recommended V_{LVR} and the value actually used by the Trace DR2424 inverter are indicated.

SYSTEM TEST RESULTS

As previously discussed, the 30-day system testing procedure had five basic steps. Figure 32 illustrates these steps in the 30-day sequence in terms of the measured values for battery voltage and net battery capacity. The first step involved typical operation or 'cycling' for several days with an ac load and starting from a condition with the battery bank at a full state-of-charge. The second step was the first measurement of usable battery capacity, with the array disconnected. The third step was the 'recovery' test to assess the system's ability to reestablish the battery bank at a full state-of-charge following a low-voltage-disconnect condition while still powering the ac load. The fourth step was a second measurement of the usable battery capacity, with the array disconnected. The fifth step was a second more rapid 'recovery' test, this time with the ac load disconnected.

The results from this sequence of tests, when coupled with the array performance model, provided a detailed characterization of the functionality and performance of the system and its separate components. Figure 33 shows the measured daily solar resource during the 30-day test period for the FireFly™ 600. Figure 34 shows the corresponding results from our array performance model, giving the daily dc energy available from the photovoltaic array assuming that the array operates continuously at its maximum-power-point. The following sections of this report quantify the effectiveness of the system in transforming this available dc energy into the ac energy delivered to the load.

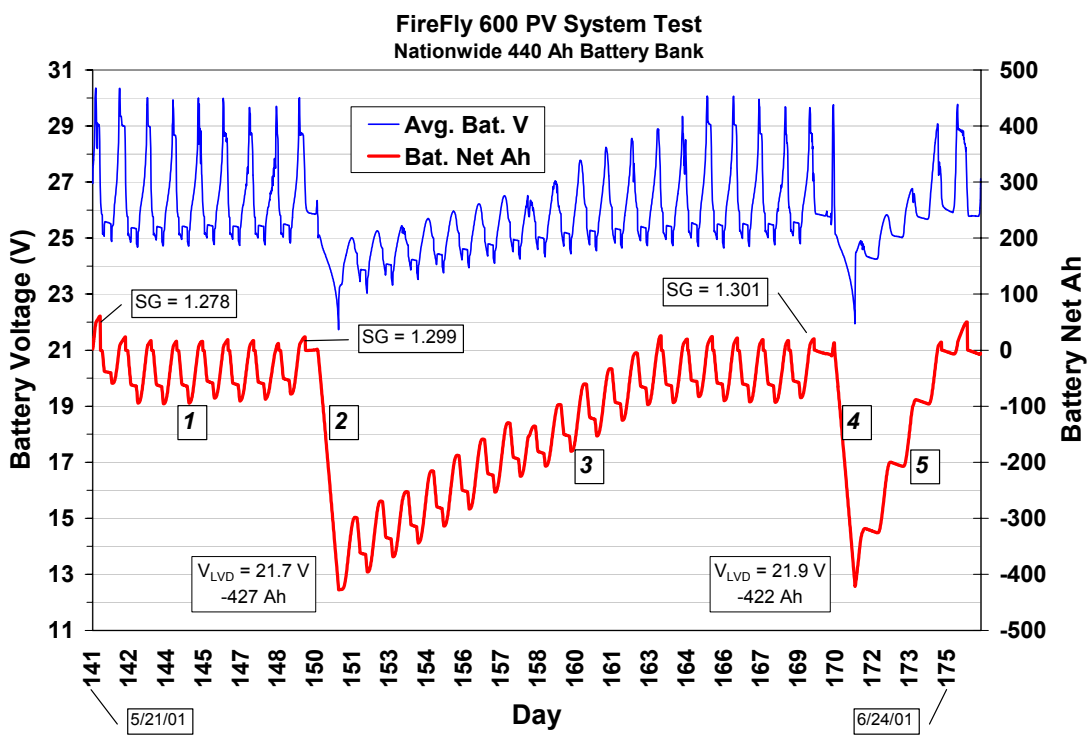

Figure 32. Battery voltage and net amp-hours during the five steps of the system test procedure: (1) initial cycling, (2) battery capacity test, (3) first recovery, (4) battery capacity test, and (5) second recovery.

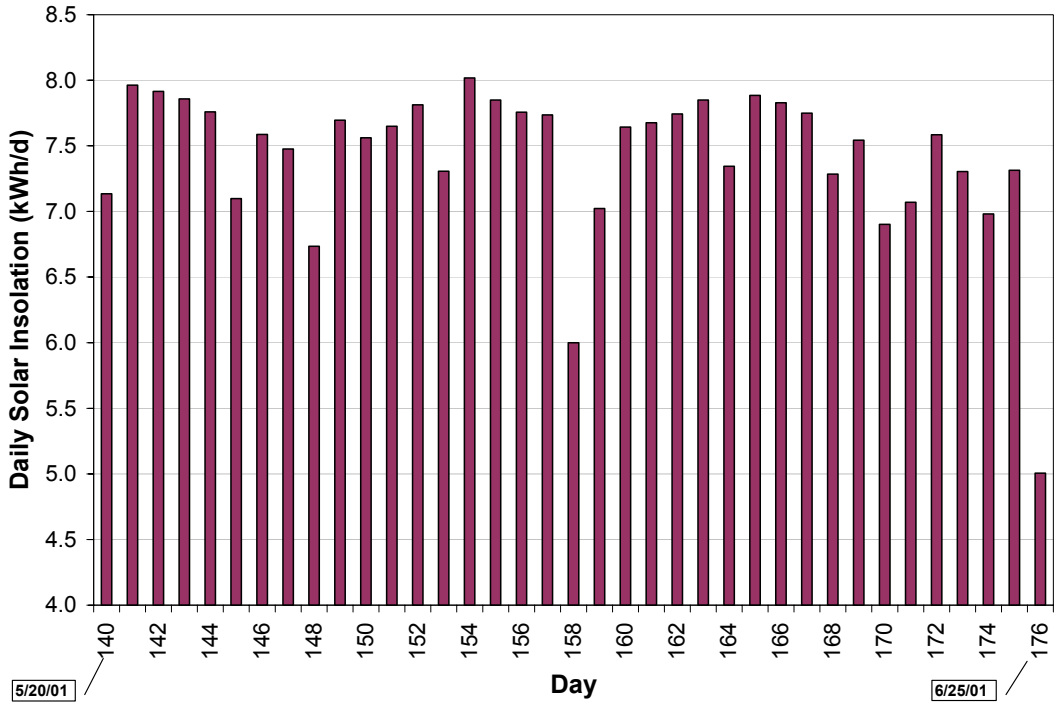

Figure 33. Measured daily solar energy (insolation) in the plane-of-array during the system performance tests for the FireFly™ 600 system.

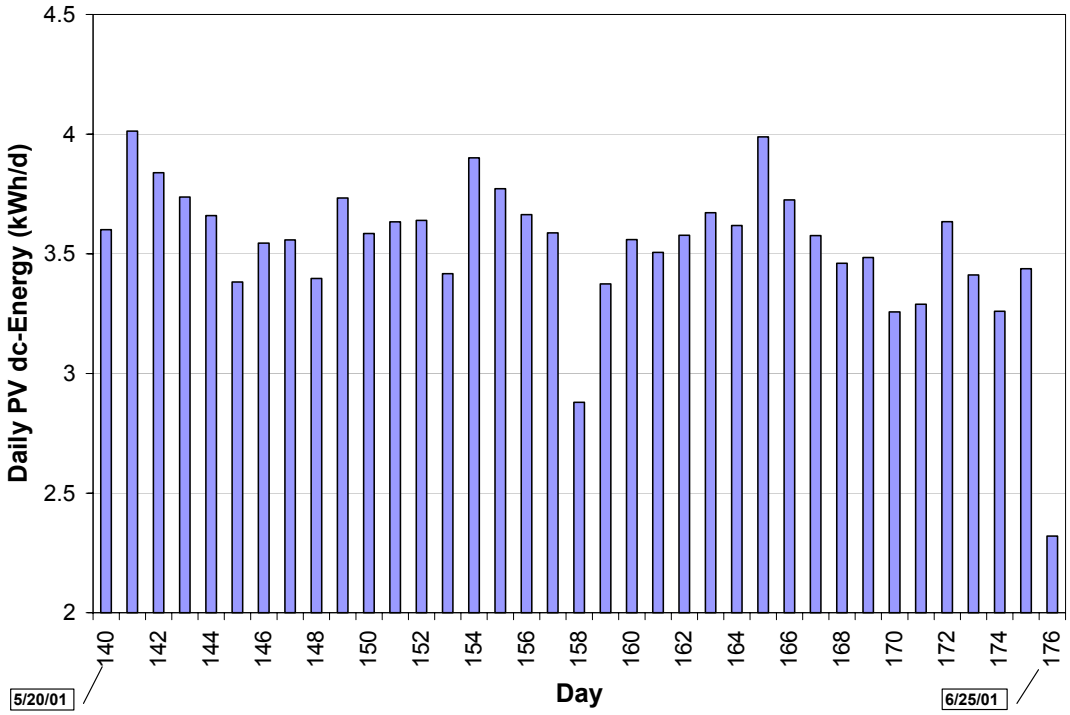

Figure 34. Calculated daily energy available at P_{mp} from the FireFly™ 600 array during the system performance test period, based on empirical array performance model.

Operation During Typical Cycling

The first step in the system test sequence involved several days of typical operation or 'cycling' with a preselected ac load, and starting from a condition with the battery bank at a full state-of-charge. As previously discussed, the ac load selected for testing was scaled in proportion to the daily solar insolation available during the preceding daytime charging period. Figure 35 shows the battery voltage and net current flow (Ah) during eight days of cycling. The ac load was applied twice during the night, once just after sunset and again prior to sunrise. The specific gravity of the electrolyte in the batteries is also indicated at the start and end of the cycling period. In order to power the ac load during this cycling period, the battery bank was discharged daily by about 90 Ah from a high state-of-charge, then on a daily basis this charge was returned plus an additional 'overcharge' of 15 to 20 Ah. Remember that a 'conservative' ac load was intentionally selected for use during this 30-day test procedure, so the daily overcharge was anticipated. By quantifying the energy consumed during the daily overcharge, the test results provide the means for optimizing the system design. Battery temperatures are indicated for three different days at the point in time when the bulk and float charging conditions occurred. The battery voltage corresponding to these temperatures indicated that the temperature compensation provision in the C40 charge controller was correctly adjusting these voltages based on battery temperature.

From a system designer's perspective, the energy used to 'overcharge' the battery bank on a daily basis can represent a significant fraction of the energy available from the photovoltaic array. Therefore, a system design tradeoff is required between using energy to 'overcharge' the batteries to maximize their lifetime and providing it to the ac load instead. One possible design alternative is to have the system perform a battery 'equalization' charge once per week instead of designing for a daily overcharge. This 'equalization' alternative should make better use of the kWh of dc energy available from the array while still maintaining battery health.

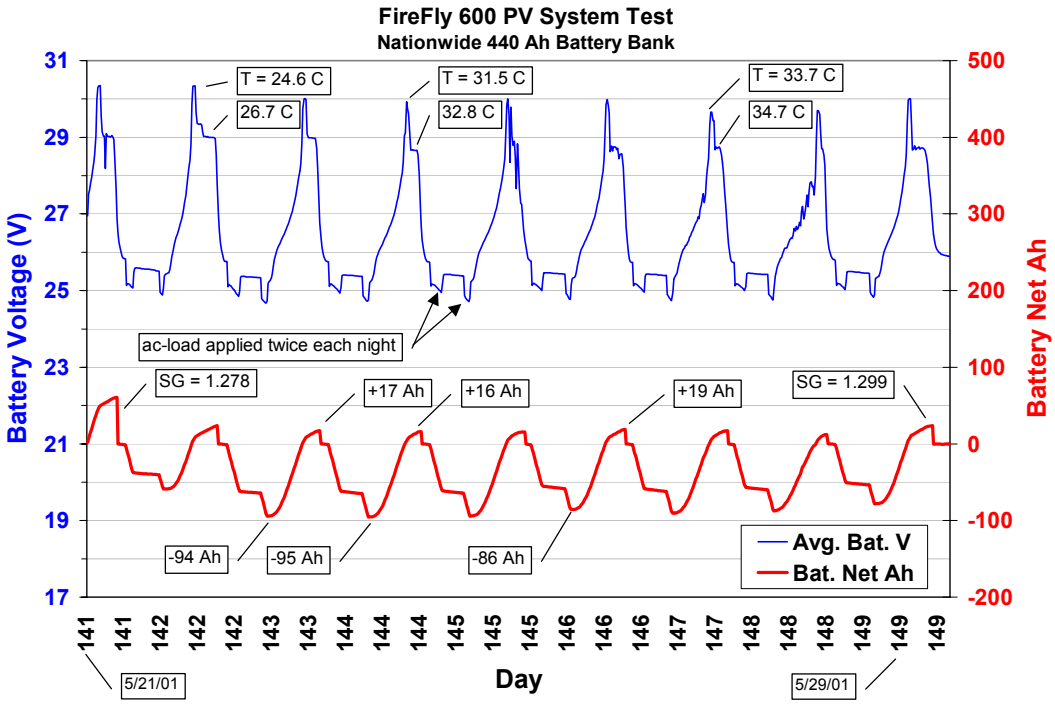

Figure 35. Battery voltage and net amp-hour flow into and out of battery bank during the initial daily 'cycling' phase of the test procedure. A variety of operating parameters are highlighted.

As previously discussed, the Trace C40 charge controller provides a 3-stage charge control process. Figure 36 illustrates the charge control process for a single day during system 'cycling.' In the first stage, current from the array is not limited and the voltage is allowed to rise until the V_{BULK} setpoint (30 Vdc) is reached. In the second 'absorption' stage, the V_{BULK} setpoint is maintained for a period of 1 hour. Then in the third stage the setpoint is changed to, and then maintained at, the V_{FLOAT} value (29 Vdc). In Figure 36, it can also be seen that the battery voltage falls off from the V_{FLOAT} plateau as the sun sets and there is less and less current available from the array. The two intervals during the night when the ac load was applied are readily evident from the associated voltage drops. For the particular day illustrated, the 111 Ah added to the battery during the daytime was about 18% greater than the 94 Ah extracted to power the ac load at night. This 18% difference doesn't sound like an excessive energy penalty to pay in order to maintain battery health, however, when the same analysis is done using true units for energy (kWh) the conclusion is different.

Figure 37 illustrates another way to interpret the same test data, but with net electrical flow into and out of the battery expressed in energy units (kWh) rather than current flow (Ah). In this case, 3.05 kWh of energy from the photovoltaic array was added to the battery during the daytime, and then 2.35 kWh was extracted from the battery to power the ac load at night. In energy units (kWh), 30% more energy was added to the battery during the day than was extracted at night! Therefore, for the ac load selected for use during the test procedure, a full 30% of the dc energy provided by the array was dissipated in the battery, and was thus not available as ac energy from the system. When conducting an energy balance, the fundamental problem with units of Ah is that battery voltage is implicitly assumed to remain constant (e.g. 24 Vdc). However, as shown in Figure 32, the battery voltage varies dramatically during typical operating conditions for a photovoltaic off-grid system.

The energy loss in the battery results from a combination of mechanisms, including fundamental battery efficiency and the energy used on a daily basis to 'overcharge' the battery. Alternative schemes for system operation need to be evaluated in order to make more efficient use of the array dc energy while still maintaining battery health. For instance, the level of overcharge required to maintain battery health needs to be carefully determined, and the daily battery charging strategy and the charge controller setpoints need to be adjusted accordingly.

Figure 38 illustrates several days of additional system 'cycling' at the end of the first 'recovery from V_{LVD}' test. The results and interpretation here are the same as for data recorded during the initial cycling step shown in Figure 35. There was evidence of temperature compensation by the Trace C40 charge controller indicated in the peak battery voltages achieved. As in the initial cycling test, the 'conservative' ac load resulted in a significant percentage of the array dc energy being used to overcharge the batteries.

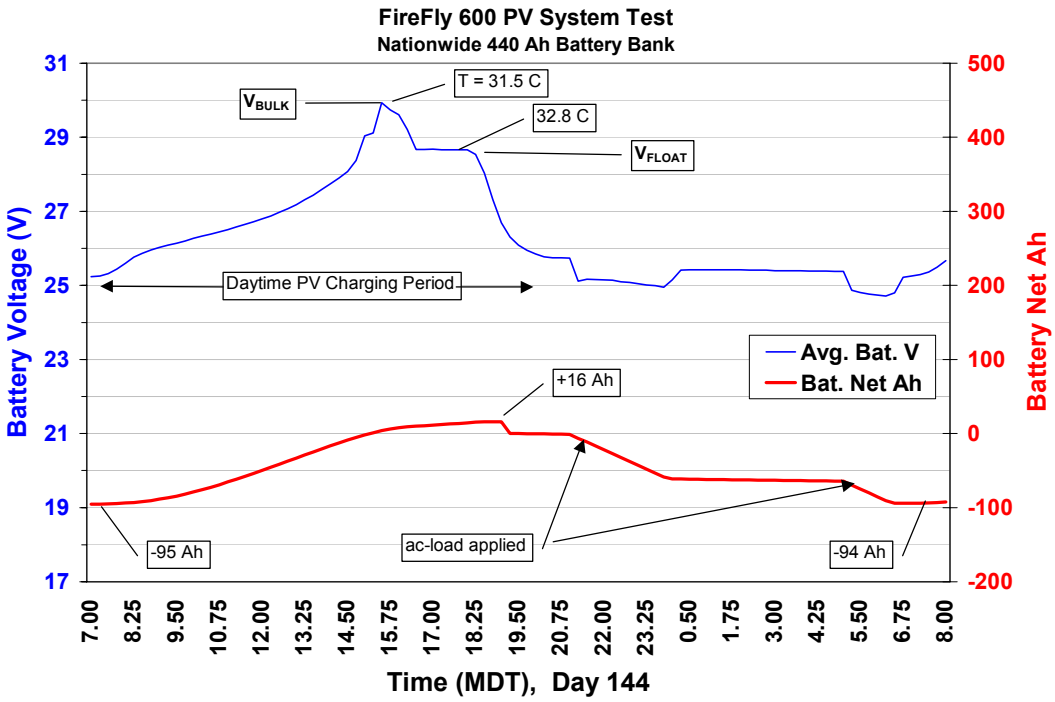

Figure 36. Example of a daily 'cycle' illustrating the 3-stage charging process (bulk, 1-hr absorption, float) controlled by the Trace C40 charge controller. The effect of applying the ac load at two different times during the night is shown.

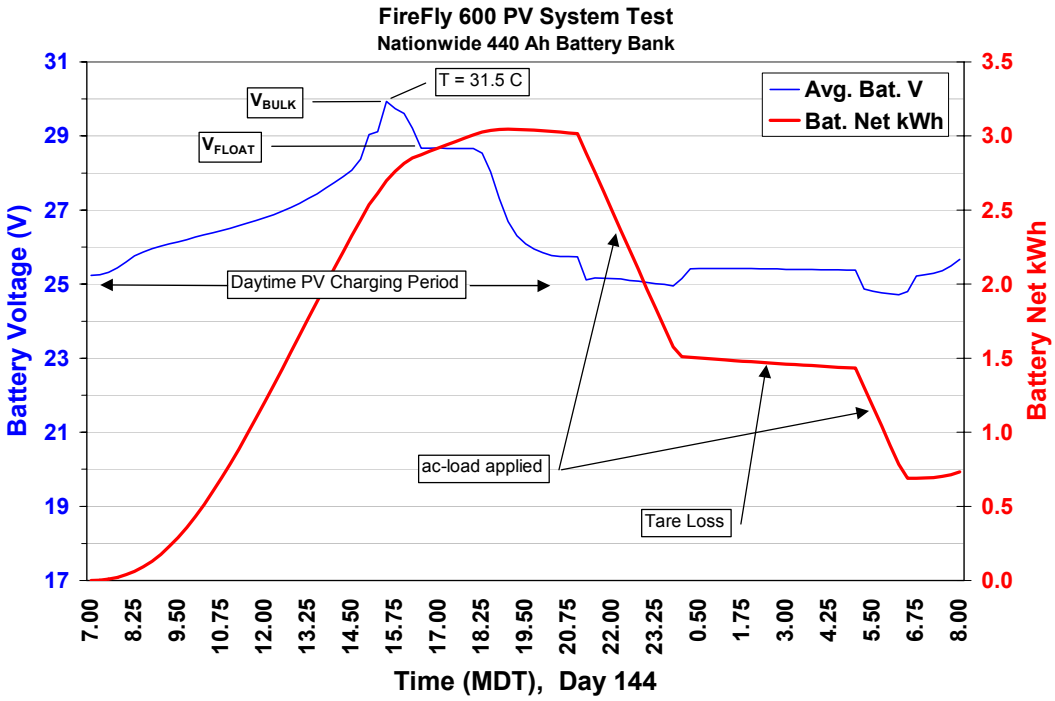

Figure 37. Example of a daily 'cycle' illustrating the 3-stage charging process controlled by the Trace C40 charge controller. Energy balance (kWh) indicated that 30% more energy was put into battery than was withdrawn.

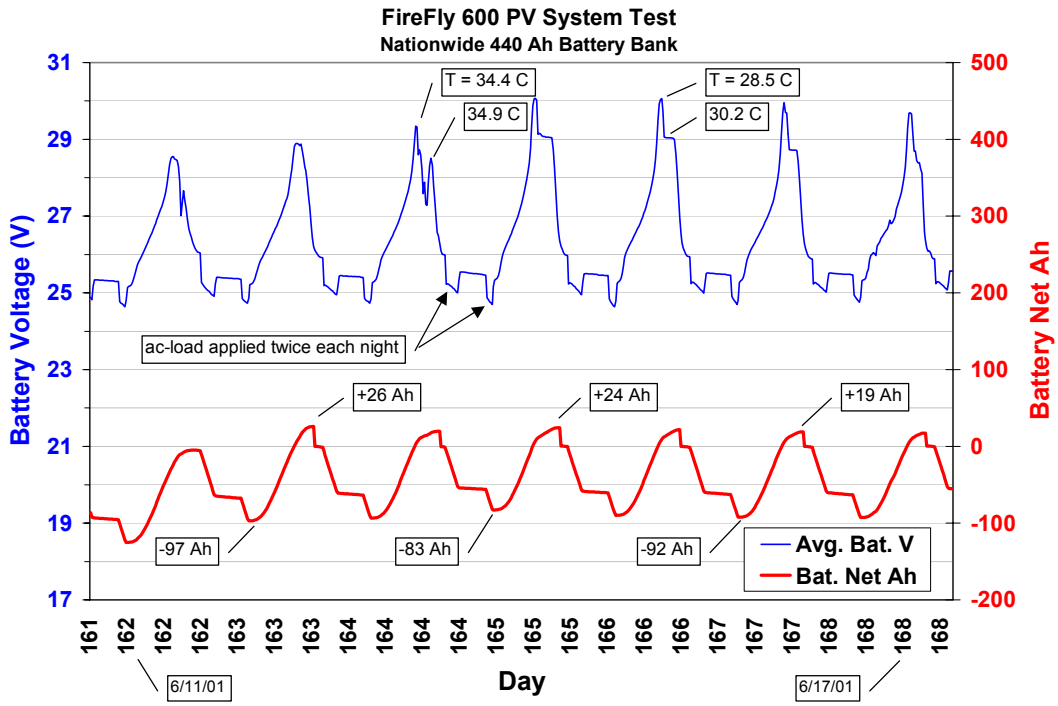

Figure 38. Battery voltage and net amp-hour flow into and out of battery bank during the daily 'cycling' at the end of the first 'recovery' test.

Recovery from Low-Voltage-Disconnect and Tare Loss

The ability of an off-grid photovoltaic system to quickly 'recover' from a low-voltage-disconnect condition, after the usable capacity of the battery bank has been depleted, is critical to both system performance and system reliability. The system must be able to continue to supply the ac load while still restoring the battery to a full state-of-charge in a relatively short period of time. If the battery is not returned to a full SOC within about 1 to 2 weeks, then permanent degradation of battery capacity is likely to result. Four parameters control system's ability to recover from a low-voltage-disconnect condition: the V_{LVD} setpoint, the V_{LVR} setpoint, the dc energy available from the array, and the size of the ac load.

As previously discussed, the setpoints for V_{LVD} and for V_{LVR} controlled by the Trace DR2424 inverter and the Trace C40 charge controller respectively, were both too low and were not user adjustable. Trace needs to modify these values, or make them adjustable, to better match the needs of typical deep-cycle lead-acid batteries used in photovoltaic systems.

Figure 39a shows the transitions from typical daily cycling (Day 149) through the first battery capacity test to a low-voltage-disconnect condition (Day 150), and then continuing for the first two days of 'recovery test #1.' Analysis of these test data indicated that the Trace DR2424 inverter reconnected the ac load to the system when the battery voltage reached 24.9 Vdc, defining the V_{LVR} condition. Because the V_{LVR} value is too low, it is likely that depending on the size of the ac load the inverter may disconnect and then reconnect the ac load unexpectedly as the system oscillates between the V_{LVD} and V_{LVR} conditions. Figure 39b shows the test results for the duration of the first 'recovery' test. Even for the 'conservative' ac load used during the 30-day test sequence, full recovery from a low-voltage-disconnect condition took about 12 days. A larger ac load would have resulted in a longer recovery time.

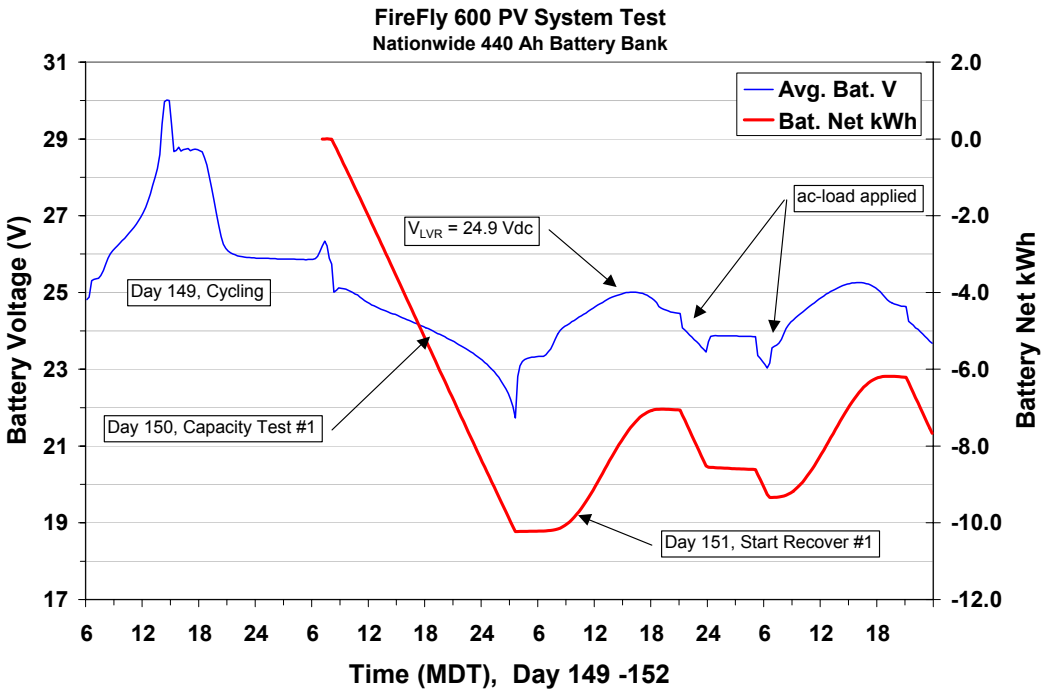

Figure 39a. Battery voltage and net energy (kWh) into and out of battery bank during battery capacity test #1, and at the start of 'recovery' test #1 including ac load application.

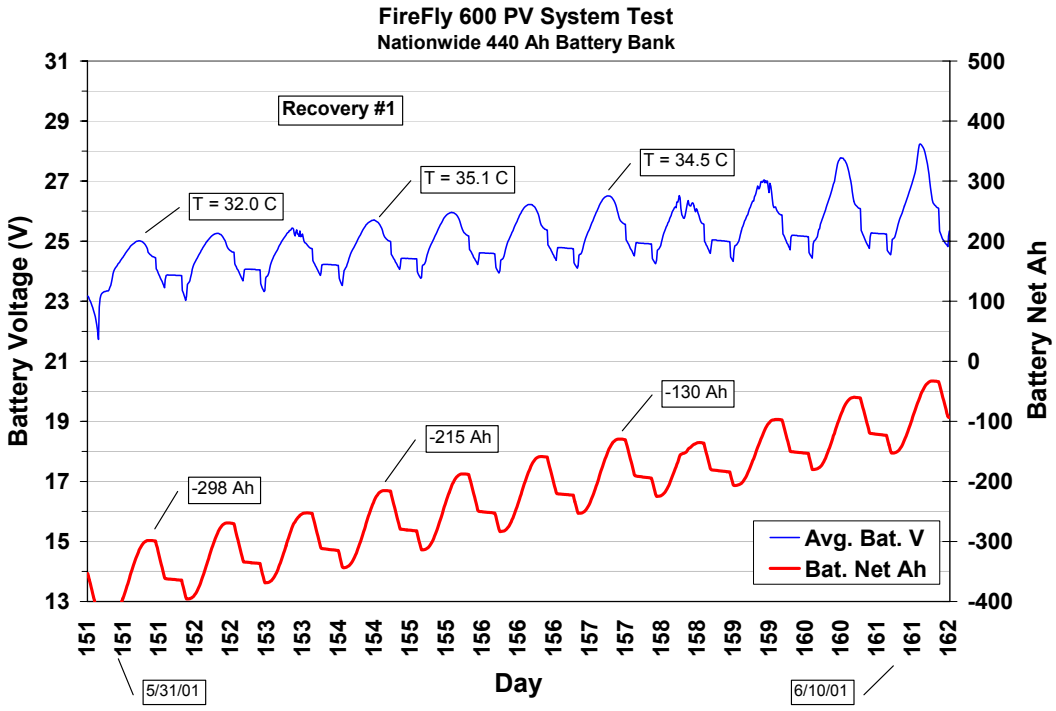

Figure 39b. Battery voltage and net amp-hour flow into and out of battery bank during the first 'recovery' test with ac load applied.

The effect of the ac load size on the time to recover from a low-voltage-disconnect condition is dramatically illustrated by data recorded during the second 'recovery' test. Following the second battery capacity test with discharge to V_{LVD}, the ac load was turned off and the array was used to recharge the battery bank. Figure 40 illustrates the results obtained during the second recovery test where the batteries reached a full state-of-charge plus a slight overcharge in 3 days.

The second recovery test also provided the means to quantify the 'tare' or 'parasitic' power loss in the system components: DR2424 inverter, Trace Meter, and wiring. Tare loss was directly available from the data because during the second recovery test there was no ac load applied. Therefore, the only parasitic load on the battery bank was the inverter and the battery capacity meter. The battery net Ah curve in Figure 40 shows the stair step improvement in the battery state-of-charge as energy was added by the array during the daytime. The slight downward slope at the top of each stair step was caused by the parasitic dc power loss. Analysis of the test data indicated this parasitic (tare) loss was about 17.5 W. Over a 24-hr period, this tare loss represents a significant percentage (~14%) of the dc energy provided by the array, and should be both accounted for and minimized during system design.

The Trace DR2424 inverter has an adjustable feature, the 'search mode' control, that is intended to control the tare loss by minimizing the inverter's output to small test pulses when there is no ac load requirement. The purpose of the test pulses is to detect the presence of a load, and if detected the inverter circuitry is activated to provide full voltage. However, the success of the 'search mode' in detecting a load and consequently minimizing tare loss is strongly dependent on the type of ac load attached to the system. For instance, small loads below the sensitivity of the search mode setpoint, loads that vary above and below the setpoint, appliances (microwave, VCR) with small continuous power requirements (clocks, displays), some fluorescent lights, and other devices may not be successfully detected by the search mode. For this reason, system users often defeat the search mode to ensure that all loads are powered correctly, but at the expense of the worst-case tare loss. The 17.5 W tare loss measured during this test procedure represents the worst case with the search mode defeated. If the system designer and/or the system user is careful in selecting the loads powered by the photovoltaic system, then the full advantage of the inverter's search mode could be realized, thus reducing tare loss to perhaps 2% of the dc energy provide by the array.

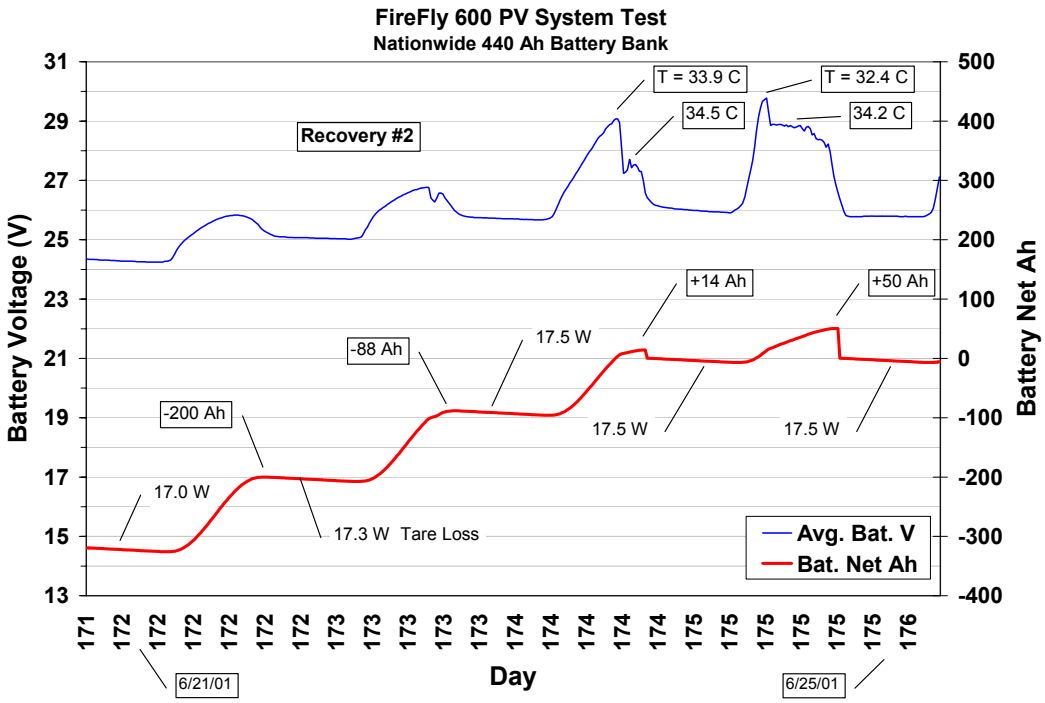

Figure 40. Battery voltage and net amp-hour flow into and out of battery bank during the second 'recovery' test without ac load applied to the system.

Daily Energy Efficiency for System and Components

The measured data from the 30-day test procedure were analyzed to provide a daily energy balance in units of kWh/d for the primary system components, as well as for the complete system. The kWh/d units provided a common basis for comparison, starting with the daily solar energy incident on the array and ending with the daily ac energy consumers are accustomed to purchasing from a utility company. By calculating the ratio of the daily energy out of a component divided by the daily energy into the component, a 'daily efficiency' was determined for each component and for the system. The results from this approach make it clear where design modifications can be made to improve system performance. The 'daily efficiencies' provide a more useful metric for the system designer than the more common instantaneous efficiency values based on power at a single operating condition. Table 5 summarizes the daily energy balance and calculated component efficiencies obtained during a 30-day test period in June 2001. The following discussion clarifies the interpretation of these results for each of the major components in the system.

Daily Array Efficiency

The daily energy efficiency for the photovoltaic array was calculated using the empirically determined performance model previously discussed. The calculated daily energy values were determined both for measured test conditions during the 30-day test period, as well as for the different months of the year (Table 1) using 'typical' solar resource and meteorological data from the National Solar Radiation Database. Array operating conditions are dictated by environmental conditions, and as a result the daily array efficiency for a latitude-tilt orientation varied seasonally with a low of about 9.5% in the summer months and a high of about 11.2% in the winter. Thus, on a relative basis the daily array energy efficiency was about 18% higher in winter than summer. If seasonal adjustments of the array tilt-angle

are done, the daily efficiency in summer and winter does not change noticeably, but the dc energy available from the array increases as previously illustrated in Figure 5.

The daily energy efficiency of the array was also directly influenced by the efficiency of the individual modules in the array. As reported earlier, the performance of the array of BP275 modules on the FireFly™ 600 array was about 6% below what would be expected based on the nameplate ratings for individual modules. If this discrepancy can be addressed through improved array design and/or negotiation with the module manufacturer, then the daily dc energy available from the array will be increased by the same percentage.

Table 5. Summary of daily energy balance with 'daily' efficiencies for the FireFly™ 600 and its components during a 30-day test sequence with array at latitude-tilt in Albuquerque, NM

Day	Sun kWh/m^{2}d	Array Eff.	Array-dc kWh/d	Array Util. Eff.	Overcharge kWh/d	Battery Eff.	Inverter Eff.	System Eff.	ac-Energy kWh/d	A:L,dc	A:L,ac
140	7.02	0.102	3.60								
141	7.88	0.101	4.01				0.852	0.313	1.254		
142	7.83	0.097	3.84	0.604	0.704		0.879	0.538	2.064	1.64	1.86
143	7.80	0.095	3.74	0.819	0.508	0.780	0.864	0.552	2.063	1.56	1.81
144	7.71	0.094	3.66	0.833	0.473	0.773	0.867	0.558	2.042	1.55	1.79
145	7.02	0.096	3.38	0.890	0.458	0.709	0.861	0.543	1.836	1.59	1.84
146	7.44	0.095	3.54	0.809	0.553	0.789	0.866	0.553	1.960	1.57	1.81
147	7.22	0.098	3.56	0.824	0.496	0.746	0.870	0.535	1.902	1.63	1.87
148	6.39	0.105	3.40	0.795	0.356	0.727	0.862	0.498	1.693	1.73	2.01
149	7.54	0.098	3.73	0.754	0.69						
150	7.46	0.095	3.58		**Battery Capacity Test #1**						
151	7.60	0.095	3.63					0.550	2.000		1.82
152	7.75	0.093	3.64	0.867	0	0.751	0.864	0.562	2.045	1.54	1.78
153	7.15	0.095	3.42	0.853	0	0.751	0.861	0.551	1.883	1.56	1.81
154	7.88	0.098	3.90	0.834	0	0.732	0.868	0.530	2.068	1.64	1.89
155	7.72	0.097	3.77	0.856	0	0.722	0.870	0.537	2.026	1.62	1.86
156	7.64	0.095	3.66	0.879	0	0.719	0.872	0.551	2.018	1.58	1.82
157	7.60	0.094	3.59	0.897	0	0.730	0.856	0.561	2.011	1.53	1.78
158	5.67	0.101	2.88	0.808	0	0.758	0.843	0.517	1.488	1.63	1.94
159	6.81	0.098	3.37	0.863	0	0.712	0.863	0.530	1.788	1.63	1.89
160	7.50	0.094	3.56	0.908	0	0.715	0.860	0.558	1.987	1.54	1.79
161	7.54	0.092	3.51	0.924	0	0.708	0.868	0.568	1.993	1.53	1.76
162	7.61	0.093	3.58	0.913	0	0.707	0.867	0.559	2.000	1.55	1.79
163	7.75	0.094	3.67	0.914	0.748	0.696	0.872	0.555	2.037	1.57	1.80
164	7.10	0.101	3.62	0.856	0.561	0.667	0.883	0.504	1.824	1.75	1.98
165	7.82	0.101	3.99	0.749	0.700	0.756	0.888	0.503	2.005	1.77	1.99
166	7.71	0.096	3.72	0.830	0.642	0.746	0.877	0.543	2.023	1.61	1.84
167	7.61	0.093	3.58	0.855	0.549	0.760	0.868	0.564	2.017	1.54	1.77
168	7.14	0.096	3.46	0.869	0.512	0.709	0.873	0.538	1.862	1.62	1.86
169	7.40	0.093	3.48	0.827	0.597						
170	6.81	0.095	3.26		**Battery Capacity Test #2**						
171	6.87	0.095	3.29								
172	7.44	0.097	3.63	0.884	0	0.057	0.00	0.000	0.0		
173	7.13	0.095	3.41	0.922	0	0.060	0.00	0.000	0.0		
174	6.82	0.095	3.26	0.945	0.393	0.060	0.00	0.000	0.0		
175	7.09	0.096	3.44		1.462						
176	4.89	0.094	2.32								
Avg. =	7.41	0.096	3.59	0.848	0.57	0.733	0.867	0.542	1.945	1.60	1.85
S =	0.48	0.003	0.20	0.067	0.11	0.064	0.009	0.020	0.137	0.07	0.07

Daily Array Utilization Efficiency

The daily array utilization efficiency quantifies how effectively the system's power conditioning system (charge controller, battery, inverter) uses the dc energy available from the array. The maximum energy available from the array can be captured only if the charge controller has a dedicated maximum-power-point-tracking (MPPT) function. The Trace C40 does not have a MPPT function, and as a result the

operating point for the array used with the FireFly™ system was typically well off the maximum-power-point, as previously illustrated in Figure 7. For the 30-day test period in June, the daily 'array utilization' efficiency was measured to be about 85%, meaning that 15% of the dc energy potentially available from the array was lost. The array utilization efficiency will be even lower in the winter months, estimated at about 75%, when array voltage is higher. This is clearly an area for improvement in the performance of the FireFly™ system. The energy loss can be addressed by using a different charge controller with a MPPT function and/or by selecting a photovoltaic array with voltage characteristics that more closely match the voltage requirements of the battery bank.

Daily Battery Efficiency

The daily battery efficiency was defined as the daily energy provided by the battery divided by the daily energy supplied to the battery from the photovoltaic array. The goal in system design is to maximize the daily battery efficiency while still overcharging the battery sufficiently to maintain its health. The maximum battery efficiency is achieved when overcharging is eliminated. However, eliminating periodic overcharging is a costly operational alternative because the lifetime of the batteries will be dramatically shortened. Daily battery efficiency, reliability, and maintenance requirements are also strongly influenced by operating temperature. Therefore, battery enclosure designs that minimize temperature deviations from a nominal 25°C are highly desirable for improving system performance and reliability. With the lid closed on the current enclosure design, battery temperature will be excessive in the summer requiring frequent addition of water, and excessive hydrogen generation will present a potential safety hazard. During the 30-day test period in June, the average daily battery efficiency was measured to be about 73% for a relatively conservative (small) ac load that resulted in more overcharging than necessary to maintain battery health.

If the ac load used during the 30-day test period had been increased then the dc energy available to overcharge the battery would have been reduced, and the calculated battery efficiency would be higher. In the limit, if battery overcharging had been eliminated entirely during the test period, then the average daily battery efficiency would have increased to about 92%. Another way to express the importance of optimizing the battery charging/overcharging strategy is in terms of the potential improvement in the ac energy delivered by the system. The average ac energy provided per day during the test period (1.94 kWh/d) could have been increased by 25% to 2.41 kWh/d if the dc energy used in overcharging the batteries was delivered to the load instead. Therefore, it is very important to determine the minimum level of overcharge (array energy expenditure) necessary to maintain battery health. Additional investigation will be required to fully understand this performance/reliability trade off for the battery.

Daily Inverter Efficiency

Inverter efficiency varies with the magnitude of the load, the load type (resistive, inductive, capacitive), tare loss, and operating temperature. As a result, the 'daily inverter efficiency' will be lower than the peak efficiency specified for a specific load and operating temperature. Data recorded during the 30-day test period quantifies both the daily inverter efficiency for a resistive-load and the sensitivity of instantaneous efficiency to operating temperature. As indicated in Table 5, the average daily energy efficiency was measured to be about 87%. During the test, the inverter was operated twice each night when the resistive ac load was applied. The ac load applied resulted in a constant ac power level of 475 Wac. This load coincided closely with the peak efficiency level reported by the manufacturer for the Trace DR2424 inverter. As previously discussed, the total daily energy dissipated in the ac load was scaled to the preceding day's total insolation level by varying the duration the load was applied.

By applying the ac load just after sunset and again just before sunrise, the operating temperature range for the inverter was maximized during the test period providing additional efficiency information. The

influence of operating temperature on instantaneous efficiency at a 475 Wac load is shown in Figure 41. The instantaneous efficiency measured, at a 25°C operating temperature and 475-W power level, is in good agreement with laboratory test results for a similar inverter given in Appendix A.

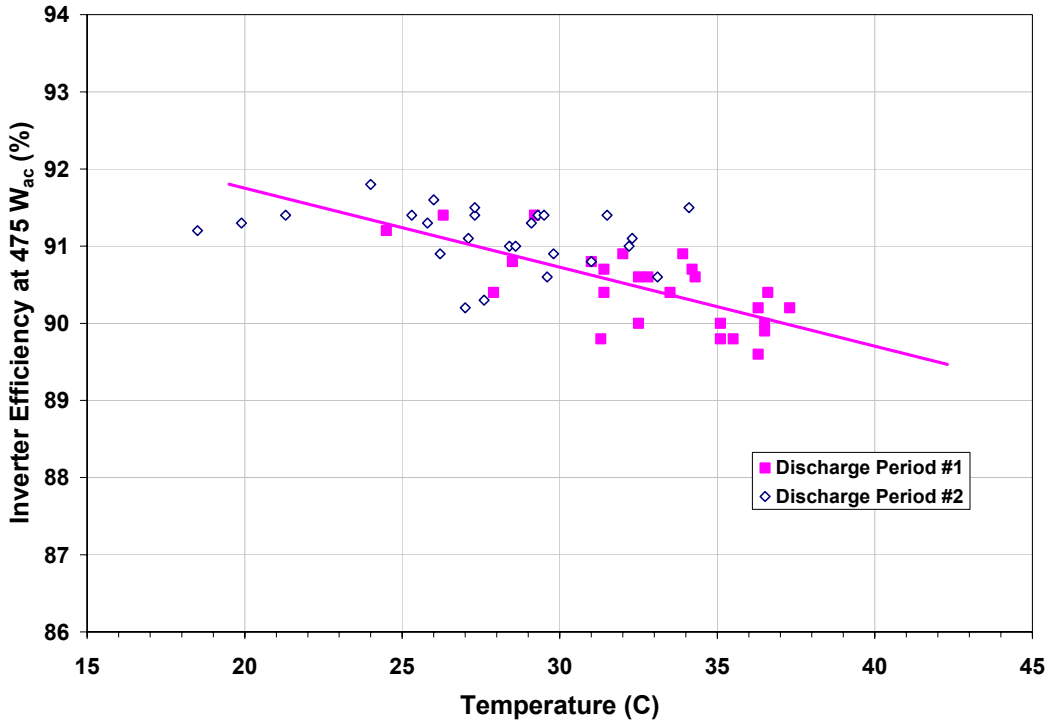

Figure 41. Instantaneous efficiency measured for Trace DR2424 inverter at 475-Wac output for a range of air temperature inside the insulated enclosure used to house the inverter.

System designers should attempt to address three factors in optimizing daily inverter efficiency. First, the design ac load for the system should result in the inverter operating at power levels consistent with its peak efficiency. If the ac load is too small or too large, the inverter efficiency can be significantly reduced. Second, the inverter should be selected to minimize the daily parasitic (tare) power loss. Tare losses are a 24-hour-per-day energy loss, and they can represent a large fraction of the dc energy available from the array. Third, the enclosure used to house both the inverter and the charge-controller should be designed to minimize operating temperature for these components during the summer months. Reduced operating temperatures will increase system efficiency and extend the lifetime of both components.

The operating temperature range for the Trace DR2424 inverter was specified as 0°C to 50°C, and for the Trace C40 as 0°C to 40°C. As previously shown in Figures 23 and 24, charge controller operating temperatures were just reaching this upper limit for summer conditions in Albuquerque. In addition, the low temperature limits on the component specifications need to be considered when designing the enclosure for winter conditions. Perhaps the best thermal compromise is an insulated enclosure that is closed during the winter, but vented during the summer.

Daily System Efficiency

Finally, the 30-day test procedure was used to determine the daily energy efficiency for the entire system. This efficiency represents the percentage of the energy available from the photovoltaic array that was actually delivered to the load as ac energy. The average daily efficiency determined for the FireFly™ 600

system, using the 'conservative' ac load previously discussed, was about 54%. Figure 42 summarizes the daily efficiencies for the separate system components during the 30-day test period in June in Albuquerque. As previously mentioned, the measured array performance was about 6% below the array rating derived from module nameplate ratings. Therefore, the daily system efficiency, if related to the nameplate power rating for the array, would be about 51%.

A number of opportunities for improvement of system performance were identified during the test procedure. System optimization will increase the overall system efficiency and daily ac energy available. The next section of this report discusses options for system improvement.

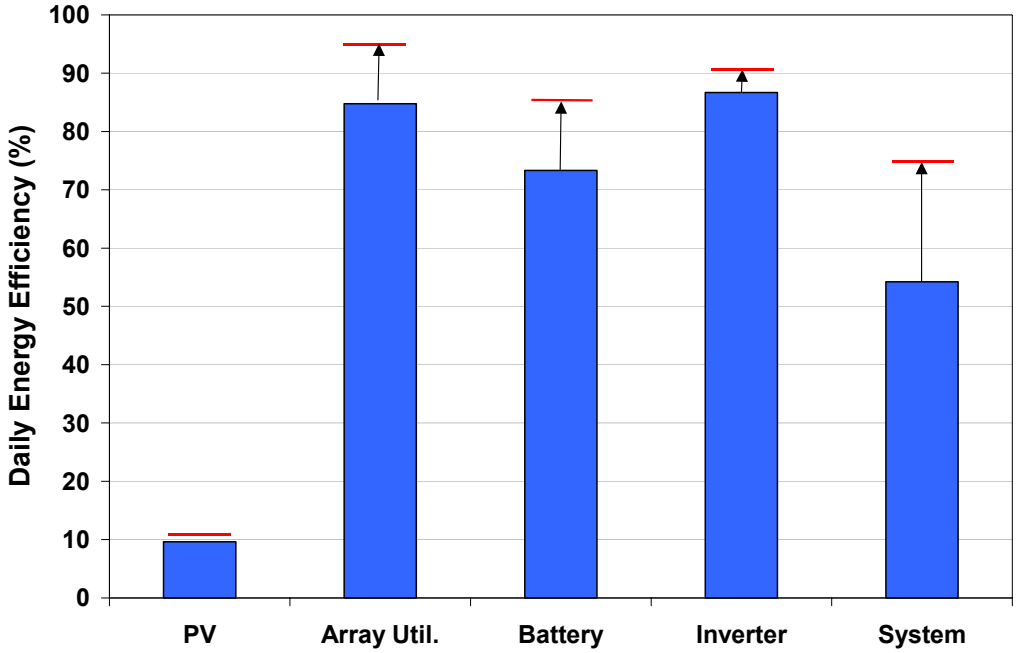

Figure 42. Daily energy efficiency measurements for the FireFly™ 600 components and system during the 30-day test period in June in Albuquerque, using a 'conservative' ac load. Arrows indicate range for potential improvement through system optimization.

System Performance Optimization

The possibilities for improvement in performance and reliability of the FireFly™ 600 system were addressed in two different scenarios. The first scenario required specific design modifications to the existing hardware, modification of electronic setpoints in charge-controller and inverter, and a specific system operating procedure, but all of the current system components were used. The second scenario required an alternative selection of components in order to achieve a further enhancement in system performance.

First Scenario

In the first optimization scenario, it was assumed that all mechanical and wiring changes previously discussed were addressed in order improve system safety, reliability, and compliance with NEC requirements. In addition, it was assumed that the recommended modifications are made by Trace for the DR2424 inverter setpoints for low-voltage-disconnect (V_{LVD}) and low-voltage-reconnect (V_{LVR}), plus the

input voltage range is increased to at least 32 Vdc to accommodate battery 'equalization.' The modifications by Trace are necessary in order to obtain the maximum battery lifetime. The results given in Table 6 summarize the expected daily ac energy available from the FireFly™ 600 for four different operational strategies (Cases 1-4).

Case 1 represents the 'conservative' load situation as tested, where a significant percentage (0.57 kWh/d, or ~15%) of the daily dc energy delivered by the array was expended in daily overcharge. Figure 42 previously illustrated the daily energy efficiencies for the system and components for the Case 1 situation. Case 2 is for the same situation as Case 1, except that the array tilt-angle was adjusted seasonally to increase the dc energy available from the array. As indicated in Table 6, this strategy increased the ac energy available in winter by about 10%, and in summer by about 5%.

Case 3 takes the performance optimization a step further by using a battery charging strategy that significantly reduced the dc energy used to overcharge the batteries. For this charging strategy, it was assumed that on a daily basis enough energy was provided to the battery to achieve the regulation voltage (29 Vdc), but no higher. The V_{FLOAT} and V_{BULK} settings in the Trace C40 would both be set to about 29 Vdc. Instead of daily overcharge, once per week a 3-hr equalization (boost) charge at 31 Vdc and 16-A was assumed. This charging strategy reduced the average daily dc energy used for battery maintenance from 0.57 kWh/d to 0.21 kWh/d and resulted in a noticeable boost (~16%) in ac energy available from the system. There are two additional benefits for this alternative charging strategy; the input voltage to the Trace DR2424 inverter could be kept below the upper limit of 31 Vdc, and less frequent battery 'watering' would be required. Unfortunately, the Trace C40 has a provision for automatic equalization but only every 30 days. So, the user of the system would have to manually initiate the equalization mode for the other 3 weeks of the month. Alternatively, the system designer or user could consider installing a small auxiliary generator that was used only to provide the energy needed for weekly equalization of the batteries.

Case 4 further improves ac energy production by minimizing the inverter tare loss. The DR2424 tare loss can be reduced from 17.5 W to less than 2 W assuming that all system ac loads can be effectively powered with the inverter in the 'search' mode. Taking advantage of this tare loss optimization will require that system ac loads are carefully selected or specified, but will also provide an 8% increase in the ac energy capacity for the system.

Second Scenario

In the second optimization scenario, different system components will be needed in order to obtain optimum performance. In particular, the array and/or charge controller will need to be different. In addition, it was assumed that all mechanical and wiring changes previous discussed were implemented.

As previously illustrated in Figure 7, the maximum-power-voltage, V_{mp}, for the FireFly™ 600 array is consistently much higher than the operating voltage dictated by the battery voltage, and as a result about 15 to 20% of the dc energy available from the array, on an annual basis, was lost. In addition, the array output power at ASTM Standard Reporting Conditions was measured to be over 6% below that expected from module nameplate ratings. The net result from these two factors was about 25% less dc energy available from the system than expected. In order to eliminate this lost energy, the system integrator should first verify that the array power at Standard Reporting Conditions closely matches the expectation based on nameplate ratings, and second address the mismatch between array V_{mp} and system operating voltage. One possible solution, if the Trace C40 charge-controller was retained, would be to select modules that have an array V_{mp} about 4 to 5 Vdc lower than the array of BP275 modules. Another possibility would be to select a different charge controller with a maximum-power-point-tracking (MPPT) capability.

The combination of all improvements discussed could result in an 'optimized' system with the higher daily efficiencies for components shown in Figure 42. Table 7 gives the resulting dc and ac energy available from an optimized FireFly™ 600 system for the array oriented at a latitude tilt-angle (Case 5) and for seasonal tilt adjustment (Case 6). *Relative to the conditions as tested at Sandia, the improvements in component performance, array orientation, setpoint selection, battery overcharge philosophy, and inverter tare loss result in a substantial 50% increase in the ac energy production capacity of the system.*

Table 6. Estimated dc Energy Availability and ac Load Capacity for FireFly™ 600 System in Albuquerque for Different System Operation Philosophies. Array has eight BP275 modules with total area of 5.04 m^2

Month	Lat. Tilt Solar kWh/m^{2}d	Tilt Adjust Solar kWh/m^{2}d	Daily Array Efficiency	Lat. Tilt Array-dc kWh/d	Tilt Adjust Array-dc kWh/d	Case 1 ac-Energy kWh/d	Case 2 ac-Energy kWh/d	Case 3 ac-Energy kWh/d	Case 4 ac-Energy kWh/d
Jan	5.09	5.61	0.112	2.88	3.16	1.55	1.70	1.97	2.13
Feb	5.82	6.09	0.108	3.18	3.33	1.71	1.79	2.08	2.24
Mar	6.31	6.30	0.107	3.40	3.40	1.83	1.83	2.12	2.28
Apr	7.12	7.20	0.102	3.65	3.69	1.97	1.99	2.30	2.46
May	7.47	7.87	0.098	3.69	3.89	1.99	2.10	2.43	2.59
Jun	7.23	7.78	0.095	3.47	3.72	1.87	2.00	2.32	2.48
Jul	7.24	7.66	0.095	3.45	3.64	1.86	1.96	2.27	2.43
Aug	7.01	7.17	0.096	3.37	3.45	1.82	1.86	2.15	2.31
Sep	6.60	6.46	0.097	3.23	3.23	1.74	1.74	2.02	2.18
Oct	6.33	6.47	0.102	3.27	3.27	1.76	1.76	2.04	2.20
Nov	5.46	5.94	0.108	2.98	3.23	1.61	1.74	2.02	2.18
Dec	4.89	5.49	0.112	2.76	3.08	1.49	1.66	1.92	2.08
Year	6.38	6.67	0.102	3.28	3.43	1.77	1.85	2.14	2.30

Case 1: As tested, latitude tilt, daily 0.57 kWh battery overcharge.

Case 2: Seasonal array tilt, daily 0.57 kWh overcharge.

Case 3: Seasonal array tilt, weekly 1.5 kWh equalize charge instead of daily overcharge.

Case 4: Seasonal tilt, weekly 1.5 kWh equalize, inverter tare 2W for 12h vs. 17.5W.

Table 7. With Design Optimization, dc Energy Availability and ac Load Capacity for FireFly™ 600 System in Albuquerque for Different System Operation Philosophies

Month	Lat. Tilt Solar kWh/m^{2}d	Tilt Adjust Solar kWh/m^{2}d	Daily Array Efficiency	Lat. Tilt Array-dc kWh/d	Tilt Adjust Array-dc kWh/d	Case 5 ac-Energy kWh/d	Case 6 ac-Energy kWh/d
Jan	5.09	5.61	0.119	3.06	3.36	2.23	2.44
Feb	5.82	6.09	0.115	3.38	3.54	2.46	2.57
Mar	6.31	6.30	0.114	3.62	3.62	2.63	2.63
Apr	7.12	7.20	0.108	3.88	3.93	2.82	2.85
May	7.47	7.87	0.104	3.93	4.14	2.85	3.01
Jun	7.23	7.78	0.101	3.69	3.96	2.68	2.88
Jul	7.24	7.66	0.101	3.67	3.87	2.67	2.81
Aug	7.01	7.17	0.102	3.59	3.67	2.61	2.67
Sep	6.60	6.46	0.103	3.43	3.44	2.49	2.50
Oct	6.33	6.47	0.109	3.48	3.48	2.53	2.53
Nov	5.46	5.94	0.115	3.18	3.44	2.31	2.50
Dec	4.89	5.49	0.119	2.93	3.28	2.13	2.38
Year	6.38	6.67	0.108	3.49	3.65	2.53	2.65

Case 5: Latitude tilt, array meets spec, 95% array utilization, 85% battery, 90% inverter, <0.1 kWh/d tare.

Case 6: Seasonal tilt, array meets spec, 95% array utilization, 85% battery, 90% inverter, <0.1 kWh/d tare.

CONCLUSIONS

Although the effort documented in this report was highly successful in meeting the original objectives, additional improvements in the test procedure and data interpretation are needed to further optimize system performance and reliability for all sites and seasons. An abbreviated version of the work documented in the report has also been published elsewhere [17].

- Seasonal influence on the dc energy available from the array (energy efficiency) was well understood. However, the seasonal (operating temperature) influence on daily energy efficiencies for array utilization, the battery, and the inverter were not fully determined for all operating conditions.
- As tested, a constant ac load was applied during two separate periods during the night with a total duration of 4 to 5 hours. The combined effect of tare loss and inverter efficiency versus load size was not fully quantified for a variety of load sizes and durations.
- As tested, the ac load was a purely resistive load. Additional tests with combinations of resistive, inductive, and capacitive loads should be conducted to determine the magnitude of their influence on the daily energy efficiency for the system.

REFERENCES

[1] Owner's Manual FireFly Solar Electric System, Energia Total, Ltd., Corrales, NM. http://www.energiatotal.com .

[2] Zomeworks Corporation, Battery Enclosures. http://www.zomeworks.com

[3] DR Series Owner's Manual, Version 3.2, 1998, Trace Engineering, Arlington, VA. http://www.xantrex.com

[4] C-Series Multifunction DC Controllers, Installation and Operation Guide, 1999, Trace Engineering, Arlington, VA. http://www.xantrex.com

[5] Trace Meter, Battery Status Meter, 1999, Trace Engineering, Arlington, VA. http://www.xantrex.com

[6] ASTM E 1036, *Standard Test Methods for Electrical Performance of Nonconcentrator Terrestrial Photovoltaic Modules and Arrays Using Reference Cells*.

[7] Anon., "NSRDB Vol. 2. Final Technical Report National Solar Radiation Database, (1961-1990)." National Renewable Energy Laboratory Technical Report, NREL/TP-463-5784, Jan 1995. http://rredc.nrel.gov/solar/

[8] D. King, J. Kratochvil, and W. Boyson, "Temperature Coefficients for PV Modules and Arrays: Measurement Methods, Difficulties, and Results," *26th IEEE PVSC*, 1997.

[9] D. King, J. Kratochvil, and W. Boyson, "Measuring Solar Spectral and Angle-of-Incidence Effects on Photovoltaic Modules and Solar Irradiance Sensors," *26th IEEE PVSC*, 1997.

[10] B. Kroposki, W. Marion, D. King, W. Boyson, and J. Kratochvil, "Comparison of Module Performance Characterization Methods,' *28th IEEE PVSC*, Anchorage, 2000.

[11] D. King, J. Kratochvil, and W. Boyson, "Field Experience with a New Performance Characterization Procedure for Photovoltaic Arrays," *2nd World Conference on Photovoltaic Solar Energy Conversion*, July 1998.

[12] D. King, W. Boyson, and J. Kratochvil, "Analysis of Factors Influencing the Annual Energy Production of Photovoltaic Systems," *29th IEEE PVSC*, 2002.

[13] PV-DesignPro photovoltaic system design software by Maui Solar Software Corporation, Haiku, HI. http://www.mauisolarsoftware.com

[14] National Electrical Code and NEC Handbook are available from the National Fire Protection Agency, 11 Tracy Drive, Avon, MA, 02322. Articles 250, 690, and 100. Email: custserv@nfpa.org Website: www.nfpa.org

[15] *Home Power Magazine*, 'Code Corner' editorials by John Wiles, issues #62, 72, 74.

[16] IEEE Std 450-1995, "IEEE Recommended Practice for Maintenance, Testing, and Replacement of Vented Lead-Acid Batteries for Stationary Applications"

[17] D. King, T. Hund, W. Boyson, and J. Kratochvil, "Experimental Optimization of the Performance and Reliability of Stand-Alone Photovoltaic Systems," *29th IEEE PVSC*, 2002.

APPENDIX A

TRACE DR2424 INVERTER TESTS

This Appendix provides typical performance test results obtained in the inverter research lab at Sandia National Laboratories for a Trace DR2424 inverter like the one in the FireFly 600 system.

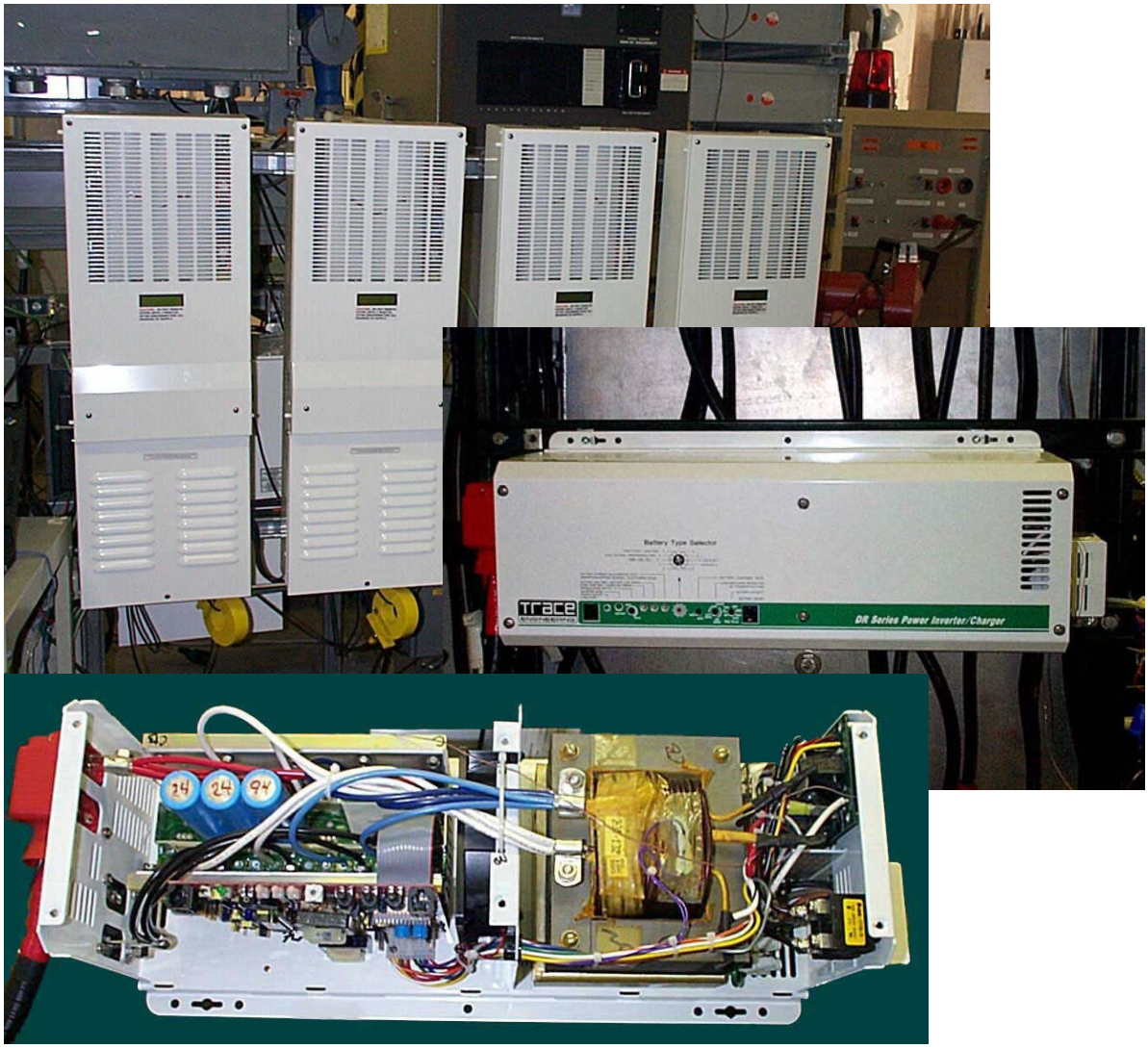

Photos of inverters being evaluated in Sandia's inverter testing laboratory.

Trace Engineering DR2424 2.4kW Modified-sine-wave Inverter

{refer to test plan at http://www.sandia.gov/pv/bos/sstndaln/gnrctst.htm}

manufacturer's specifications

model evaluated	DR2424	input voltage	21.6 – 31.0 Vdc
rated power	2.4 kWac	output voltage	120 V +/-5%
rated voltamperes	2400 VA	voltage distortion	not specified (quasi-sine)
surge power (overload)	7.0 kW (1 minute)	dc disconnect voltage	20.8 Vdc
efficiency (inverter mode)	95% peak	efficiency (charge mode)	not specified
tare power	10.8 Wdc (0.72 Wdc in search mode	max charge rate	70 Adc
charge control[1]	3-stage manual equalize	temperature compensation	optional sensor

[1] User-controlled voltages set based upon battery type (10 settings).

dc evaluation using 2030 A-H Battery (GNB Absolyte IIP)

Parameter	Quantity
inverter mode	
battery disconnect voltage	20.8 to less than 19.2 V [2]
charge mode	
dc ripple voltage (26.9 V float)	4.9V (max peak to peak)
dc ripple current (0.13 A float)	2.3 A (max peak to peak)
battery float voltage	26.9 V
bulk charging efficiency	79 %
bulk charging ac current distortion	96 %
bulk ac power factor	0.63

[2] Disconnect voltage dependent on actual current and battery capacity setting on inverter (50 – 1000 Ah).

Efficiency

(tare power = 7.7 watts, 0.8 watts in search mode.)

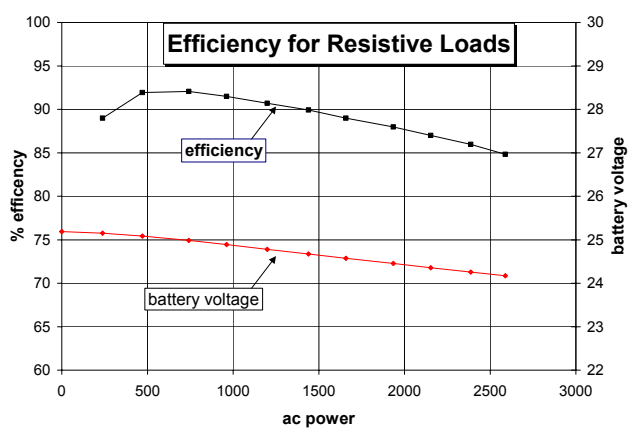

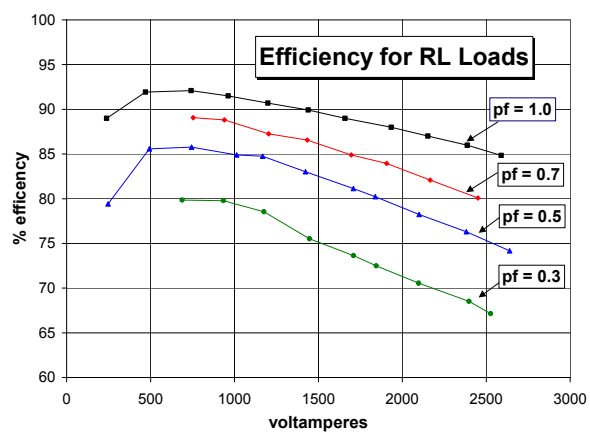

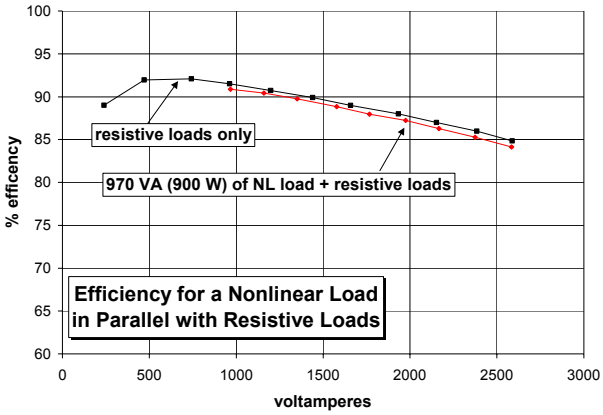

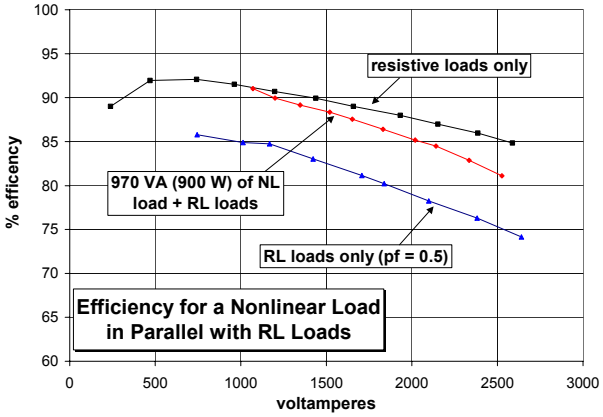

voltage and frequency regulation, and distortion

Note: Regulation is referenced to no-load values of 119 Vac and of 60.0 Hz.			
Test Configuration	% Voltage Regulation	% Frequency Regulation	Voltage Distortion (% THD) [3]
% full load (pf=1.0)			
no load	0.0	0.0	39
20% full load	2.5	0.0	37
50% full load	2.7	0.0	30
90% full load	2.8	0.0	25
100% full load	2.8	0.0	25
full load reactive			
pf=0.35 @ 2400 VA	4.0	0.0	30
pf=0.54 @ 2380 VA	0.9	0.0	29
pf=0.71 @ 2450 VA	1.0	0.0	28
non-linear loads in parallel with R			
NL=970 VA (R+NL=1770 VA ≈ 75% full load)	3.5	0.0	27
NL=970 VA (R+NL=2370 VA ≈ 100% full load)	3.5	0.0	26
motor loads (1/2 hp motor)			
motor only	1.0	0.0	31
motor with 1.8 kW in parallel (2210 W total)	2.0	0.0	27

[3] High distortion values are expected due to quasi-sine waveform.

inverter overload

Test Configuration	Planned Load Duration	Measured Load Duration	Measured Power / Voltage	Test Termination
Full load (2400 W)	5 hr	>> 5 hr	2400 W/116 V	operator shutdown
Full load + 20% (2880 W)	15 min	15 min	2685 W/115 V	operator shutdown
Full load + 50% (3600 W)	2 min	2 min	3712 W/116 V	operator shutdown
Full load + 100% (4800 W)	30 sec	30 sec	3800 W/116 V	operator shutdown

motor starting ½ hp motor fully loaded by dynamometer brake

	SNL line Motor Only	Inverter Motor Only	Inverter with 1.7kW Parallel Preload
initial ac voltage (rms)	121	119	119
voltage sag	1.7%	24%	25%
surge current (peak amps)	68	36	45
time to steady state (seconds)	0.20 sec (12 cycles)	0.5 sec (30 cycles)	0.3 sec (18 cycles)
steady-state current (rms)	9.2	9.1	21.6
steady-state voltage (rms)	120.3	118	117
voltage regulation	0.4%	0.9%	1.9%

Transfer Waveforms

*Many pieces of equipment are designed to operate through momentary voltage deviations. Computer and telecommunications manufacturers design to the ITI curve (CBEMA). Voltage deviations that lie between the two lines in the ITI curve should not adversely effect these types of equipment. The points overlaying the ITI curve result from plotting the moving average of the rms voltage through the transition. This envelope is not a pass-fail test, but a general indication that equipment will typically continue to operate correctly when the inverter provides a voltage waveform within the limits stated.

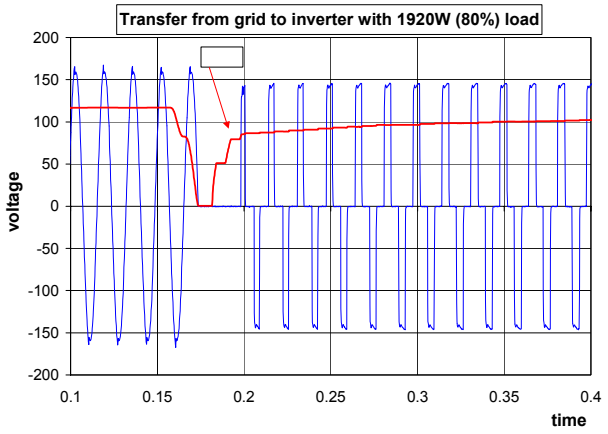

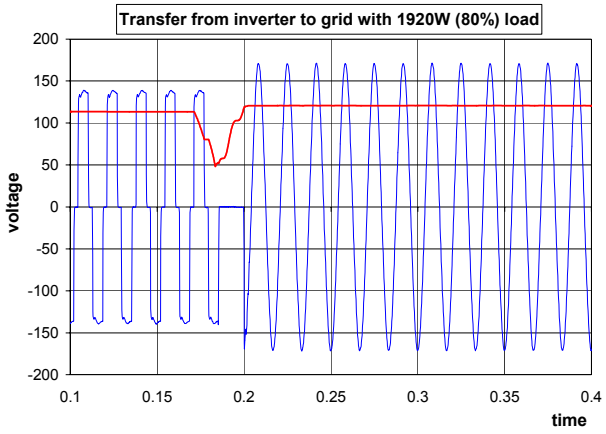

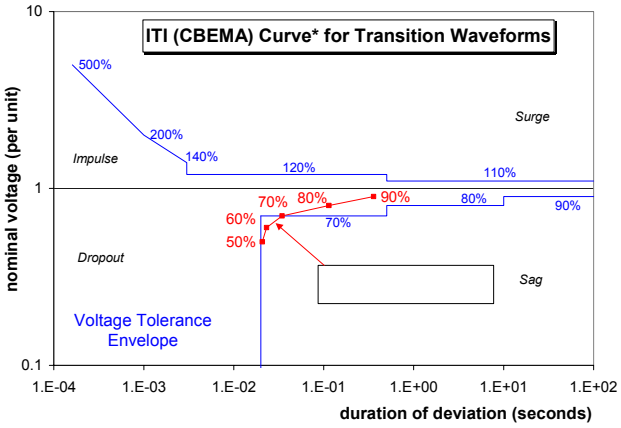

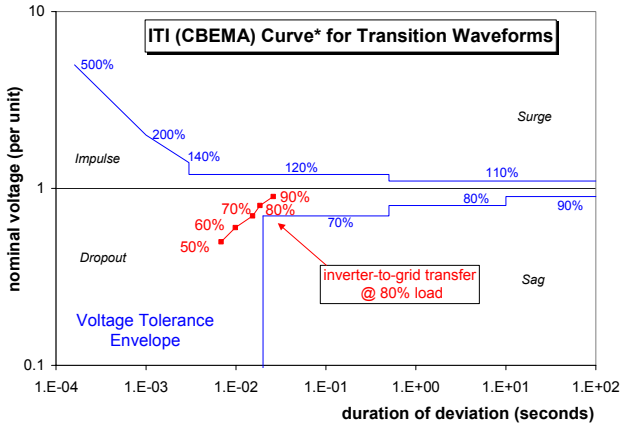

Battery Charging Algorithm The following chart tracks battery voltage and current through one complete charge cycle. Switch settings set to 1000 amp hour AGM/gel battery.

Parameter	Control Setting
battery type	AGM/gel
battery size	1000 amp-hour
temperature compensation	not connected
	Setpoint Corresponding to Control Settings
bulk charge regulation voltage	28.2 Vdc
float voltage	27.0 Vdc
bulk charge current	70 Adc
end of absorption charge	charge current < 25 Adc or 12 hr (lesser)

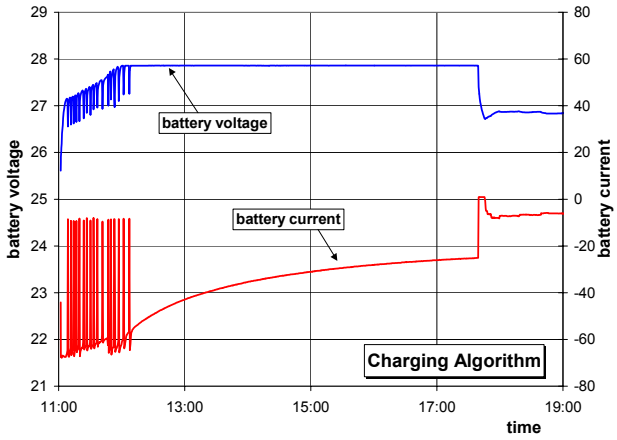

APPENDIX B

TRACEABILITY STATEMENT
Photovoltaic Systems Evaluation Laboratory
Sandia National Laboratories

Pyranometer and Pyrheliometer Calibrations

Pyranometer and pyrheliometer calibrations by the Photovoltaic Systems Evaluation Laboratory (PSEL) at Sandia National Laboratories are performed in a manner consistent with applicable ASTM test methods, and are traceable to the World Radiometric Reference (WRR) supported by the World Radiation Center in Davos, Switzerland. Sandia maintains three absolute cavity radiometers that have all been calibrated during international inter-comparisons. Two absolute cavity radiometers are used at the PSEL; one was manufactured by Technical Measurements Incorporated, Model MK-VI (s/n 67603) and the other by Eppley AHF (Hickey/Frieden, s/n 31108), both are maintained by Sandia's Primary Standards Laboratory. The TMI and the AHF instruments were calibrated through the international NREL Pyrheliometer Comparisons conducted in October 2001; both instruments were within 0.2% of the WRR reference instruments. Previous inter-comparisons for the TMI were conducted in 10/98, 10/94, 11/84, 11/80, 11/79, and 11/78. In addition, the radiometers' calibrations have been checked annually since 1980 using a laser light source and a Scientech (s/n 356) laser power meter with calibration traceable to the National Institute for Standards and Technology (NIST). A secondary reference standard Kipp&Zonen CM21 pyranometer (s/n 980505) and a secondary reference standard Kipp&Zonen CH-1 pyrheliometer (s/n 990202) serve as the working standards for our calibrations of other instruments. Another Eppley PSP (s/n 18527F3) shaded with a moving disk is used for diffuse irradiance measurements. All the instruments are calibrated relative to the absolute cavity radiometer. All resistors, temperature references, and voltmeters used are calibrated annually with traceability to NIST through Sandia's Primary Standards Laboratory.

Photovoltaic Module Calibrations

Photovoltaic module calibrations and performance measurements by the Photovoltaic Systems Evaluation Laboratory are performed in accordance with applicable ASTM test methods, and are traceable to the World Radiation Reference. Traceability is established through secondary reference Eppley pyranometers or Eppley pyrheliometers calibrated with our TMI MK-VI absolute cavity radiometer, or through a secondary silicon reference cell (MK-022) with transfer calibration from our primary silicon reference cells (MK-025 and MK-034). Direct traceability to the World Photovoltaic Scale (WPVS) is achieved using a separate secondary silicon reference cell (PRC 980512-5). Our primary silicon reference cells have traceability to the WRR through calibration at the National Renewable Energy Laboratory relative to their absolute cavity radiometer, and they are traceable to NIST through calibration relative to standard FEL lamp sources there.[1] In addition, the reference cells are also traceable to the international World Photovoltaic Scale.[2] All resistors, temperature references, and voltmeters used for these measurements are calibrated annually with traceability to NIST through Sandia's Primary Standards Laboratory. The LI-COR LI-1800 spectral radiometer used to measure the outdoor solar spectrum during tests is calibrated annually by LI-COR Incorporated with calibration traceable to NIST through their secondary FEL lamps.

[1] D. L. King, B. R. Hansen, and J. K. Jackson, "Sandia/NIST Reference Cell Calibration Procedure," 23rd IEEE PVSC, May 1993, pp1095-1101.

[2] C. R. Osterwald, et al., "World Photovoltaic Scale: International Reference Cell Calibration Program," Prog. in Photovolt: Res. Appl. **7**, 287-297 (1999).